

The mechanism of peptide exchange by MHC class II molecules

Inaugural – Dissertation
to obtain the academic degree
Doctor rerum naturalium (Dr. rer. nat.)

submitted to
the Department of Biology, Chemistry and Pharmacy of
Freie Universität Berlin

by
Monika-Sarah Schulze
from Giessen

2012

This thesis is based on research conducted from 2008 to 2012 at the Dana-Farber Cancer Institute in Boston, MA, USA, under the supervision of Prof. Dr. Kai Wucherpennig.

Gutachter:

Erster Gutachter: Prof. Dr. Kai Wucherpennig
Dana-Farber Cancer Institute
Harvard Medical School

Zweiter Gutachter: Prof. Dr. Udo Heinemann
Max-Delbrück-Center for Molecular Medicine
Freie Universität Berlin

Disputationstermin: 15. Mai 2012

Declaration

I hereby declare that the work presented in this thesis has been conducted independently and without any inappropriate support, and that all sources of content, experimental or intellectual, are suitably referenced and acknowledged. I further declare that this thesis has not been submitted before, either in the same or a different form, to this or any other university for a degree.

Boston, 26 February 2012

Monika-Sarah Schulze

Acknowledgment

First of all, I would like to thank Professor Dr. Kai Wucherpfennig for giving me the opportunity to carry out my PhD project in his lab and work on a scientifically extremely interesting but also highly challenging project. Thanks to him I could work in a stimulating multi-disciplinary environment and learn a lot about immunology research, a field I am very interested in. I also want to thank him for his continuous support and confidence in me throughout the years and his interest in and guidance during the project as well as his valuable advice during the writing process of my thesis.

Furthermore, I would like to thank Prof. Dr. Andreas Ziegler for making it possible for me to start as a PhD student at the Freie Universität Berlin many years ago. I also would like to thank him and Dr. Barbara Uchanska-Ziegler for their advice and feedback concerning my projects during our annual meetings. I extend my special thanks to Prof. Dr. Udo Heinemann who agreed to be my second reviewer from the beginning and Prof. Dr. Beate Koksche for being the chair of my defense committee.

Special thanks also goes to our collaborators Prof. Dr. James Chou from the Department of Biological Chemistry and Molecular Pharmacology of Harvard Medical School and, especially, Dr. Matt Call, who introduced me to the field of protein NMR spectroscopy and helped me carrying out and analyzing the multidimensional NMR experiments during this dissertation.

I am also most grateful to the people in the Wucherpfennig lab throughout the years for creating such an enjoyable and encouraging work environment and providing motivation during difficult times. Especially, Dr. Melissa Call I want to thank for her continuous input and inspiring discussions about my projects. Kathrin Anders, who taught me the method of surface plasmon resonance, and Bettina Franz I want to thank for their scientific help and friendship throughout the common journey towards the PhD. Furthermore, I would like to thank Dr. Dhruv Sethi for his crystallographic advice and his help with installing software programs. For reading parts of my thesis and giving feedback I would like to thank Don Shaffer, Jessica Dobbins, Howell Moffett, Torsten Meissner and Chris Harvey.

Last but not least I would like to thank my parents for giving me the freedom and constant support to do what I am really interested in.

Summary

Presentation of antigenic peptides by major histocompatibility complex class II (MHC II) molecules on the cell surface is essential as it evokes different immune responses including antibody production, cell destruction, and initiation of regulatory mechanisms. Peptide loading and formation of stable MHC II/peptide complexes is catalyzed by the MHC II like protein HLA-DM (DM). A major focus of this work was to understand the molecular mechanism of DM-mediated peptide exchange which would aid in efforts to predict immunogenicity of known and emerging pathogens. Furthermore, enhanced peptide exchange of MHC II molecules by a synthetic small molecule, J10, was investigated. This small molecule has therapeutic potential as it could allow actively modifying the presented peptide repertoire which is of interest for various medicinal applications, e.g. peptide based vaccination. To address the dynamic process of peptide exchange, which involves breaking and reforming multiple peptide-MHC II interactions, various methods were applied including X-ray crystallography, NMR spectroscopy and surface plasmon resonance (SPR).

SPR experiments undertaken during this doctoral work revealed definitive DM binding at increased temperature to the high-affinity MHC II/peptide complexes DR1/HA and DR2/MBP previously exhibiting no or only little DM susceptibility. This finding supports the model of a common transient MHC II/peptide conformation for high- and low-affinity MHC II/peptide complexes which is dependent on kinetic parameters and more abundant at higher temperature. Furthermore, the functional significance of the SPR data was demonstrated by correlating DM binding to a high- and a low-affinity MHC II/peptide complex with DM activity on the two complexes as measured by fluorescence polarization, showing that the two assays were in agreement.

Previous studies showed that release of the peptide N-terminus is crucial for DM binding and may be facilitated by spontaneous peptide motion which is also supported by SPR and NMR data obtained during this doctoral work. However, the structural implications of a partial peptide release were unknown. In this doctoral thesis a DR1 structure is presented carrying an HA peptide variant missing the two N-terminal peptide residues (P-2, P-1) that represents an intermediate state of a MHC II molecule during peptide release. Surprisingly, no major but small conformational changes were

observed including a small divergence of the DR α and DR β helices normally adjacent to the peptide N-terminus and an altered conformation of the conserved residue Val β 85 which partially opens up the P1 pocket. Overall, the DR1 structure seems to be relatively stable even if three conserved hydrogen bonds are disrupted and small conformational changes appear to destabilize the P1 anchor, which may facilitate peptide release.

Peptide mobility in the MHC II peptide-binding groove was further investigated in this study by NMR experiments and revealed the presence of multiple conformations for MBP (myelin basic protein) peptide bound to DR2 molecule. These data advance the structural understanding of MHC II/peptide complexes which is so far mainly deduced from the static picture of crystal structures of MHC II/peptide complexes. The NMR approach, including biosynthetic production of isotope-labeled MBP peptide and subsequent loading onto DR2 molecules, resulted in high-quality NMR spectra and can be used to further explore details about peptide dynamics in the MHC II/peptide complex.

During this work, the established NMR system was applied to investigate peptide release catalyzed by the small molecule J10 in solution. Although comparison of NMR data before and after J10 addition revealed subtle changes in peak intensities, which could indicate that the small molecule induces one of the peptide conformations, further experiments are necessary to confirm this effect. The ^{19}F -NMR experiments performed in this study revealed a higher affinity of the small molecule to low-stability MHC II/peptide complexes than to high-stability complexes. This finding could direct co-crystallization approaches of the small molecule that aim to identify its binding site on MHC II molecules, which could in turn be important for further improvement of the function of the therapeutically interesting J10.

Zusammenfassung

Präsentation antigener Peptide durch Klasse II Moleküle des Haupthistokompatibilitätskomplexes (*major histocompatibility complex*, MHC) auf der Zelloberfläche ist entscheidend für den Ablauf der adaptiven Immunantwort, die Prozesse wie Antikörperproduktion, Zellerstörung und Initiierung von Regulationsmechanismen beinhaltet. Die Peptidbeladung und Ausbildung von stabilen Peptid-MHC-Klasse-II-Komplexen wird katalysiert von HLA-DM (DM), ein untypisches MHC-Klasse-II-Molekül. Ein Schwerpunkt dieser Doktorarbeit war es, den molekularen Mechanismus des von DM katalysierten Peptidaustausches besser zu verstehen, welches Bemühungen vorantreiben könnte, die Immunogenität bekannter und neuer pathogener Organismen vorherzusagen. Desweiteren wurde der von einem kleinen Molekül beschleunigte Peptidaustausch von MHC-Klasse-II-Molekülen untersucht. Das synthetisch hergestellte kleine Molekül namens J10 hat Potential therapeutisch angewandt zu werden, da es ermöglichen könnte, aktiv das präsentierte Peptidrepertoire zu verändern, welches von Interesse ist für mannigfaltige medizinische Anwendungen, wie z.B. verbesserte Effizienz von peptidbasierten Impfstoffen. Um den dynamischen Prozess des Peptidaustausches zu untersuchen, welcher das Unterbrechen und Wiederausbilden von vielfachen Peptid-MHC-Klasse-II Interaktionen beinhaltet, wurden unterschiedliche Methoden angewandt, wie Röntgenkristallographie, NMR Spektroskopie und Oberflächenplasmonresonanz.

Oberflächenplasmonresonanzexperimente in der Doktorarbeit demonstrieren, dass DM an die stabilen Peptid-MHC-Klasse-II Komplexe DR1/HA und DR2/MBP bindet, welche bis dahin keine oder nur geringe Empfindlichkeit gegenüber DM gezeigt hatten. Diese Ergebnisse unterstützen das Model eines gemeinsamen Übergangszustandes für Peptid-MHC-Klasse-II Komplexe mit hoher und geringer Affinität, welcher abhängig ist von kinetischen Parametern und bei höherer Temperatur häufiger vorkommt. Desweiteren wurde in dieser Arbeit die funktionelle Bedeutung von den Oberflächenplasmonresonanzexperimenten demonstriert, indem DM Bindung und DM katalysierter Peptidaustausch von zwei Peptid-MHC-Klasse-II Komplexen mit hoher und geringer Affinität verglichen wurden. DM Aktivität wurde mit Hilfe von Fluoreszenzpolarisation gemessen und die Resultate beider Methoden zeigten gute Übereinstimmung.

Vorherige Studien haben gezeigt, dass die Loslösung des Peptid-N-Terminus entscheidend ist, damit DM an MHC-Klasse-II Moleküle bindet, was wahrscheinlich durch spontane Peptidbewegung möglich ist und auch durch SPR und NMR Daten in dieser Arbeit unterstützt wird. Die Auswirkungen der partiellen Peptidloslösung auf die MHC-Klasse-II Struktur waren jedoch unbekannt. In dieser Doktorarbeit wird die Kristallstruktur eines DR1 Moleküls präsentiert, welches mit einer Variante des HA (*hemagglutinin*) Peptids ohne die zwei N-terminalen Aminosäuren beladen ist und somit einen Übergangszustand während der Peptidloslösung von MHC-Klasse-II Molekülen darstellt. Erstaunlicherweise weist die Struktur keine grossen, sondern kleine konformationelle Unterschiede auf, wie z.B. ein geringes Auseinandergehen der DR α und DR β -Ketten, die sich normalerweise neben dem Peptid-N-Terminus befinden, und eine veränderte Seitenkettenkonformation von Val β 85, was zu einer teilweisen Öffnung der P1 Tasche führt. Im Allgemeinen scheint die DR1 Struktur relativ stabil zu sein, auch wenn drei konservierte Wasserstoffbrücken unterbrochen sind. Geringe konformationelle Veränderungen scheinen die P1 Bindungstasche zu destabilisieren, was eventuell die Peptidloslösung erleichtert.

Darüberhinaus wurde in dieser Arbeit die Peptidmobilität in der Bindungstasche von Peptid-MHC-Klasse-II Komplexen mit NMR Experimenten untersucht, welche die Anwesenheit mehrerer Konformationen für das MBP (*myelin basic protein*) Peptid im Komplex mit DR2 zeigten. Diese Daten geben ein besseres strukturelles Verständnis des Peptid-MHC-Klasse-II Komplexes, welches bisher vor allem durch das statische Bild von Kristallstrukturen beeinflusst ist. Der NMR Ansatz, welcher die biosynthetische Produktion von isotopen-markiertem MBP Peptid und anschliessender Beladung von DR2 Molekülen beinhaltet, ergab qualitativ hochwertige NMR Spektren und kann angewandt werden, um weitere Details der Peptiddynamik in der Bindungstasche zu untersuchen.

Das oben beschriebene NMR System wurde während dieser Arbeit angewandt, um die von dem kleinen Molekül J10 katalysierte Loslösung des Peptids in Lösung zu untersuchen. Obwohl der Vergleich von NMR Daten vor und nach J10 Zugabe geringe Unterschiede von Signalintensitäten zeigte, welches bedeuten könnte, dass J10 eine bestimmte Peptidkonformation induziert, sind weitere Experimente erforderlich, um diesen Effekt zu bestätigen. ^{19}F -NMR Experimente in dieser Arbeit zeigten höhere J10

Affinität zu Peptid-MHC-Klasse-II Komplexen mit geringer Affinität im Vergleich zu Komplexen mit hoher Affinität. Diese Ergebnisse können genutzt werden, um Ko-kristallisationsexperimente anzuleiten, die darauf gezielt sind, die Bindungsstelle des kleinen Moleküls zu bestimmen. Die Information der spezifischen Interaktionen zwischen J10 und MHC-Klasse-II Molekül könnte zur Verbesserung von J10 eingesetzt werden, welches Potential hat, therapeutisch eingesetzt zu werden.

List of publications

Schulze, M.S., A.K. Anders, M.J. Call, K.W. Wucherpfennig: Structure of a human MHC class II molecule with a partially filled peptide-binding groove. 2012, (manuscript in preparation).

Schulze, M.S., K.W. Wucherpfennig: The mechanism of HLA-DM induced peptide exchange in the MHC class II antigen presentation pathway. *Current Opinion in Immunology*. 2012, 24:105-111.

Anders, A.K., M.J. Call, **M.S. Schulze**, K.D. Fowler, D.A. Schubert, N.P. Seth, E.J. Sundberg, K.W. Wucherpfennig: HLA-DM captures partially empty HLA-DR molecules for catalyzed removal of peptide. *Nature Immunology*. 2011, 12:54-61.

List of abbreviations

ASU	-	asymmetric unit
CAPS	-	<i>N</i> -cyclohexyl-3-aminopropanesulfonic acid
CD	-	cluster of differentiation
CHO	-	chinese hamster ovarian
CIITA	-	class II transcriptional transactivator
CLIP	-	class-II-associated invariant chain peptides
DMSO	-	dimethyl sulfoxide
DNP	-	dinitrophenyl
DTT	-	dithiothreitol
<i>E. coli</i>	-	<i>Escherichia coli</i>
ER	-	endoplasmatic reticulum
FP	-	fluorescence polarization
GM/CA-CAT	-	General Medicine and Cancer institutes Collaborative Access Team
HA	-	hemagglutinin
HLA	-	human leukocyte antigen
HPLC	-	high-performance liquid chromatography
HSQC	-	heteronuclear single quantum coherence
Ii	-	invariant chain
MBP	-	myeline basic protein
MES	-	2-morpholinoethanesulfonic acid
MHC	-	major histocompatibility complex
MHC I	-	major histocompatibility complex class I
MHC II	-	major histocompatibility complex class II
MLE	-	MHC loading enhancer
MOI	-	multiplicity of infection
MPD	-	2-methyl-2,4-pentandiol
MWCO	-	molecular weight cut off
NE-CAT	-	Northeastern Collaborative Access Team
NMR	-	nuclear magnetic resonance
nOe	-	nuclear Overhauser effect
NOESY	-	Nuclear Overhauser effect spectroscopy
PAGE	-	polyacrylamide gel electrophoresis
PDB	-	protein data bank
PEG-x	-	polyethylene glycol with a mean molecular mass of x g/mol
RU	-	response unit
SDS	-	sodium dodecyl sulfate
<i>Sf</i>	-	<i>Spodoptera frugiperda</i>
SPR	-	surface plasmon resonance
TFA	-	trifluoroacetic acid
tr	-	transverse relaxation-optimized
TROSY	-	transverse relaxation optimized spectroscopy

Table of contents

Gutachter	II
Declaration	III
Acknowledgment	IV
Summary	V
Zusammenfassung	VII
List of publications	X
List of abbreviations	XI
Table of contents	XII
1 Introduction	1
1.1 The major histocompatibility complex	1
1.2 MHC class II dependent pathway of antigen presentation	2
1.3 Structure and function of MHC class II/peptide complex and comparison with MHC class I/peptide complex	5
1.4 The role of HLA-DM in the MHC class II presentation pathway and comparison to the peptide loading complex of MHC class I molecules	9
1.5 Structure of HLA-DM and lateral interaction with HLA-DR	11
1.6 Proposed mechanisms for HLA-DM-catalyzed peptide exchange	14
1.7 HLA-DO: a negative regulator of HLA-DM	16
1.8 MHC loading enhancers	17
1.9 Scopes and objectives of this study	21
2 Chapter I: Investigating enhanced peptide exchange of MHC class II molecules by the small molecule catalyst J10	22
2.1 Introduction	22
2.2 Materials and Methods	24
2.2.1 Preparation and crystallization of HLA-DR2/MBP in the presence of J10-1 and J10-12.	24
2.2.2 Preparation of isotope labeled MBP peptide	25
2.2.3 Preparation of HLA-DR2/peptide complexes	26
2.2.4 NMR experiments	27
2.3 Results and discussion	28

2.3.1	Preparing and crystallizing HLA-DR2/MBP in the presence of J10-1 or J10-12	28
2.3.2	Preparing and characterizing ¹⁵ N-labeled MBP peptide.....	29
2.3.3	Preparing the complex of HLA-DR2 and ¹⁵ N-labeled MBP peptide	31
2.3.4	Measuring ¹ H- ¹⁵ N HSQC spectra of ¹⁵ N-labeled MBP peptide free in solution and in complex with HLA-DR2.....	31
2.3.5	Deuterating MBP peptide to improve signal intensity of the HSQC spectrum of isotope labeled MBP peptide in complex with HLA-DR2	35
2.3.6	Measuring and comparing HSQC spectra of HLA-DR2/ ¹⁵ N, ¹³ C, ² H-MBP before and after addition of J10-1	36
2.3.7	Performing HNCA and ¹⁵ N-NOESY experiments of HLA-DR2/ ¹⁵ N, ¹³ C, ² H-MBP to determine resonance assignments	39
2.3.8	Measuring ¹⁹ F-NMR spectra of J10-11 in the presence of HLA-DR2/MBP and HLA-DR2/CLIP	40
2.4	Conclusion.....	42
3	<i>Chapter II: Structural effects of destabilizing peptide-MHC II interactions and implications for the peptide exchange mechanism of HLA-DM.....</i>	46
3.1	Introduction.....	46
3.2	Materials and Methods	47
3.2.1	Preparation of biotinylated HLA-DM and HLA-DM mutant.....	47
3.2.2	Preparation of HLA-DM used for crystallization.....	48
3.2.3	Preparation of covalently linked HLA-DR1/peptide complexes and of HLA-DR1 mutant.....	48
3.2.4	Preparation of HLA-DM with an N-terminally truncated α chain	49
3.2.5	Surface plasmon resonance experiments.....	49
3.2.6	Protein crystallization, collection of diffraction data and structure solving	50
3.2.7	Eluting covalently linked peptide from HLA-DR1	51
3.2.8	Mass spectrometry	51
3.3	Results and discussion.....	51
3.3.1	Preparing HLA-DM and HLA-DR1 carrying a truncated HA peptide, both used for crystallization experiments.....	51
3.3.2	Measuring pH-dependent affinity of HLA-DM to HLA-DR1 carrying an N-terminally truncated HA peptide using surface plasmon resonance	53
3.3.3	Crystallizing HLA-DR1 carrying a truncated HA peptide, in the presence of HLA-DM and alone	55
3.3.4	Solving the structure of HLA-DR1 carrying an N-terminally truncated HA peptide....	56
3.3.5	Structure of HLA-DR1 carrying an N-terminally truncated HA peptide	57
3.3.6	Eluting N-terminally truncated HA peptide from HLA-DR1 protein used for crystallization and analyzing by mass spectrometry	65

3.3.7	Measuring HLA-DR binding to N-terminally truncated HLA-DM using surface plasmon resonance	67
3.3.8	Measuring HLA-DM binding to HLA-DR1 carrying an HA peptide variant with a valine at P1 position and two N-terminal peptide residues absent	68
3.3.9	Measuring HLA-DM binding to HLA-DR1 mutant (Val β 85Asp) using surface plasmon resonance	69
3.4	Conclusion.....	71
4	<i>Chapter III: Investigating HLA-DM binding to high-affinity MHC II/peptide complexes.....</i>	74
4.1	Introduction	74
4.2	Materials and Methods	75
4.2.1	Preparation of HLA-DR/peptide complexes	75
4.2.2	Surface plasmon resonance experiments	76
4.2.3	Fluorescence polarization experiments	76
4.3	Results and discussion.....	76
4.3.1	Preparing the high-affinity complexes HLA-DR2/MBP and HLA-DR1/HA	76
4.3.2	Measuring HLA-DM binding to HLA-DR2/MBP and HLA-DR1/HA using surface plasmon resonance	77
4.3.3	Comparing HLA-DM binding detected by surface plasmon resonance with HLA-DM catalysis measured by fluorescence polarization	78
4.4	Conclusion.....	79
5	<i>Final discussion and outlook.....</i>	80
6	<i>References</i>	84

1 Introduction

1.1 The major histocompatibility complex

The major histocompatibility complex (MHC; human leukocyte antigen (HLA) complex in humans) is a highly polymorphic region on chromosome 6 in humans with genes that encode MHC molecules that play a fundamental role in the immune system and autoimmunity (figure 1.1). For example, lack of expression of MHC class II (MHC II) molecules results in severe immunodeficiency with defects in both cellular and humoral immunity causing extreme vulnerability to infections (Reith and Mach, 2001). Genetic susceptibility to many autoimmune diseases, including multiple sclerosis and rheumatoid arthritis, has been linked directly to the MHC II locus (Goronzy and Weyand, 2005; Svejgaard, 2008). The MHC first received attention in the context of tissue and organ transplantation studies which showed that this locus was involved in graft acceptance and rejection (histocompatibility).

The class I molecules are expressed in most nucleated cells where they present mainly endogenous peptides on the cell surface to effector cells such as CD8⁺ T cells (cytotoxic T lymphocytes). The presented peptide repertoire can be derived from either normally-expressed self proteins or microbial proteins in the case of an infected cell. Presentation of pathogen-derived peptide by MHC class I molecule to an effector cell allows for recognition and killing of the infected cell, while presentation of normal self-peptide induces tolerance.

In comparison, the class II molecules (HLA-DR, -DQ and -DP) are presented on specialized antigen presenting cells including macrophages, dendritic cells and B cells. During infection MHC II molecules present exogenous peptides to CD4⁺ T cells derived from extracellular pathogens. Upon recognition of pathogenic peptides CD4⁺ T cells activate and direct other immune cells to the site of inflammation and therefore play a crucial role in initiating an adequate immune response. Both MHC class I and II molecules show extensive sequence polymorphisms especially in the peptide-binding region allowing different types of peptides to bind (Germain, 1994).

The MHC III region, also called central MHC, as it is flanked by the centromeric MHC II and the telomeric MHC I genes, is less polymorphic and encodes protein families involved in various aspects of innate immunity (complement proteins,

inflammatory cytokines, and heat shock proteins) as well as some proteins not directly involved in the immune system (Hauptmann and Bahram, 2004).

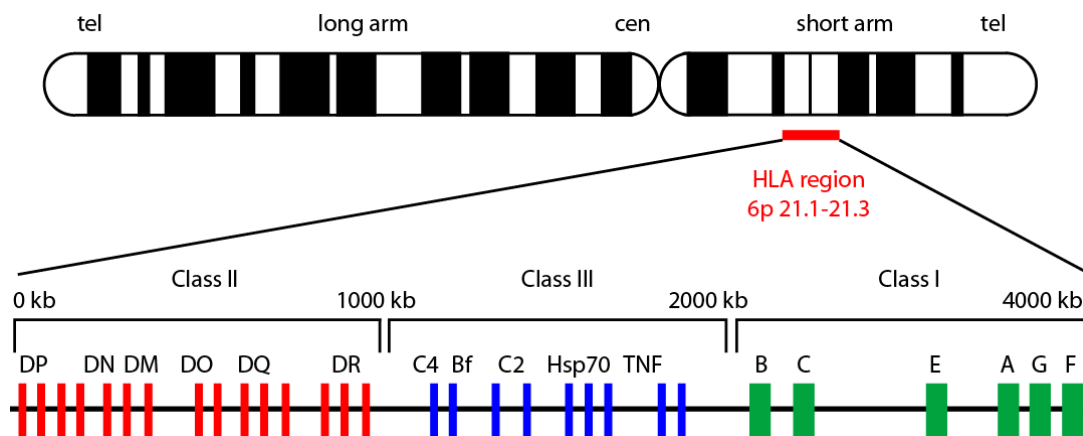


Figure 1.1: Schematic representation of the HLA locus on chromosome 6 in humans. The HLA region is located on the short arm of chromosome 6 from 6p21.1 to p21.3 indicated by a red bar. The extent of the class II (red), class III (blue) and class I (green) genes that spans from the centromeric (cen) to the telomeric (tel) end is shown. The class II region includes the genes for α and β chains of the MHC class II molecules HLA-DR, -DP, and -DQ. In addition, the genes encoding the DM α and DM β chains, and the genes encoding α and β chains of the DO molecule (DN α and DO β , respectively) are also located in the MHC class II region (adapted from (Mehra and Kaur, 2003)).

1.2 MHC class II dependent pathway of antigen presentation

Like other cell-surface glycoproteins, MHC class I (MHC I) and MHC class II (MHC II) molecules assemble in the endoplasmic reticulum (ER). As shown in figure 1.2, unlike MHC I molecules which bind endogenous peptides in the ER, MHC II molecules must protect their peptide-binding site until they reach the late endosomal compartment where they bind exogenous peptides. Therefore the α - and β - subunits which form the MHC II molecule associate with a third molecule, the MHC class II-associated invariant chain (Ii), which partially binds to and occludes the peptide-binding groove. In the ER lumen the invariant chains first form a trimer and successively three MHC II α/β - heterodimers bind noncovalently to each subunit (Lamb and Cresswell, 1992) with the chaperone calnexin binding and stabilizing the different components (Anderson and Cresswell, 1994). After assembly, the nonameric complex is directed through the Golgi apparatus to a low pH endosomal compartment via a signal sequence in the cytoplasmic region of the invariant chain. The main site of peptide loading in the MHC II pathway is the endocytic MHC class II-containing compartment (MIIC) (Anderson and Cresswell, 1994). During transport and within these late endocytic, early

lysosomal structures, the invariant chain is gradually cleaved by lysosomal proteases (Cresswell, 1996; Newcomb and Cresswell, 1993; Roche et al., 1991) such as the cysteine proteases cathepsins S and L (Deussing et al., 1998; Nakagawa et al., 1998; Riese et al., 1996). After initial C-terminal truncation of the invariant chain, further degradation leaves only short peptide fragments, called CLIP (class II-associated invariant-chain peptides), bound to MHC II molecules. As CLIP binds in the peptide-binding groove of MHC II molecules, it must be removed in order for other antigenic peptides to bind and later on to be presented on the cell surface.

HLA-DM (DM), another transmembrane protein also encoded in the MHC and regulated by the class II transcriptional transactivator (CIITA) like MHC II molecules, undertakes the task of peptide exchange and plays an important role in the process of peptide loading and formation of stable MHC II/peptide complexes. Forming stable complexes between MHC II molecules and peptides is crucial for a specific immune response as these complexes can be present on the cell surface for days (Lanzavecchia et al., 1992). During this time peptide loss due to weak interactions and binding of locally available peptides outside the cell by empty MHC II molecules could lead to ineffective and uncontrolled peptide presentation. The important function and activity of DM will be further discussed in section 1.4.

In uninfected cells, similar to MHC I molecules, MHC II molecules bind peptides derived from self proteins, frequently originating from aggregated and degraded MHC II and invariant chain molecules (Vogt et al., 1994). In case of infection MHC II molecules present exogenous peptides derived from internalization of pathogens and pieces of pathogenic organisms or eukaryotic parasites residing in intracellular vesicles. The loaded peptides are products of proteolytic degradation by proteases that are activated at low pH in the late endosomes and lysosomes. Among these proteases are the cysteine proteases cathepsins B, D, S, and L whereas cathepsins S and L are most predominant. There are also other proteases involved in antigen processing and the overall peptide repertoire presumably reflects the activities of the many proteases that are present in the endosomal pathway.

After forming stable MHC II/peptide complexes the molecules are transported to the cell surface where bound peptides are presented to T cell receptors (TCR) which are present on T cells. As T cell recognition of antigens is MHC restricted, the TCR has to recognize the peptide and the specific MHC II molecule. In order to achieve full activation of a naïve T cell, the activated antigen presenting cell must also provide

appropriate costimulation, usually via expression of CD80 or CD86 (B7-1 and -2, respectively), which bind to CD28 expressed on the naïve T cell. Stimulation through the TCR without costimulation induces T cell anergy, a state in which the T cell becomes unresponsive to antigen stimulation, even in the context of costimulation. Furthermore, the co-receptor molecule CD4 which associates on the T cell surface with components of the T cell receptor binds to the membrane-proximal domain of MHC II molecules. Binding of T cell receptor and co-stimulatory factors results in recruitment of other molecules and further signaling in the T cell ultimately leading to the activation of nuclear transcription factors turning on new gene expression. Once the T helper cell is activated it is involved in activating and directing other immune cells and thereby orchestrating the immune response.

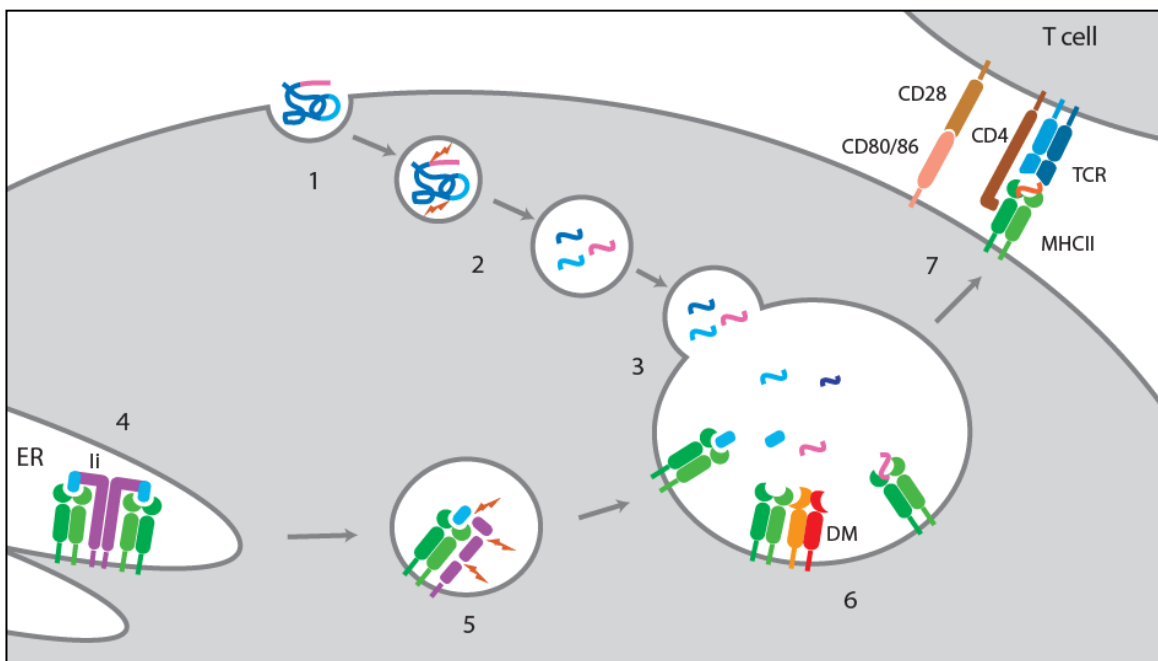


Figure 1.2: Schematic representation of antigen presentation pathway of MHC II molecules. (1) Antigen is taken up into intracellular vesicles. (2) Acidification of vesicles activates proteases which degrade antigen into peptide fragments. (3) Vesicles containing peptide fragments fuse with vesicles containing MHC II molecules. (4) Invariant chain (Ii) binds to newly synthesized MHC II molecules partially occupying the peptide-binding groove. (5) Invariant chain is proteolytically degraded. (6) DM binds to MHC II molecules and catalyzes peptide exchange. (7) MHC II molecules loaded with peptide are transported to the cell surface where they can bind to T cell receptor. The co-receptor molecule CD4 present on T cells also binds to MHC II molecules. In order for T cell activation to occur the co-stimulatory molecules CD80 or CD86 expressed on the antigen presenting cell has to bind to the co-stimulatory molecule CD28 expressed on T cells.

1.3 Structure and function of MHC class II/peptide complex and comparison with MHC class I/peptide complex

Structure of MHC II/peptide complex

MHC II molecules are heterodimers consisting of an α and a β chain which associate non-covalently and are similar in size with about 190 residues each. Both chains are type I transmembrane proteins which span the membrane once and have a C-terminal cytosolic domain and an N-terminal extracellular domain. The external part of each chain contains two domains - $\alpha 1$, $\alpha 2$ and $\beta 1$, $\beta 2$, respectively (figure 1.3, B). The membrane-proximal domains ($\alpha 2$, $\beta 2$) show structural similarities with immunoglobulin domains whereas the membrane-distal domains ($\alpha 1$, $\beta 1$) pack closely together and form the peptide-binding groove. This extended cleft where a peptide can bind is composed of a 'platform' shaped by an anti-parallel β sheet consisting of eight strands (four from the $\alpha 1$ domain and four from the $\beta 1$ domain) and two α helices (one from each domain) flanking the groove (figure 1.3, D).

Comparison with MHC I/peptide complexes

The three-dimensional structure of MHC II molecules is very similar to the appearance of MHC I molecules although the subunit structure is distinct as MHC I molecules consist of an α chain subdivided into $\alpha 1$, $\alpha 2$ and $\alpha 3$ with $\alpha 1$ and $\alpha 2$ forming the peptide-binding groove and $\alpha 3$ an Ig-like domain (figure 1.3, A). The other Ig-like domain is formed by β_2 -microglobulin. But the major structural and functional difference between MHC I and II molecules lies in the ends of the peptide-binding cleft (figure 1.3, C, D). In MHC I molecules the termini of the peptide are tightly bound at either end of the cleft by several contacts with conserved residue clusters and the typical peptide length is 8-10 residues. In comparison, peptides bound to MHC II molecules extend beyond the cleft and are usually 13 amino acids long or longer. The length of bound peptides is not constrained and partially unfolded proteins have been shown to bind to MHC II molecules through the peptide-binding groove (Runnels et al., 1997). However, it is likely that proteins and longer peptides are trimmed by proteases to a length of 13-17 residues.

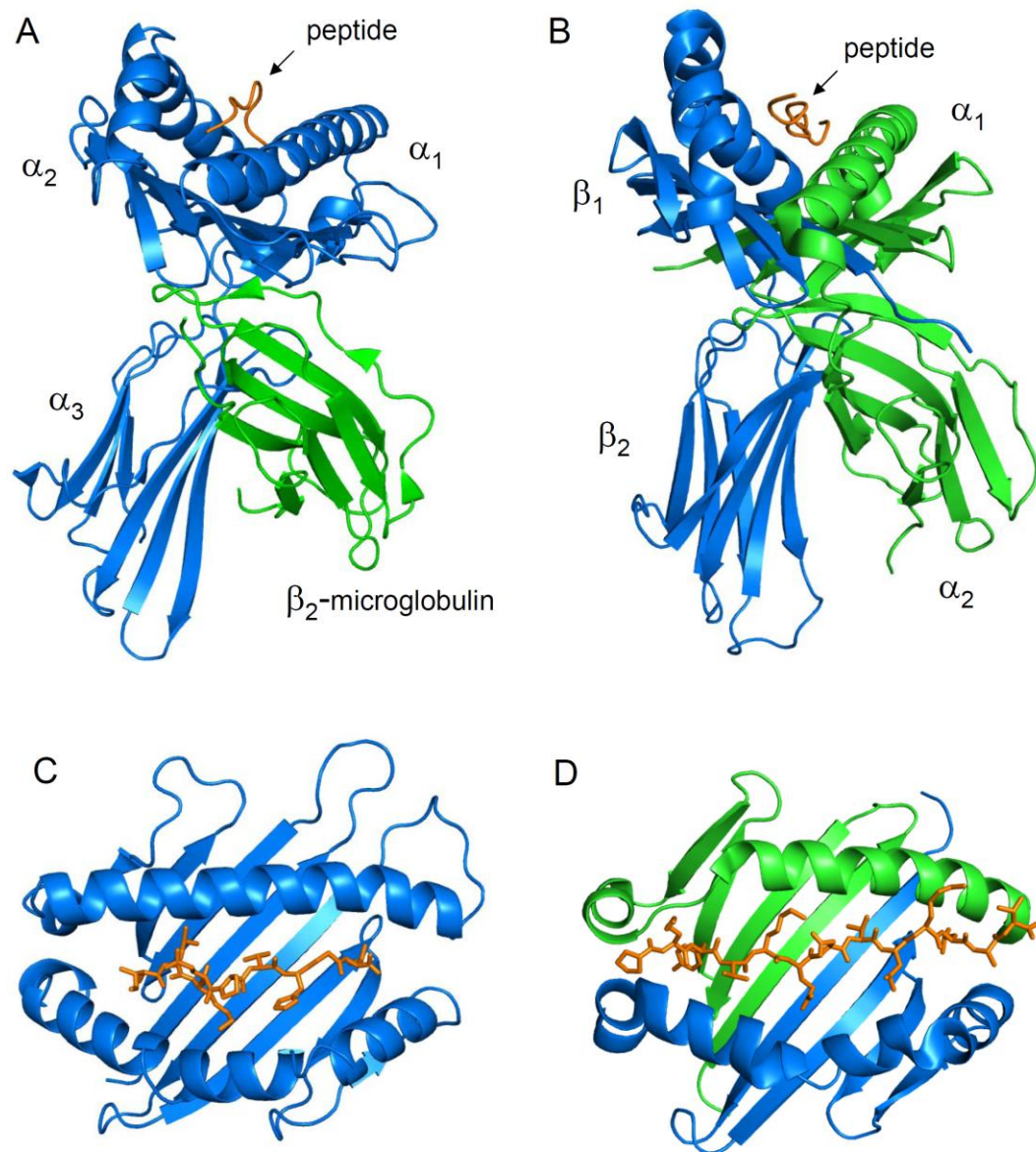


Figure 1.3: Comparison of the protein structures of MHC class I and MHC class II molecules. (A) A MHC I molecule with peptide is shown as ribbon diagram with the α chain (blue) and the β_2 -microglobulin domain (green). (B) A MHC II molecule with peptide is shown as ribbon diagram with the α chain (green) and the β chain (blue). (A, B) Different protein domains are indicated. (C, D) The peptide-binding groove of MHC molecules is composed of a β sheet building the base and two α helices flanking the peptide. Peptides are shown with N-terminus on the left and C-terminus on the right. (C, D) The peptide-binding groove is formed by part of the α chain (blue) for MHC I molecules (C) and by parts of α (green) and β chains (blue) for MHC II molecules (D). The peptide is shown in orange as ribbon diagram (A, B) or as stick model (C, D). To display the models of MHC I and MHC II molecules structures of A2 (PDB: 3HLA) and DR1 (PDB: 1DLH) were used, respectively.

How are peptides presented by MHC II molecules?

As MHC molecules have to present peptides with various sequences arising from a wide range of different pathogens their binding patterns have to be quite distinct from receptors which bind only one specific peptide. Thus, on the one hand the binding groove has to target common peptide features to accommodate different peptides and on the other hand has to build tight and specific interactions to form a long-lasting individual complex. Therefore, peptides are bound in an elongated orientation enabled by two major interactions between peptide and MHC molecule.

First, a set of conserved hydrogen bonds between residues of the MHC molecule and the peptide backbone fix the peptide along the groove. In the case of MHC II molecules, conserved amino acids of the $\alpha 1$ (Phe51, Ser53, Asn62, Asn69 and Arg76) and $\beta 1$ domain (Trp61, His81 and Asn82) form 12 hydrogen bonds to the peptide backbone which are located close to the peptide N-terminus (6), the middle part of the peptide (2) and the peptide C-terminus (4) (figure 1.4, B). The second main contribution to peptide-binding and alignment is the tight interaction of peptide residues with shallow and deep pockets formed by MHC molecules (figure 1.4, A, C). Peptide residues protrude into these pockets and are partially or entirely covered by residues of the MHC molecule. Peptide residues residing in deep pockets are particularly important as they provide anchor points for the peptide along the binding groove. For MHC I and MHC II molecules the binding pockets are located at fixed positions of the binding cleft. Therefore, for efficient binding peptides have to contain anchor residues at consistent positions. For MHC II molecules the binding pockets are at positions P1, P4, P6, and P9 (figure 1.4, D).

As the amino acids which form the binding pockets are highly polymorphic, the cavity size can vary between different MHC alleles. This divergence results in binding preference of MHC molecules for different peptides. In contrast MHC residues which form the hydrogen bond network between peptide and MHC molecules are highly conserved and as they interact with peptide backbone and not peptide side chains, these interactions target most peptides equally.

The peptide is an integral part of the MHC molecule as it stabilizes the structure. In the absence of bound peptide or chaperones, MHC I and MHC II molecules readily aggregate. This ensures that only stable MHC/peptide complexes are transported to the cell surface and MHC molecules present peptides that were processed within the cell.

Until some time ago, crystal structures of MHC II/peptide complexes had shown only one conserved N- to C-terminal orientation of the peptide with the peptide N-terminus being located in the proximity of the P1 pocket (figure 1.4, D). But recent studies showed that a CLIP peptide can also bind to an MHC II molecule (DR1) in an inverted orientation (Gunther et al., 2010). Whether this flipped orientation also applies to other peptides and MHC II molecules and whether peptides with an inverse alignment are also presented on the cell surface and recognized by T cell receptors still has to be investigated.

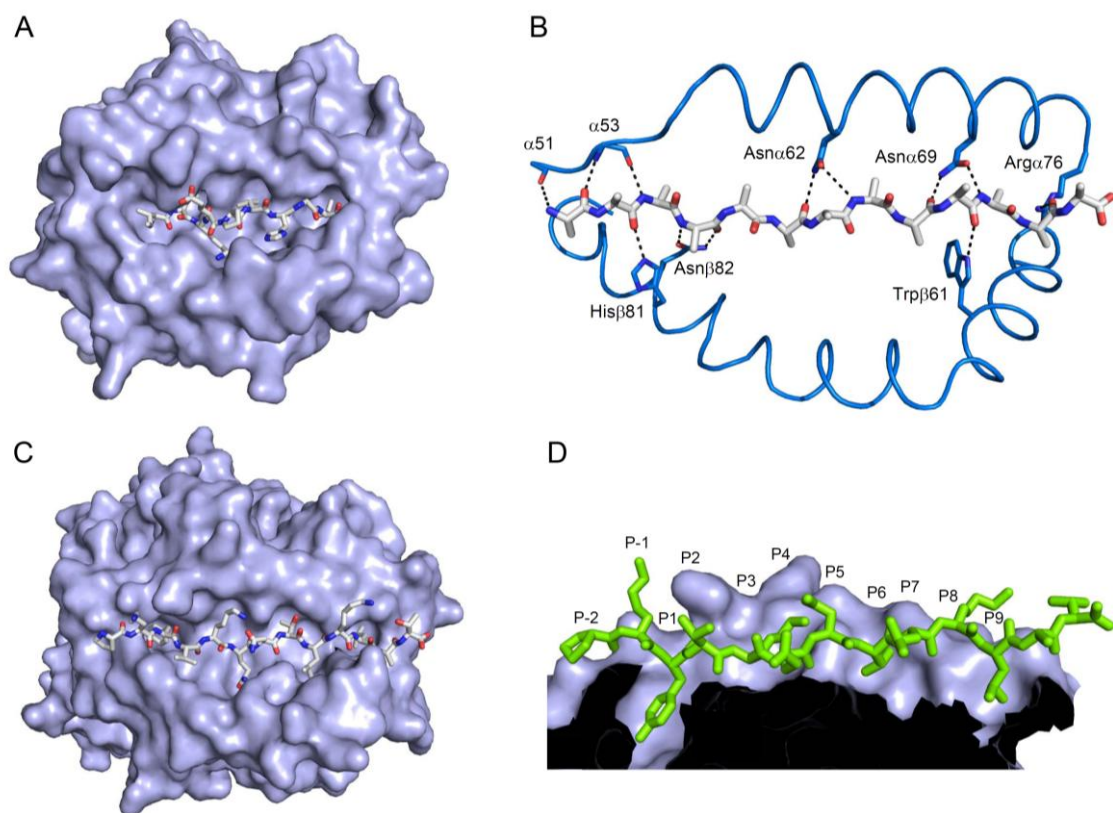


Figure 1.4: Comparison of the peptide-binding groove of MHC I and MHC II molecules and crucial peptide/MHC II interactions. (A, C) Top views of the peptide-binding grooves of a MHC I (A) and a MHC II molecule (C) are shown with the MHC molecules as surface presentation and the peptide as stick model. The peptide-binding groove of MHC I molecules is closed on both ends whereas in the peptide-binding groove of MHC II molecules the peptide termini protrude on both sides. (B, D) The two main interactions between peptide and MHC II molecule are a conserved hydrogen bond network (B) and a series of pockets filled by peptide side chains (D). (B) Helices of the α (top) and β chains (bottom) are shown as ribbon diagram (blue) and the peptide backbone as stick model with the N-terminus on the left side. (D) Cross section of the peptide-binding groove of MHC II molecules with the peptide shown as stick model (green) and the MHC II molecule as surface presentation. Peptide positions are indicated. The models of MHC I and MHC II molecules were generated using structures of A2 (PDB: 3HLA) and DR1 (PDB: 1DLH), respectively.

1.4 The role of HLA-DM in the MHC class II presentation pathway and comparison to the peptide loading complex of MHC class I molecules

As already mentioned above, HLA-DM (DM, H-2M in mice) plays a crucial role in peptide loading of MHC II molecules and therefore can modify the peptide repertoire presented to T cells. DM was discovered by analysis of mutant human B cell lines with a defect in antigen presentation (Kelly et al., 1991). Although MHC class II molecules in these cells assembled correctly and entered the endosomal pathway they failed to bind internalized peptides and mostly presented only CLIP on the cell surface. Later, it was discovered that these cells had a genetic defect in the DM β gene (Morris et al., 1994). At that time it was proposed that DM plays an important role in peptide-loading of MHC II molecules, which was confirmed later by experiments *in vitro* and *ex vivo* (Denzin and Cresswell, 1995; Sloan et al., 1995).

DM is directed to the MHC class II-containing compartment through a targeting sequence in the cytoplasmic tail of the β chain (Marks et al., 1995). But in contrast to MHC II molecules, DM also carries a cytoplasmic internalization signal which prevents it from being stably expressed on the cell surface (Lindstedt et al., 1995). DM fulfills several functions during peptide loading and exchange of MHC II molecules. First, it catalyzes the release of CLIP peptide which occupies the binding groove of MHC II molecules following partial proteolysis of the invariant chain (Denzin and Cresswell, 1995). During this process DM also assists binding of other peptides to MHC II molecules that are present in the late endosome (Sloan et al., 1995). In addition, DM stabilizes empty MHC II molecules and prevents them from aggregating (Kropshofer et al., 1996; Weber et al., 1996). Lastly, by continuous binding and rebinding to the MHC II/peptide complex DM facilitates the removal of weakly bound peptides and allows peptides with higher affinity to bind, ensuring that predominantly stable MHC II/peptide complexes are transported to the cell surface (Kropshofer et al., 1996). This function of DM is also referred to as ‘editing’ of the peptide repertoire.

Some of these key principles are similar to the peptide loading process of MHC I molecules (figure 1.5). As mentioned above, MHC I molecules are loaded with peptides in the ER after their assembly. Compared to MHC II molecules, there are more proteins involved in the process of peptide loading of MHC I molecules, including chaperones for protein folding. After assembly of the MHC I heavy chain with β_2 -microglobulin the

hetero-dimer associates with the multi-subunit peptide loading complex (PLC) in the ER (Wearsch and Cresswell, 2008). One of the key components of the PLC is tapasin, which directly binds to the MHC I molecule and also makes contact with the TAP peptide transporter (Sadasivan et al., 1996). Furthermore, tapasin forms a covalently linked dimer with ERp57, which interacts with calreticulin, which in turn is bound to the MHC I molecule through a glycosylation site (Wearsch and Cresswell, 2007, 2008). It has been shown that the disulfide-linked dimer of tapasin and ERp57 is sufficient for peptide exchange and might have a similar function to DM in the MHC II pathway (Peaper et al., 2005; Wearsch and Cresswell, 2007). Similarly to what has been observed for DM and MHC II molecules, the covalent tapasin-ERp57 dimer stabilizes MHC I molecules in a peptide-receptive conformation and greatly enhances peptide-binding. It also favors binding of high-affinity peptides which are then displayed on the cell surface. Furthermore, binding of high-affinity peptide induces dissociation of MHC I molecules from the PLC (Wearsch and Cresswell, 2007), in the same way that the complex between MHC II molecules and DM is disrupted by binding of high-affinity peptide (Anders et al., 2011).

These are striking similarities between the peptide loading processes of MHC I and MHC II molecules even though peptide exchange is facilitated by different proteins and in distinct cellular compartments (Sadegh-Nasseri et al., 2008; Wearsch and Cresswell, 2008). However, in both cases the peptide to be exchanged is buried deep within the binding groove, and MHC I and MHC II molecules are highly unstable in the absence of any peptide (Germain and Rinker, 1993; Wearsch and Cresswell, 2008), which seem to be similar preconditions and likely require similar functions.

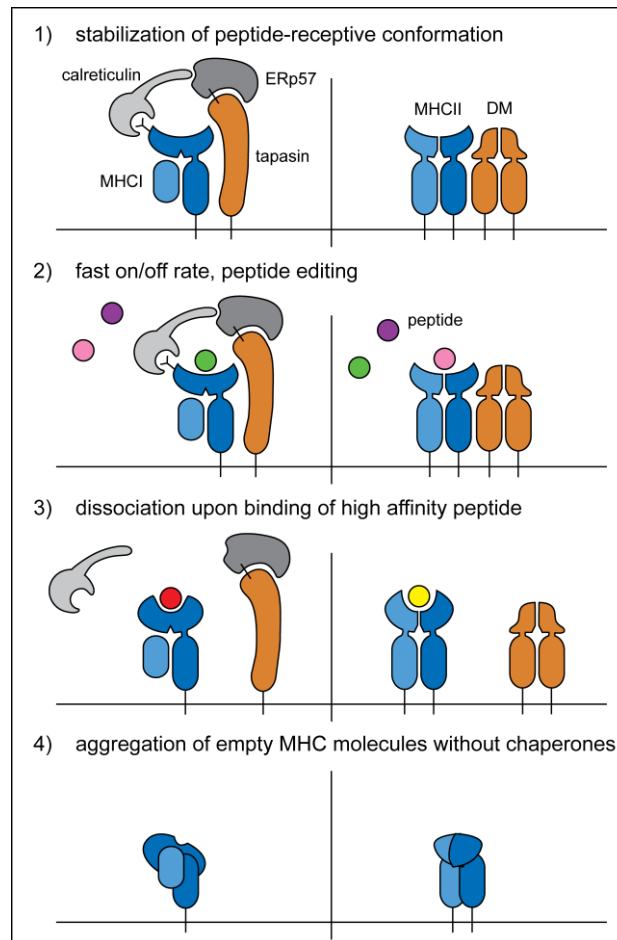


Figure 1.5: Similarities between the peptide loading mechanisms facilitated by MHC I and MHC II molecules. Peptide loading occurs in different compartments for MHC I (ER) and MHC II (endosomes-lysosomes) molecules, but key features of the peptide loading/editing process are similar, as illustrated here. Empty MHC I molecules become part of a peptide-loading complex involving tapasin, ERp57 and calreticulin; tapasin links the peptide loading complex to the peptide transporter TAP (not shown). Tapasin is covalently linked to ERp57 and this hetero-dimer performs a peptide editing function. Empty MHC I and MHC II molecules are highly unstable in the absence of peptide, and peptide loading requires chaperones that stabilize the empty state in a functional form. In both cases, binding of high-affinity peptides results in release from the respective chaperones. (Schulze and Wucherpennig, 2012)

1.5 Structure of HLA-DM and lateral interaction with HLA-DR

As expected from the high overall sequence similarity (Cho et al., 1991; Kelly et al., 1991) DM is a hetero-dimer with an overall fold and domain organization similar to that of classical MHC II molecules (Mosyak et al., 1998). The major difference compared to MHC II molecules lies in the peptide-binding groove. The α helices of the $\alpha 1$ and $\beta 1$ domains of DM, which build the rim of the peptide-binding cleft for MHC II molecules, are closer together and make several contacts which preclude peptide-binding (figure 1.6, A, C). At both ends of the cleft, bulky hydrophobic residues protrude into the

groove displaying a small and a large hydrophobic cluster where the N- and accordingly C-termini of the peptide normally bind to MHC II molecules. In the middle part, polar and charged residues form a deep pocket which is very different from the peptide-binding pockets of classical MHC II molecules (figure 1.6, B, C). Whether this pocket has a function or binding capability is unknown. The two outer hydrophobic clusters and the central polar cavity are divided and flanked by three distinct kinks formed by the $\beta 1$ domain α helix. The conformation of the closed groove of DM shows similarities to the structure of the neonatal Fc receptor, which binds immunoglobulin, has a protein fold similar to MHC I molecules, and also contains a collapsed peptide-binding groove (Mosyak et al., 1998). Aside from minor differences in loop conformations, the $\alpha 2$ and $\beta 2$ domains of DM are very similar to the corresponding domains of classical MHC II molecules.

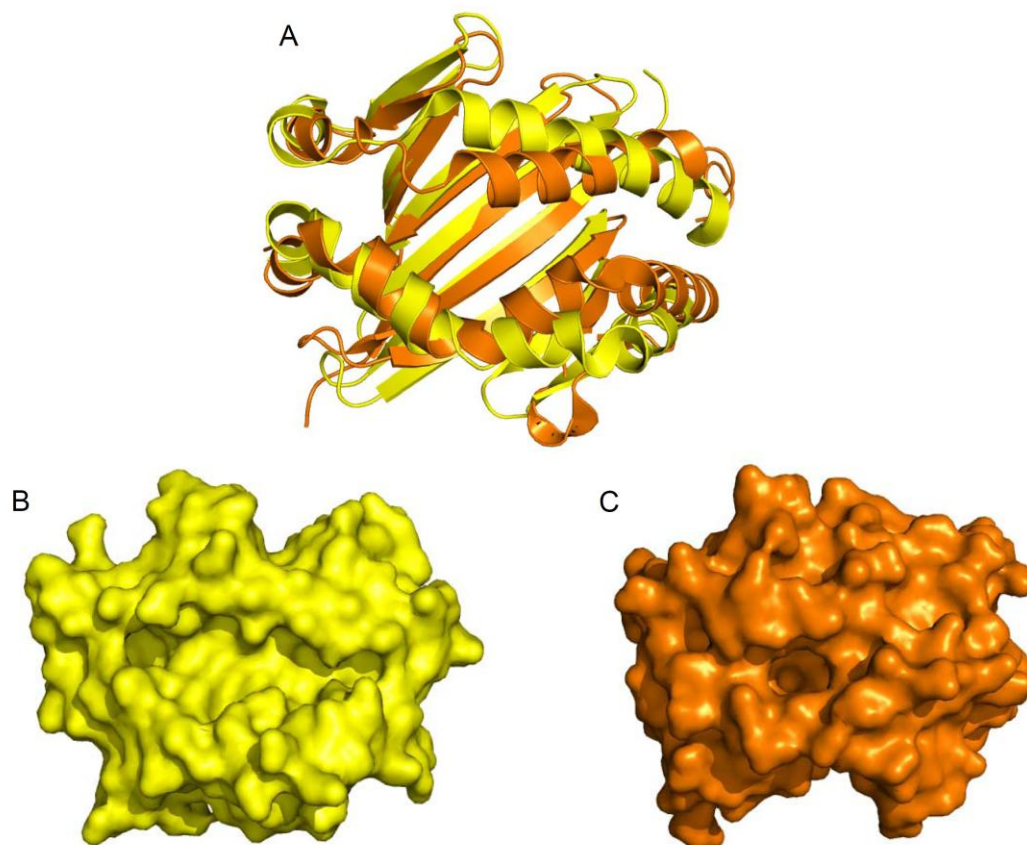


Figure 1.6: Comparison of the protein structures of DM and MHC II molecules. (A) An overlap of the $\alpha 1/\beta 1$ membrane-distal domains of DM (orange) and MHC II molecules (yellow) is shown as ribbon diagram. (B) Top view of the peptide-binding groove of MHC II molecules is displayed as surface representation. (C) Top view of the $\alpha 1/\beta 1$ membrane-distal domains of DM is depicted as surface representation revealing a deep pocket in the center. Models are based on crystal structures of DM (PDB: 2BC4) and DR1 (PDB: 1DLH).

Interestingly, residues that are part of the tight interactions between the α helices of the $\alpha 1$ and $\beta 1$ domains are conserved among human DM and homologous murine, rabbit and bovine sequences. However, residues that are pointing away from this interface are variable and show limited polymorphism (Mosyak et al., 1998). This stands in contrast to classical MHC II molecules that show extensive polymorphism of amino acids that are located within the peptide-binding groove, which allows capturing a variety of peptides.

Mutagenesis studies of DM and MHC II molecules (Doebele et al., 2000; Pashine et al., 2003) revealed a lateral binding site between both molecules (figure 1.7) which comprises part of the concave side of DM and the DR side close to the peptide-binding groove where the peptide N-terminus binds.

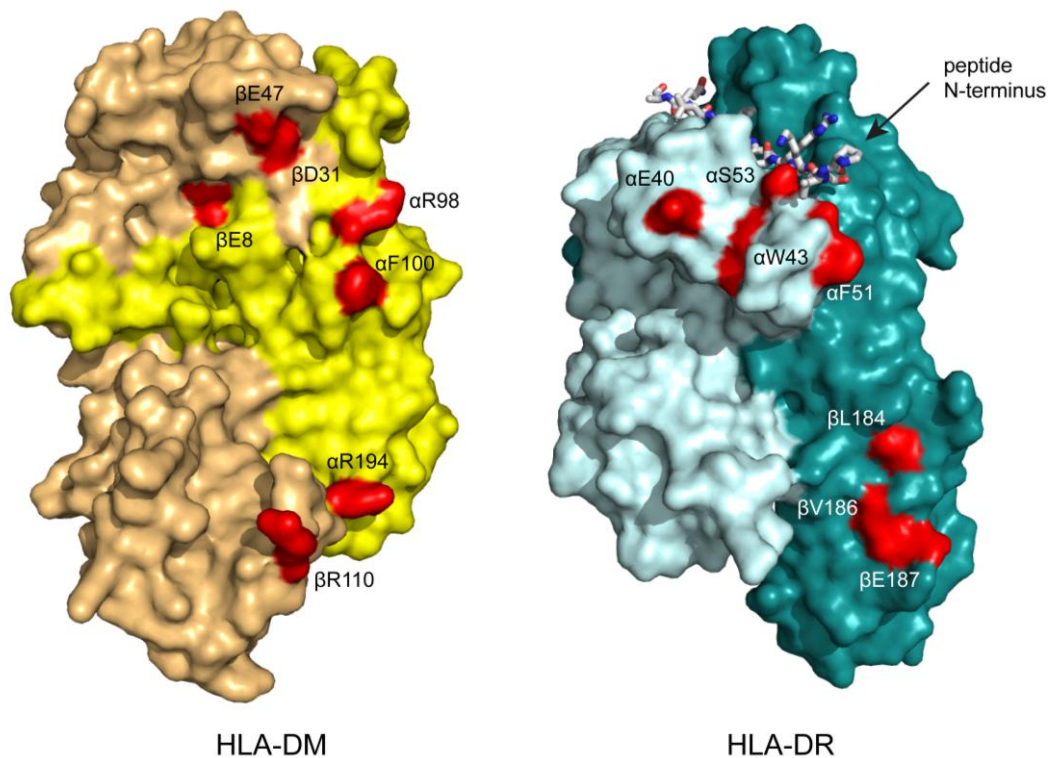


Figure 1.7: Lateral interaction surfaces of HLA-DM and HLA-DR molecules. Contact residues are colored red on both proteins, based on mutations that substantially reduced susceptibility of DR/peptide complexes to DM (Anders et al., 2011; Doebele et al., 2000) or the activity of DM (Pashine et al., 2003). Mutants that only showed small effects or introduced a glycosylation site (and thereby steric hindrance) were omitted. A functionally important cluster is located in the DR $\alpha 1$ domain close to the peptide N-terminus; a second cluster is present in the membrane proximal DR $\beta 2$ domain. DM also shows two clusters of contact residues, located in the membrane-distal $\alpha 1/\beta 1$ domains and the membrane proximal $\alpha 2/\beta 2$ domains. DM chains are colored yellow (DM α) and orange (DM β), DR chains light blue (DR α) and turquoise (DR β). Models are based on crystal structures of DM (PDB: 1HDM and 2BC4) and DR3/CLIP (PDB: 1A6A). (Schulze and Wucherpennig, 2012)

Together with other mutagenesis studies and functional experiments (Anders et al., 2011) two clusters of interacting residues were found for both molecules, respectively (figure 1.7). For DR, one cluster is present in the DR α 1 domain close to the peptide N-terminus and a second cluster is located in the membrane-proximal DR β 2 domain. The contact residues for DM are located in the membrane-distal α 1/ β 1 domains and the membrane-proximal α 2/ β 2 domains. The same lateral interaction surface was confirmed by functional experiments in which DM was tethered either to the peptide N- or C-terminus (Stratikos et al., 2002). Enhanced peptide release was observed with DM covalently bound to the peptide N-terminus, but not to the C-terminus. Although the overall binding site has been identified, the molecular mechanism of DM-catalyzed peptide exchange is still unknown.

1.6 Proposed mechanisms for HLA-DM-catalyzed peptide exchange

As described in the previous section, the general interaction site between DM and MHC II molecules has been identified. However, crucial residues important for peptide exchange which could elucidate how DM catalyzes peptide exchange are still unidentified. An attractive potential target for DM activity is the conserved hydrogen bond network between peptide and MHC II molecules because it is a prominent sequence-independent feature, and it has been shown that DM acts promiscuously on different DR alleles and catalyzes the exchange of various peptides (Weber et al., 1996). For example, Weber et al. discovered that the rate of enhancement of peptide dissociation catalyzed by DM is directly proportional to the intrinsic dissociation rate of a peptide from its DR molecule (Weber et al., 1996). Several studies have been already carried out investigating whether DM targets some of these conserved hydrogen bonds, but the results have been somewhat conflicting. Sadegh-Nasseri and colleagues perturbed the conserved hydrogen bond between histidine 81 of the DR β chain and peptide backbone with a histidine-to-asparagine mutation, which abolished DM enhancement of peptide dissociation (Narayan et al., 2007). The conserved residue His β 81 is located close to the peptide N-terminus and, therefore, also close to the interaction surface of DM and DR. A ‘hit-and-run’ mechanism was proposed by Sadegh-Nasseri and colleagues in which DM transiently but repeatedly interacts with a DR/peptide complex and thereby induces a conformational change leading to disruption

of the hydrogen bond between His β 81 and bound peptide and initiating peptide dissociation. However, studies by Ferrante et al. investigating the mutation His81Asn of the DR β chain showed no impairment of DM activity, excluding residue His β 81 as special target of DM activity (Ferrante and Gorski, 2010). Furthermore, in a comprehensive study, Jensen and colleagues mutated six conserved DR residues to alanines, including residue β His81. These residues normally form nine conserved hydrogen bonds with the peptide backbone (the other three conserved hydrogen bonds are between peptide and the backbone of DR α chain). No altered susceptibility to the catalytic activity of DM was found, suggesting that no single conserved hydrogen bond is directly targeted by DM catalysis (Zhou et al., 2009), leaving the role of residue His β 81 controversial.

While disruption of the hydrogen bond network between peptide and MHC II residues might not be the only target of DM it definitely plays an important role in the peptide exchange mechanism as has been shown by Stern and colleagues. Backbone amide N-methylation and truncation of the peptide allowed systematic elimination of the hydrogen bonds between peptide N-terminus and conserved DR residues including hydrogen bonds to the DR α backbone (Stratikos et al., 2004). Interestingly, elimination of the three hydrogen bonds between peptide and the DR α backbone involving residues α 51-53 increased susceptibility to DM, indicating that these hydrogen bonds might be disrupted in the MHC conformation recognized by DM.

Concluding, disruption of the hydrogen bond network to the peptide backbone is likely involved in the peptide exchange mechanism catalyzed by DM, however, additionally DM might impact the structural flexibility of the peptide-binding groove and thereby alter the interactions of peptide anchor residues with the deep pockets formed by MHC II molecules. Global conformational change in the peptide-binding groove has been previously proposed (Belmares et al., 2002) as well as direct DM interactions with and involvement of the P1 pocket (Chou and Sadegh-Nasseri, 2000; Sato et al., 2000).

1.7 HLA-DO: a negative regulator of HLA-DM

There are at least three factors that determine peptide editing activity of DM, which in turn influences the peptide repertoire presented on MHC II positive cells: the overall expression levels of DM, the extent of co-localization of DM with MHC II molecules in endosomal compartments, and the expression of another non-classical MHC II molecule, HLA-DO (DO, H-2O in mice), which seems to play an important role in modulating DM activity (Leddon and Sant, 2010).

DO is expressed in B cells, thymic epithelial cells and certain subsets of dendritic cells (Hornell et al., 2006) and its expression level is further regulated by cell maturation. The gene products of DO are structurally similar to classical MHC II molecules and even display more similarity to MHC II molecules than does DM with approximately 60% similarity compared to approximately 28% (Cho et al., 1991; Kelly et al., 1991; Servenius et al., 1987; Tonnellet et al., 1985; Trowsdale and Kelly, 1985). Similar to DM, DO genes show limited polymorphism (Inoko et al., 1985; Jonsson and Rask, 1989; Naruse et al., 1999; Naruse et al., 2002; Servenius et al., 1987; van Lith et al., 2002). But the expression pattern of DO is different from that of DM and classical MHC II molecules which are controlled by the class II transactivator (CIITA) and upregulated by the cytokine interferon- γ . Whereas the DO α chain transcription is dependent on CIITA, the DO β chain seems to be subject of tight and differential regulation independent of CIITA even though CIITA expression can still increase DO β chain expression (Nagarajan et al., 2002).

It has been shown that DO requires DM association to efficiently exit the ER and associates with DM during and after transport to the endosomal/lysosomal compartment (Liljedahl et al., 1996). Mutagenesis studies mapped the DM binding site on the DO α chain (Deshaies et al., 2005). *Ex vivo* experiments with human T cells (Denzin et al., 1997) and melanoma cell lines (van Ham et al., 1997) revealed an inhibitory role for DO illustrated by increased levels of MHC class II/CLIP complexes on the cell surface of transfectants expressing DO. *In vitro* experiments with purified DO and DM showed decreased DM activity during class II peptide loading reactions (Denzin et al., 1997; Liljedahl et al., 1998; van Ham et al., 1997). Further studies have suggested that DO inhibition of DM-catalyzed peptide exchange is dependent on pH with lower inhibitory function at pH lower than pH 5.0 (Kropshofer et al., 1998; Liljedahl et al., 1996; van

Ham et al., 2000), indicating that DO may preferentially inhibit DM activity in early endocytic compartments.

Studies in human B cell lines and primary B cells showed that DO binds to 50-70% of the available DM (Chen et al., 2002; Kropshofer et al., 1998). Association of DO and DM seems to prevent binding of MHC II molecules. Therefore, a large pool of DM may not be available for peptide editing of MHC II molecules in human B cells. An attractive model proposes that MHC II molecules and DO may compete for the same DM binding site resulting in DO indirectly influencing peptide loading of MHC II molecules.

1.8 MHC loading enhancers

Several groups of small molecules have been identified which, like DM, catalyze peptide exchange of MHC II molecules. These are referred to as MHC loading enhancers (MLE). Surprisingly, these small molecules with molecular weights of less than 500 Da accomplish a similar function as the large protein DM with a molecular weight of ~ 60 kDa. Changing the peptide repertoire presented towards CD4⁺ T cells is of great therapeutic interest and therefore much effort is put into finding a small molecule that modulates peptide presentation through the MHC II pathway. As can be seen in table 1.1, MLE exhibit various chemical properties and likely act by different mechanisms.

alcohols

The approach of Strominger and colleagues was to identify a small molecule which could interrupt the hydrogen bond network formed between peptide and MHC II molecules and thereby facilitate peptide exchange. At first, simple alcohols such as ethanol, propanol and butanol were found to exchange CLIP peptide on DR1 and DR2 molecules (Falk et al., 2002). Introducing aromatic alcohols increased activity (Marin-Esteban et al., 2003, 2004), but high concentrations (10^{-4} – 1 M) are still required for activity.

di-peptides

Instead of altering the strength of hydrogen bonds between peptide and MHC II molecules, the strategy of Falk, Roetzschke and colleagues was to target the P1 pocket of DR1 which anchors the N-terminal part of the peptide. The di-peptide Tyr-Arg was found to accelerate peptide exchange in DR1 molecules (Gupta et al., 2008). Assuming the tyrosine binds in the P1 pocket, the N- and C-termini of the di-peptide were chemically modified with the intent to optimize putative hydrogen bonds which resulted in increased activity with effective concentrations of 10^{-4} to 10^{-3} M. Furthermore, mutations in the P1 pocket affected the activity of the di-peptides, supporting the hypothesis that the di-peptide targeted the area of the P1 pocket.

adamantyl compounds

The adamantyl compounds were found by Roetzschke, Falk and colleagues using an ELISA-based assay immobilizing DR1 molecules and measuring peptide loading by detection of biotinylated HA peptide (Hopner et al., 2006). Enhanced peptide loading was observed in the absence of DM and most of the activity could be attributed to the adamantane group. Similar to the di-peptides described above, the adamantyl compounds are selective for MHC II alleles with a large P1 pocket versus a smaller P1 pocket, indicating that the adamantyl compounds may act by binding directly to that site.

inorganic metal complexes

Another group of MLE was found by a high-throughput approach, screening for small molecules that remove peptides from MHC II molecules. Two metal complexes were found, cis-platin and carboplatin, which are typically used as chemotherapy agents, and also related metal complexes with palladium and gold showed activity (De Wall et al., 2006). The different metal complexes have a square-planar configuration with the metal ion acting as a weak Lewis acid which might suggest interactions with sulphur atoms of cysteines or methionines (De Wall et al., 2006). The most potent metal complex, cis-platin, is active in the range of 10^{-6} – 10^{-5} M.

small molecule enhancers of HLA-DM

In another high-throughput approach around 100,000 compounds of drug-like small molecule libraries were screened by Wucherpfennig and colleagues (Call et al., 2009;

Nicholson et al., 2006). By tracking fluorescence polarization of a labeled peptide bound to soluble DR2 in the presence of soluble DM, four small molecules were found that substantially enhanced peptide exchange ($10^{-6} - 10^{-4}$ M). Two of the small molecules also showed activity in the absence of DM although to a smaller extent. Microdialysis experiments indicated direct binding to DM for one of the small molecules (M19, see table 1.1) being active only in the presence of DM. Binding to both proteins, DM and DR2, was observed for a small molecule (F15, see table 1.1) that showed activity even without DM. Furthermore, three of the four small molecules were sensitive to DM mutations localized at the hydrophobic ridge at the top of the concave side of DM, which is very likely part of the interaction surface of DM and DR (see figure 1.7), indicating that some of the small molecules may support the DM-DR interface by contacting residues of both proteins.

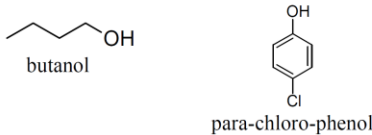
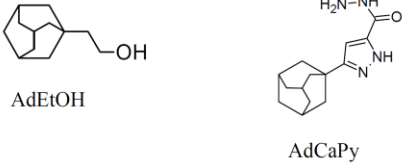
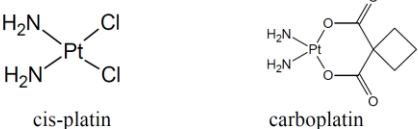
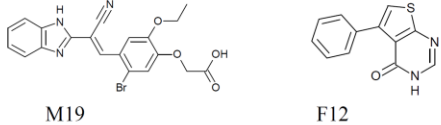
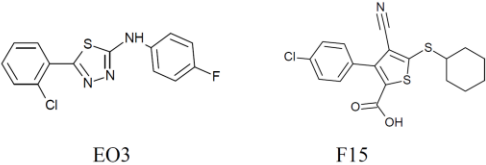
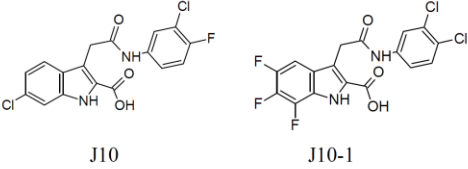
J10 and its analogs

Among the most potent loading enhancers of MHC II molecules acting in the absence of DM are J10 and its analogs discovered by Wucherpfennig and colleagues by a high-throughput screening (Call et al., 2009). The J10 series of molecules is active on all tested DR alleles (DR1, DR2, DR4) and showed no sensitivity to polymorphism involving the P1 pocket, suggesting the peptide exchange mechanism of J10 may be distinct from the mechanism of the di-peptides and the adamantyl compounds described above. Extensive medicinal chemistry improved the activity of the small molecules used at a concentration of $10^{-5} - 10^{-4}$ M and enhancement of peptide presentation has been demonstrated both *in vitro* in a cellular assay and *in vivo*.

In general, MLE are remarkably diverse and might use distinct mechanisms to influence peptide exchange. However, it is likely that the small molecules interfere either directly or allosterically with one of the two main interactions between peptide and MHC II molecules, i.e. conserved hydrogen bond network between peptide and MHC II residues and occupancy of a series of deep pockets formed by MHC II residues.

During these studies, the peptide exchange mechanism of J10 and its analogs was investigated in the absence of DM applying X-ray crystallography and NMR spectroscopy as can be seen in chapter I. The J10 series of small molecules has a strong potential for use as adjuvant for peptide vaccination and in therapeutics due to the low concentration needed for activity and showed already promising results *in vivo*.

Table 1.1: MHC loading enhancers (MLE). MLE are small molecules that influence peptide-binding by MHC II molecules. Representative structures from each reference are shown. (adapted from (Call, 2011)).

MLE group	structure (eg.)	effective concentration range	functional outcome	
alcohols	 <p>butanol</p> <p>para-chloro-phenol</p>	mM	peptide exchange	Falk et al., <i>JBC</i> , 2002. Marin-Esteban et al., <i>J Auto Immun</i> , 2003. Marin-Esteban et al., <i>JBC</i> , 2004.
dipeptides + modified dipeptides	Tyr-Arg Ac-Tyr-Arg-NH ₂ Ac-Phe-Arg-NH ₂	mM	peptide exchange	Gupta et al., <i>PLoS One</i> , 2008.
adamantyl compounds	 <p>AdEtOH</p> <p>AdCaPy</p>	mM – μ M (allele-specific)	peptide exchange	Hoepner et al., <i>JBC</i> , 2006. Dickhaut et al., <i>PLoS One</i> , 2009.
inorganic metal complexes	 <p>cis-platin</p> <p>carboplatin</p>	μ M	peptide removal	De Wall et al., <i>Nature Chem Bio</i> , 2006.
various small molecules	 <p>M19</p> <p>F12</p>	μ M	peptide exchange (only when DM is present)	Nicholson et al., <i>J Immunol</i> , 2006.
various small molecules	 <p>EO3</p> <p>F15</p>	μ M	peptide exchange (optimal in the presence of DM)	Nicholson et al., <i>J Immunol</i> , 2006.
J10 + analogs	 <p>J10</p> <p>J10-1</p>	μ M	peptide exchange	Call et al., <i>J Immunol</i> , 2009.

1.9 Scopes and objectives of this study

This doctoral work aimed to elucidate molecular details of the peptide exchange mechanism of MHC II molecules catalyzed by the protein DM and the synthetic small molecule J10. To address structural and dynamic aspects of this complex process various methods were applied including surface plasmon resonance (SPR), X-ray crystallography and NMR spectroscopy.

Surface plasmon resonance experiments were carried out to investigate DM binding to high-affinity MHC II/peptide complexes. Recent studies have shown that for DM binding to occur, the N-terminal part of the peptide has to leave the binding groove. This partial peptide release could be due to spontaneous peptide motion which should be enhanced at higher temperature and implies DM binding to all MHC II/peptide complexes even if to a small extent. To test this hypothesis SPR experiments were carried out at different temperatures investigating whether DM binding can be induced to high-affinity MHC II/peptide complexes previously exhibiting no or only little DM susceptibility.

Crystallographic studies were applied to reveal the MHC II conformation with a partially empty peptide-binding groove, which could determine whether release of the peptide N-terminus induces conformational changes of the MHC II structure. Knowing how the MHC II conformation adapts to loss of crucial interactions between peptide and MHC II molecule could display important molecular details of the peptide exchange mechanism. Furthermore, using X-ray crystallography we aimed to identify the binding site of the small molecule J10, which would allow structure based design to further improve affinity and activity of the MHC loading enhancer J10.

Applying NMR spectroscopy, the dynamics of the peptide bound to MHC II molecule were explored in solution. To date, the molecular understanding of the MHC II/peptide complex is mainly deduced from the static image given by crystal structures. Investigating MHC II/peptide complexes in solution could advance this understanding by taking the dynamics of the complex and especially peptide mobility into account. Furthermore, using the NMR approach, peptide release facilitated by the small molecule J10 was followed in solution to explore the peptide exchange mechanism catalyzed by J10.

2 Chapter I: Investigating enhanced peptide exchange of MHC class II molecules by the small molecule catalyst J10

2.1 Introduction

Peptides presented by MHC II molecules on the cell surface play a pivotal role as they can evoke different immune responses upon interaction with CD4⁺ T cells which can lead to antibody production (Vinuesa et al., 2005), cell destruction by cytotoxic T cells (Behrens et al., 2004) or formation of CD4⁺ regulatory T cells (Sakaguchi, 2010). Actively modifying the repertoire of presented peptides is therefore of interest for various medicinal applications including peptide based vaccination (e.g. therapeutic cancer vaccination) and treatment with peptide immunomodulators (e.g. Copaxone used for treatment of multiple sclerosis). However, the efficiency with which administered peptides are loaded onto MHC II molecules is usually very low, with the therapeutic peptide often proteolytically degraded before it can be loaded onto a MHC II molecule. Therefore, enhancing MHC II loading could improve the efficacy of peptide-based therapeutics.

Our lab previously identified a small molecule (Nicholson et al., 2006) called J10 that significantly accelerates the rate of peptide loading onto DR molecules in the absence of DM. Different from previously discovered MHC II loading enhancers (MLE) with activities at millimolar concentrations, J10 is active in the low micromolar range, which makes it more suitable as a potential adjuvant for peptide vaccination and immunotherapies. Different from DM, J10 catalyzes peptide exchange also at neutral pH although it has optimal activity at an acidic pH, like DM. Catalyzing peptide exchange at neutral pH could be advantageous if J10 is used as adjuvant for peptide therapeutics as it could load peptides on MHC II molecules present in early endosomes and on the cell surface. Furthermore, it was shown that J10 enhances peptide presentation by MHC II molecules *in vivo* (Call et al., 2009). Extensive medicinal chemistry has been already carried out which improved the activity of the small molecule. However, as J10 and its derivatives have high potential as adjuvant for peptide therapeutics and might reveal a highly peptide receptive DR conformation also relevant for the peptide exchange mechanism of DM, it is of great interest to understand how the small molecules catalyze peptide exchange.

Two methods were applied to investigate the peptide exchange mechanism of J10; first, X-ray crystallography to explore the binding site of the small molecule, and second, NMR spectroscopy to investigate peptide release catalyzed by the small molecule in solution. At first, attempts to crystallize J10 derivatives (J10-1, J10-12, see figure 2.1) together with the MHC II/peptide complex DR2/MBP were carried out using co-crystallization and ligand soaking. Identification of the specific binding site of J10 would help to design small molecules with a higher affinity and therefore higher potency for potential therapeutic applications. To investigate the effect of J10 binding on DR2/MBP in solution, NMR experiments were performed. HSQC spectra of isotope labeled MBP peptide in complex with DR2 were measured before and after addition of a J10 derivative. By comparing the HSQC spectra chemical shifts and intensity changes could be detected and together with the peak assignment could provide information about which part of the peptide is affected by small molecule binding. For isotope labeling, the peptide had to be expressed separately from DR2 and subsequently quantitatively exchanged against an already bound lower-affinity peptide (in this case CLIP peptide). The most active J10 derivative was chosen for small molecule addition (J10-1, see figure 2.1). Furthermore, to qualitatively measure binding of J10 to low- and high-affinity MHC II/peptide complexes ^{19}F -NMR experiments of a J10 derivative were performed (J10-11, see figure 2.1).

The application of these two complementary methods was utilized to gain a comprehensive molecular understanding of the MHC II/J10 interactions and their interplay with peptide-binding. The findings could guide further small molecule design as well as provide new information about peptide-binding to and release from MHC II molecules in general.

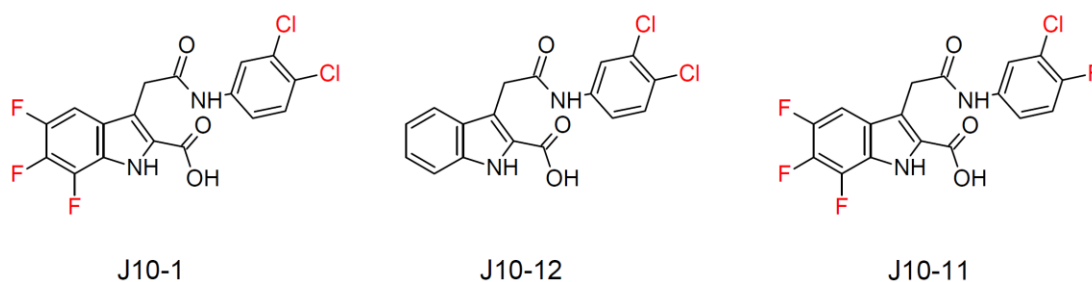


Figure 2.1: Chemical structures of the most active J10 derivatives enhancing MHC II loading. From right to left the activity of the small molecules increases. The small molecules J10-1 and J10-12 were used for co-crystallization trials. NMR experiments with isotope-labeled MBP peptide were carried out using the small molecule J10-1 and ^{19}F -NMR spectra were collected of the small molecule J10-11.

2.2 Materials and Methods

2.2.1 Preparation and crystallization of HLA-DR2/MBP in the presence of J10-1 and J10-12

Soluble DR2/MBP was expressed in *Sf9* insect cells using the baculovirus system (pAcDB3 plasmid with BaculoGold Baculovirus; BD Biosciences). The MBP (85-99) peptide (ENPVVHFFKNIIVTPR) was covalently linked to the N-terminus of the DR β chain with a thrombin-cleavable linker. The hydrophobic transmembrane regions of DR α and DR β were replaced with leucine zipper dimerization domains from the transcription factors Fos and Jun (Kalandadze et al., 1996). The protein was purified by affinity chromatography using mAb L243 (American Type Culture Collection). The leucine zipper dimerization domains were cleaved with V8 protease, and for some DR2/MBP complexes the peptide linker was cut with thrombin. The protein was further purified by anion exchange chromatography.

For co-crystallization experiments DR2/MBP was concentrated to ~ 10 mg/mL and incubated with 2 mM J10-1 or 2 mM J10-12 at 25 °C or 37 °C. Crystals were obtained at 18 °C in 100 mM glycine, pH 5.1-5.4, 14-18% PEG 6000 and 20 mM or 50 mM sodium acetate using the hanging drop method. For soaking experiments the crystals were transferred into a solution containing the crystallization conditions and 2 mM J10-1 or 2 mM J10-12, crystals were incubated at 25 °C for 4 h. Crystals were flash cooled in liquid nitrogen using 30 % glycerol or 35 % ethylene glycol as cryoprotectant.

Diffraction data were collected on beamline X25 at the National Synchrotron Light Source (Brookhaven Laboratories, Upton, NY, USA) with a resolution of up to 3 Å. Data were processed with HKL2000 (Otwinowski and Minor, 1997). DR2/MBP crystallized in the hexagonal space group P3₁ with unit cell dimensions $a = b = 118.6$ Å, $c = 75.4$ Å and two molecules per asymmetric unit. The structure was determined by molecular replacement with the program MOLREP (Vagin and Teplyakov, 2010) using the already solved DR2/MBP structure (PDB: 1BX2, (Smith et al., 1998)) as a search model. For structure refinement the program CNS (Brunger, 2007; Brunger et al., 1998) was used. Manual model building was carried out in O (Jones et al., 1991) and COOT (Emsley and Cowtan, 2004). To model the small molecules into observable electron density coordinates and molecular topologies of the small molecules were generated

with the ProdrG server (Schuttelkopf and van Aalten, 2004). To assess the accuracy of the crystal structure the statistical quantities R_{free} and R_{work} were used (Brunger, 1992).

2.2.2 Preparation of isotope labeled MBP peptide

The 15 amino acid peptide (ENSVVHFFKNIVTSR) was expressed as a C-terminal in-frame fusion to the trpLE sequence with an N-terminal 9-His tag in the pMM-LR6 vector (gift from S. C. Blacklow, Harvard Medical School, Boston). The trpLE fusion protein (Staley and Kim, 1994) contains the *E. coli* trp leader polypeptide L, the *E. coli* trp polypeptide E with the deletion LE 1413 (Kleid et al., 1981; Miozzari and Yanofsky, 1978) and the T7 promoter-operator sequence allowing high levels of transcription into mRNA (Studier et al., 1990). Furthermore the trpLE fusion protein directs the expression of the protein into insoluble inclusion bodies which reduces toxicity.

Transformed *E. coli* BL21(DE3) cells were inoculated into 1 L M9 minimal medium (1 liter: 4 g glucose, 1 mL 2 M MgSO_4 , 1 mL 0.1 M CaCl_2 , 40 mL Centrum multivitamins solution, 1 g NH_4Cl , 6 g Na_2HPO_4 , 3 g KH_2PO_4 , 0.5 g NaCl) with one or more stable isotope labels. Cultures were grown at 37 °C to an absorbance of ~ 0.6 at 600 nm and were induced at 37 °C with 300 μM isopropyl β -D-thiogalactopyranoside. NH_4Cl and glucose of the M9 minimal media were replaced with $^{15}\text{NH}_4\text{Cl}$ and ^{13}C -glucose (Cambridge Isotope Laboratories), respectively, to label the peptide with the stable isotopes ^{15}N and ^{13}C . Deuteration of the peptide required bacterial growth in D_2O . As bacterial growth is slow in D_2O the level of D_2O was gradually adjusted by transferring the bacterial culture from media prepared with 50% D_2O to media with 80% and finally 100% D_2O .

Inclusion bodies were extracted with 6 M guanidine HCl, 50 mM Tris (pH 8.0), 200 mM NaCl, 1% Triton X-100, and 5 mM 2-mercaptoethanol. The cleared lysate was bound to a Ni^{2+} -affinity column (Sigma) and washed with five column volumes urea buffer (8 M urea, 50 mM Tris, pH 8.0, 200 mM NaCl) under reducing conditions (5 mM 2-mercaptoethanol) and five column volumes under non-reducing conditions. After additional washing with water the protein was eluted with pure formic acid. Water was added to the eluted protein fractions until a formic acid concentration of 70% was obtained. As a methionine had been introduced between the peptide sequence and the fusion protein, both components could be separated by chemical cleavage using CNBr. 0.2 g CNBr for every 1 mL formic acid/protein solution was added and incubated at

room temperature for 1 h with exclusion of light and oxygen using a nitrogen stream. The cleavage rate was monitored using SDS-PAGE.

CNBr was removed by dialysis against water using regenerated cellulose membranes (MWCO 1000 Da). The dialyzed solution was neutralized. After precipitation of the cleaved trpLE fusion partner the supernatant which contained the peptide was shock frozen using liquid nitrogen and subsequently lyophilized. The lyophilized peptide was dissolved in 50% TFA, loaded onto a C8 column and separated on a gradient of 5%-95% acetonitrile (0.1% TFA) over 15 column volumes. The purified peptide was identified by mass spectrometry. Peptide fractions were lyophilized and dissolved in water to prepare a 1 mM stock solution.

2.2.3 Preparation of HLA-DR2/peptide complexes

For the preparation of the various DR2/peptide complexes soluble DR2/CLIP complexes were used which had been produced using stably transfected Chinese hamster ovary (CHO) cell lines in hollow fiber bioreactors as described in (Day et al., 2003). Soluble DR2/CLIP proteins were purified via affinity chromatography with monoclonal antibody L243 (American Type Culture Collection). The CLIP peptide (PVSKMRMATPLLMQA) was covalently attached via a thrombin-cleavable linker at the N-terminus of the DR β chain. After thrombin cleavage (20 units thrombin/1 mg protein, 2 h, 30 °C) the cleaved CLIP peptide was exchanged versus the respective peptide synthesized by Peptide 2.0. For peptide exchange a 5-fold molar excess of peptide was added to cleaved DR2/CLIP (0.2 mg/mL) in 50 mM citrate buffer (pH 5.2), 100 mM NaCl and incubated overnight at 30 °C.

During the preparation of DR2 complexes carrying isotope labeled MBP peptides excess peptide was removed by size exclusion chromatography (Superose 6) after the peptide exchange reaction. During chromatography the complex was also buffer exchanged to the final buffer (10 mM Tris, pH 7.0, 100 mM NaCl) and afterwards concentrated to the final concentration used for NMR experiments.

To prepare unlabeled DR2/MBP complex used for ^{19}F -NMR experiments, MBP peptide was synthesized by Peptide 2.0 with a DNP-label at the side chain of a C-terminal lysine. For peptide loading the protocol was followed as described above with the modification of adding 50 μM of the small molecule J10-1 to the peptide exchange reaction. Free peptide was removed by size exclusion chromatography (Superose 12)

and the complex was further purified by α -DNP affinity chromatography. For ^{19}F -NMR experiments DR2/MBP and cleaved DR2/CLIP were both concentrated to a final concentration of 1-2 mg/mL and buffer exchanged against 50 mM citrate buffer (pH 5.2).

2.2.4 NMR experiments

All NMR experiments with the isotope labeled MBP peptide were conducted on Bruker spectrometers equipped with cryogenic probes and were transverse relaxation optimized (tr) (Pervushin et al., 1997). The transverse relaxation-optimized ^1H - ^{15}N -labeled heteronuclear single-quantum coherence (tr-HSQC) spectrum of ^{15}N -labeled MBP peptide was collected with 0.33 mM of labeled peptide in 20 mM citrate buffer (pH 5.2) and 10% D_2O at 30 °C with a ^1H frequency of 750 MHz and four scans were measured. The tr-HSQC spectra of isotope labeled MBP peptide in complex with DR2 were measured with a protein complex concentration of 0.35 mM or 0.6 mM in either 10 mM Tris (pH 5.2) and 100 mM NaCl or 50 mM citrate buffer (pH 5.2), both including 5% D_2O . The small molecule J10-1 was added at a concentration of 1 mM. The spectra were collected at various ^1H frequencies (600 MHz, 750 MHz, 900 MHz) at 33 °C or 37 °C using Shigemi NMR microtube assemblies (Sigma-Aldrich). For the three-dimensional, ^{15}N -selected NOESY-TROSY-HSQC experiment (^{15}N -NOESY) a mixing time of 200 ms was used in order to detect long-range nOes (nuclear Overhauser effect). ^{15}N -NOESY and tr-HNCA experiments were measured with a ^1H frequency of 750 MHz. The spectra were processed and analyzed with the programs NMRPipe (Delaglio et al., 1995), CARRA (Keller, 2004) and XEASY (Bartels et al., 1995).

The one-dimensional ^{19}F -NMR experiments of the small molecule J10-11 were conducted on a Varian spectrometer with a magnetic field strength of 11.7 Tesla at 25 °C. The concentration of the small molecule J10-11 was 250 μM in 50 mM citrate buffer (pH 5.2) and the protein complexes DR2/MBP and DR2/CLIP were added at a concentration of 11 μM . Micro NMR sample tubes (New Era Enterprises) were used into which a microcapillary (New Era Enterprises) was inserted. The sample was pipetted into the microcapillary and 1 mM TFA which was used as a standard with 5% D_2O was added between the capillary and the NMR tube. Using microcapillaries (volume 50 μL) less sample had to be used. The ^{19}F -NMR experiments were processed and analyzed using the program MestReNova (Mestrelab Research).

2.3 Results and discussion

2.3.1 Preparing and crystallizing HLA-DR2/MBP in the presence of J10 derivatives

DR2/MBP was used as MHC II/peptide complex and crystallization experiments were set up together with one of the two most active J10 derivatives, J10-1 or J10-12 (see figure 2.1). MBP peptide (residues 85-99) is part of myelin basic protein and has a high-affinity for DR2 molecules. Using fluorescence polarization (FP) assay, it had been shown that J10 and its derivatives are active on DR2/MBP and catalyze the exchange of bound MBP peptide. DR2/MBP was expressed in *Sf9* insect cells and purified by affinity chromatography. For some DR2/MBP complexes, the linker between MBP peptide and DR β chain was proteolytically cleaved, but the cleaved complex yielded no well-diffracting crystals. For co-crystallization, the concentrated DR2/MBP complex was incubated with the small molecule J10-1 or J10-12 before crystallization. Alternatively DR2/MBP crystals were soaked with one of the two small molecules. Various crystallization conditions were screened including crystallization conditions of previously crystallized DR molecules. In the end a modified condition of the crystallized DR2/MBP complex (Smith et al., 1998) yielded crystals. Crystals from co-crystallization and soaking experiments were examined with X-ray radiation and some crystals diffracted up to 2.9 Å. DR2/MBP crystallized in a hexagonal lattice and the structure was determined with molecular replacement (table 2.1).

After structure refinement the electron density was searched for extra density not accounted for by the protein into which the small molecule was manually fitted. A data set from a co-crystallization trial showed larger extra electron density close to the N-terminus of the peptide in the vicinity of residue Ser53 of the DR α chain. When the small molecule J10-12 was modeled into this electron density a small drop in R_{free} factor (Brunger, 1992) was observed after refinement. But after calculating an electron density map by omitting the small molecule and part of the DR α chain (Trp α 43 to Ser α 53) only vague and noncontinuous additional electron density appeared in this region which could be also explained by several water molecules and was not large enough to accommodate the small molecule. Therefore, the small molecule could not unambiguously be built into the electron density.

Table 2.1: Data collection and refinement statistics of DR2/MBP. The data set was collected at beamline X25 at the National Synchrotron Light Source (Brookhaven Laboratories, Upton, NY, USA). The crystal was grown in 100 mM glycine (pH 5.2), 15 % PEG 6,000 and 20 mM sodium acetate at 18 °C. Values in parenthesis refer to the highest resolution shell.

Data collection	
Space group	P3 ₁
Cell dimensions	
a, b, c (Å)	119.2, 119.2, 76.2
Resolution (Å)	50.0-2.90 (2.95-2.90)
R _{merge} (%)	8.4 (44.1)
I/σI	35.0 (2.5)
Completeness (%)	98.9 (90.5)
Redundancy	4.9 (2.9)
Refinement	
Resolution (Å)	42-2.90
No. unique reflections	26527 (1229)
R _{work} /R _{free} (%)	22.4/27.5
Number of atoms (ASU)	
Protein	6116
Peptide	264
Water	183
B-factors (Å²)	
Protein	83.5
Peptide	88.2
Water	85.3
R.m.s. deviations	
Bond lengths (Å)	0.008
Bonds angles (°)	1.399

2.3.2 Preparing and characterizing ¹⁵N-labeled MBP peptide

As the small molecule might have bound to only a subset of DR molecules in the co-crystal structure and might have a fast on/off rate, NMR spectroscopy was pursued to investigate small molecule binding in solution. To track MBP peptide bound to DR2 upon small molecule binding the peptide was labeled with different isotopes. For isotope labeling, the 15 amino acid long MBP peptide (ENSVVHFFKNIVTSR) was expressed separately from the DR protein (as a trpLE fusion protein). The peptide sequence corresponds to the MBP protein sequence 85-99 except that two prolines at positions three and 14 were substituted with serine. Prolines were replaced as they generate no resonances in ¹H-¹⁵N HSQC experiments due to absence of amide protons.

For the initial NMR experiments the MBP-peptide was ¹⁵N-labeled and the yield of the peptide together with the fusion protein was 140 mg per 1 liter bacterial culture. The peptide together with the fusion protein was purified following the preparation scheme shown in figure 2.2. Using SDS-PAGE it was determined that ~ 70% of the MBP-fusion protein was cleaved using CNBr. The correct mass of the purified peptide was

verified by mass spectrometry (see figure 2.3). 3 mg of purified peptide were obtained from 1 liter of bacterial culture and around 7 mg of purified ^{15}N -labeled MBP peptide were prepared.

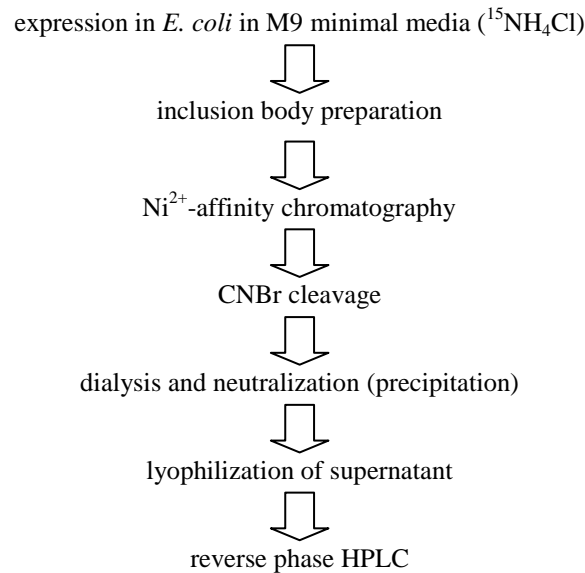


Figure 2.2: Preparation scheme of ^{15}N -labeled MBP peptide. The MBP peptide sequence together with the trpLE fusion protein was expressed in *E. coli* in M9 minimal media adding $^{15}\text{NH}_4\text{Cl}$ for isotope labeling. After inclusion body preparation the fusion protein was captured using Ni^{2+} -affinity chromatography. After elution the peptide was cleaved from the fusion protein using CNBr under acidic conditions. Upon dialyzing and neutralizing the cleaved fusion protein precipitated and the short peptide stayed in solution. The supernatant was lyophilized and the peptide was further purified by reverse phase HPLC.

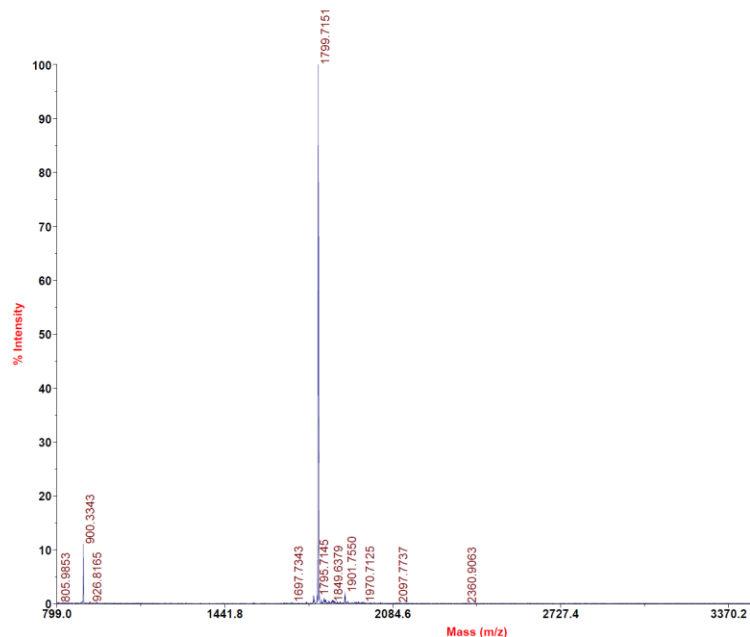


Figure 2.3: Mass spectrum of purified ^{15}N -labeled MBP peptide. The spectrum shows a single major peak at ~ 1800 Da corresponding to the mass of ^{15}N -labeled MBP peptide.

2.3.3 Preparing the complex of HLA-DR2 and ^{15}N -labeled MBP peptide

For the NMR experiments the ^{15}N -labeled MBP peptide was loaded onto DR2/CLIP molecules. DR2/CLIP had been previously expressed in CHO cells and purified by affinity chromatography. The CLIP peptide was covalently linked to the N-terminus of the DR β chain with a thrombin-cleavable linker which was cleaved before peptide exchange.

As the isotope labeled MBP peptide carried no affinity tag the DR2/ ^{15}N -MBP complex could not be separated from remaining DR2/CLIP after peptide exchange. However, MBP peptide binds with high-affinity while CLIP peptide has low-affinity for DR2 molecules. Thus, the CLIP peptide could be quantitatively exchanged with excess of ^{15}N -labeled MBP peptide present. To determine how much CLIP peptide was exchanged synthesized MBP peptide carrying a DNP-label was loaded onto cleaved DR2/CLIP molecules using the same peptide loading conditions as used for isotope-labeled MBP peptide (2.2.2). After removing free peptide by gel filtration it was determined that ~ 80% of DR2 molecules were loaded with MBP peptide measuring the absorbance at 350 nm which is specific for DNP. Furthermore, as the remaining DR2/CLIP complex was not isotope labeled it did not give rise to any NMR signal.

When ^{15}N -labeled MBP peptide was loaded onto cleaved DR2/CLIP molecules the same peptide loading protocol was followed (2.2.2) and unbound peptide separated by gel filtration. During the size exclusion chromatography the sample was also equilibrated to low salt buffer which was used for the NMR experiments. The purified DR2/ ^{15}N -MBP complex was concentrated to ~ 21 mg/mL.

2.3.4 Measuring ^1H - ^{15}N HSQC spectra of ^{15}N -labeled MBP peptide free in solution and in complex with HLA-DR2

At first a tr-HSQC spectrum of ^{15}N -labeled MBP peptide free in solution was collected. For the NMR experiments ^{15}N -labeled MBP peptide was dissolved in citrate buffer at a concentration of 0.33 mM and the spectrum measured at a ^1H frequency of 750 MHz. As can be seen in figure 2.4 the tr-HSQC spectrum of ^{15}N -labeled MBP peptide shows 13 strong peaks for the peptide backbone (see bordered peaks in figure 2.4) and some weaker peaks in the high field region of the spectrum for nitrogen-bound protons of peptide side chains (presumably asparagines and arginine). The reason why 13 instead of 15 backbone peaks were observed for the 15 amino acid long peptide is

likely due to the circumstance that the free amine at the N-terminus is in very rapid exchange with solvent and is generally not observable. This effect also sometimes broadens the signal of the backbone NH group of the second residue such that no strong signal is observed for this position either.

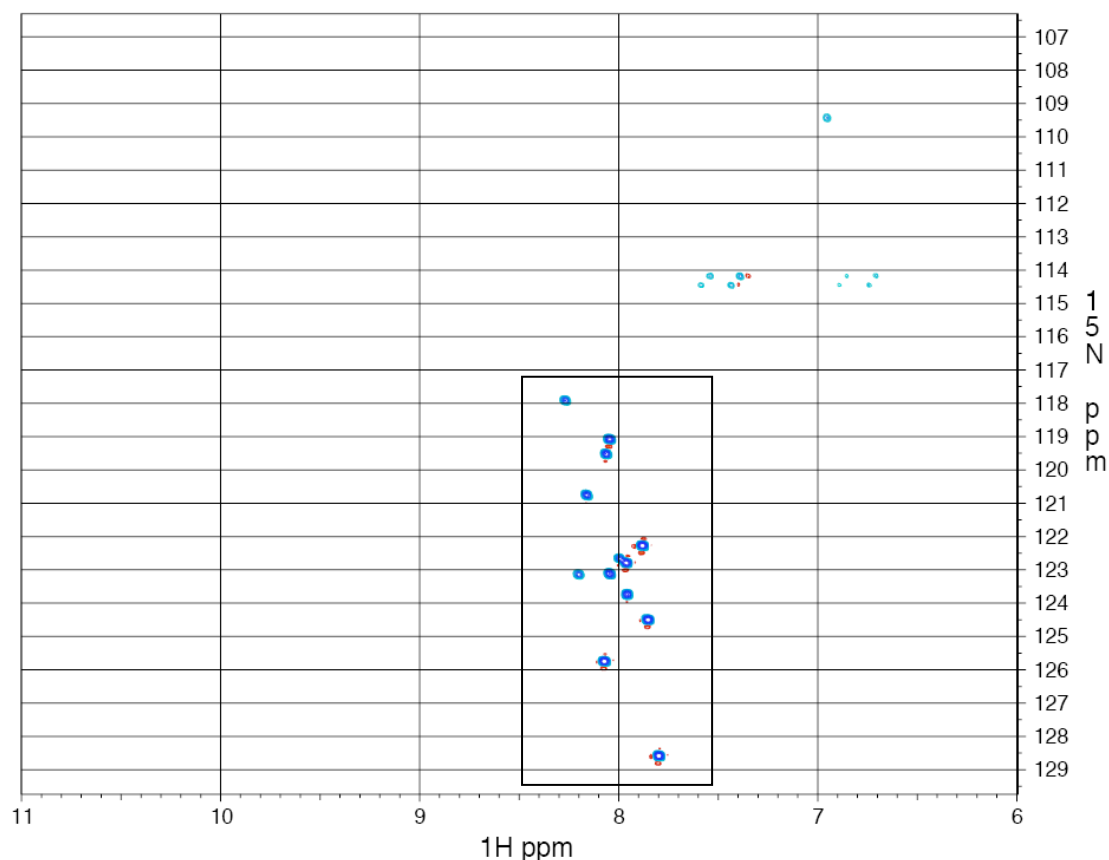


Figure 2.4: tr-HSQC spectrum of ^{15}N -labeled MBP peptide free in solution. ^{15}N -MBP peptide was dissolved in 20 mM citrate buffer (pH 5.2) at a concentration of 0.33 mM. The tr-HSQC spectrum was collected at a ^1H frequency of 600 MHz measuring four scans at 30 °C. The 13 peaks indicated by the box show 13 signals from amide protons of the peptide backbone. NH groups of the peptide backbone of the two N-terminal peptide residues likely did not give rise to signals. In the high field region of the spectrum weaker peaks of nitrogen-bound protons of peptide side chains (presumably asparagines and arginine) can be seen.

Next a tr-HSQC spectrum of ^{15}N -labeled MBP peptide in complex with DR2 was collected at a concentration of 0.35 mM at 33 °C with a ^1H frequency of 600 MHz. Figure 2.5 depicts the tr-HSQC spectrum of DR2/ ^{15}N -MBP which shows fewer and weaker peaks compared to the tr-HSQC spectrum of ^{15}N -MBP peptide free in solution (figure 2.4). Only three strong and four weak peaks could be detected for the peptide backbone besides peaks for peptide side chains.

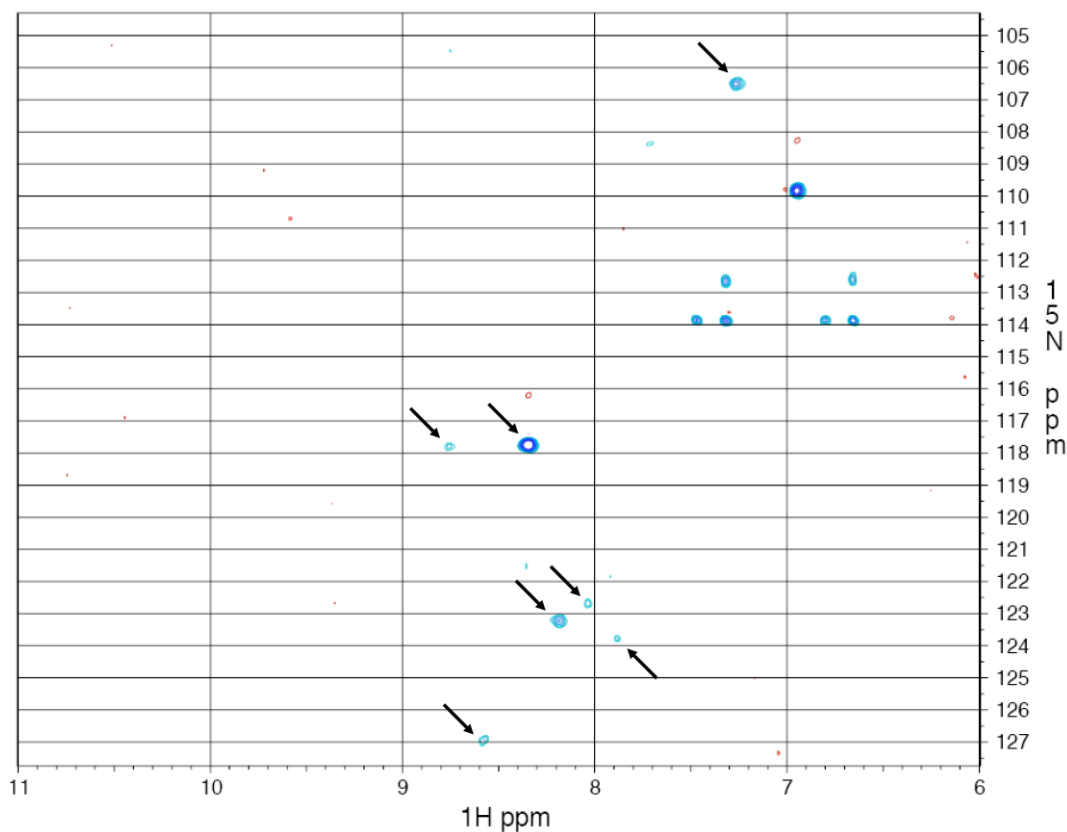


Figure 2.5: tr-HSQC spectrum of ^{15}N -labeled MBP peptide in complex with DR2 measured with a ^1H frequency of 600 MHz. The spectrum of DR2/ ^{15}N -MBP was measured in 10 mM Tris (pH 5.2), 100 mM NaCl at a concentration of 0.35 mM at 33 °C. The ^1H frequency was 600 MHz and 64 scans were measured. Observable peaks generated by backbone amide protons are indicated with arrows.

As the NMR signal is stronger if the molecule has a fast tumbling rate free MBP peptide gave rise to very strong resonances. But when the MBP peptide was bound to the DR2 protein its tumbling rate corresponded to the tumbling rate of the large protein (~ 47 kDa) and due to a shorter relaxation time the NMR signal rapidly decayed leading to weaker NMR signal and line broadening.

As the strength of the NMR signal is also dependent on the magnetic field it is possible to increase signal intensity using a stronger magnetic field. Therefore a tr-HSQC spectrum of DR2/ ^{15}N -MBP complex was measured at a ^1H frequency of 900 MHz. In addition the NMR spectrum was measured at a higher temperature and with a higher scan number which also increases signal intensity and signal to noise ratio.

As can be seen in figure 2.6 measuring the NMR signal at a stronger magnetic field (21.1 Tesla instead of 14.1 Tesla), increasing the temperature from 33 °C to 37 °C and collecting 256 scans instead of 64 scans improved the quality of the HSQC spectrum.

Thirteen instead of seven peaks were observed that were likely arising from peptide backbone, three stronger, six intermediate and four weaker peaks.

But as some peak intensities were still low and therefore peak changes upon small molecule addition might have been difficult to detect it was decided to further enhance the signal by increasing the concentration of the protein complex and by deuterating the peptide besides ^{15}N - and ^{13}C -labeling. The advantage and effects of deuterating the peptide will be explained in the next section.

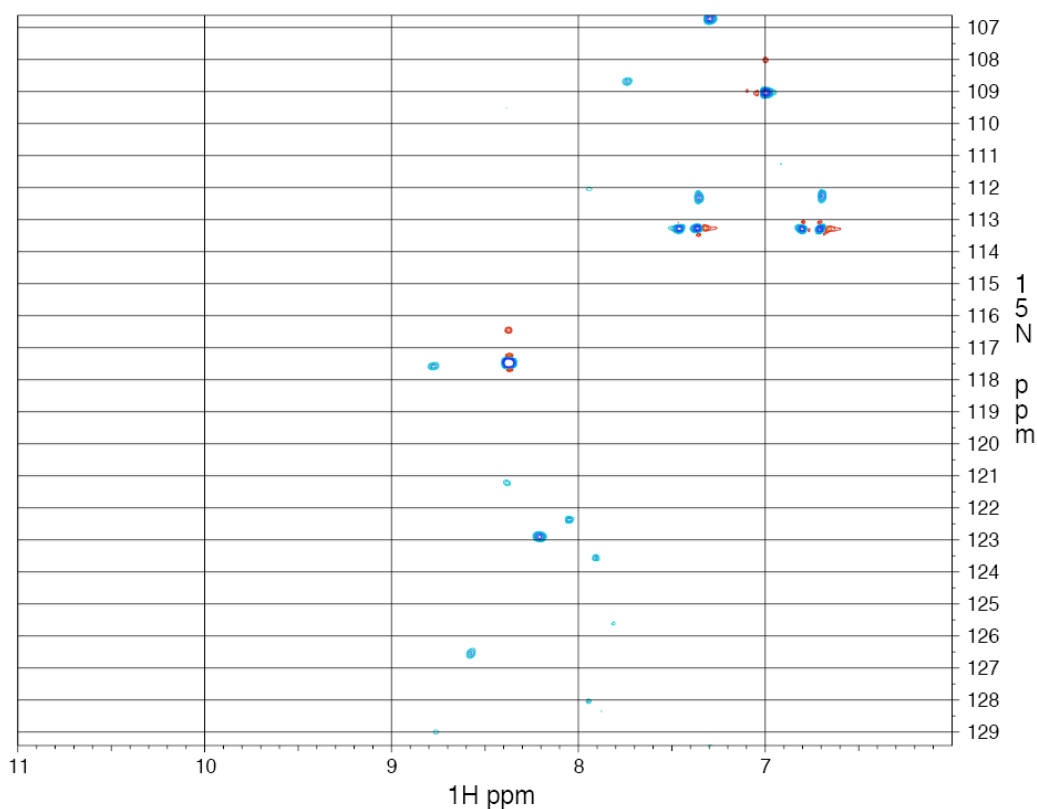


Figure 2.6: tr-HSQC spectrum of ^{15}N -labeled MBP peptide in complex with DR2 measured with a ^1H frequency of 900 MHz. The spectrum of DR2/ ^{15}N -MBP was measured in 10 mM Tris (pH 5.2) and 100 mM NaCl at a concentration of 0.35 mM at 37 °C. The ^1H frequency was 900 MHz and 256 scans were measured.

2.3.5 Deuterating MBP peptide to improve signal intensity of the HSQC spectrum of isotope labeled MBP peptide in complex with HLA-DR2

As described in the previous section the detected NMR signal resulting from ^{15}N -labeled MBP peptide in complex with DR2 was very weak. As the peptide was bound to a large protein (~ 47 kDa) its molecular tumbling rate corresponded to the molecular tumbling rate of the higher molecular weight complex leading to signal loss. To improve signal intensity temperature, magnetic field strength and scan number were increased. But still not all expected resonances from the peptide were detected. Another possibility to enhance signal intensity arising from backbone amide protons is to minimize spin-spin interactions with neighboring protons by substituting non-exchangeable protons with deuteriums.

As the MBP peptide binds to the DR2 molecule in an extended conformation the backbone amide protons are in close proximity to protons of the C_β -atom of the neighboring residue causing fast relaxation and decrease in signal strength. The same applies to the C_α -proton of the same residue which is next to the amide proton of the peptide backbone. This effect of fast relaxation can be eliminated by replacing the non-exchangeable protons of the C_α - and C_β -atoms with deuteriums.

Another factor for signal loss is the close contact of the MBP peptide with DR2 residues. Again through spin-spin interactions of the resonating protons of the peptide with resonating protons of the MHCII molecule the signal of the peptide is further depleted. But as the DR2 protein is expressed in CHO cells which is a complex expression system a new protocol in a different expression system would have had to be established. Therefore only the peptide was deuterated. Furthermore, the MBP peptide was ^{13}C -labeled to allow triple resonance experiments determining C_α -connectivity.

As bacterial growth in D_2O is very slow compared to H_2O the bacterial culture was gradually adjusted to media prepared with D_2O . For ^{15}N - and ^{13}C -incorporation $^{15}\text{NH}_4\text{Cl}$ and ^{13}C -glucose was added to M9 minimal media. The purification protocol was the same as for ^{15}N -labeled MBP peptide (figure 2.2). 3 mg of $^{15}\text{N},^{13}\text{C},^2\text{H}$ -MBP peptide were prepared and the yield was 2.5 mg of triple-labeled MBP peptide per 1 liter bacterial culture. Successful triple-labeling of the MBP peptide was confirmed by mass spectroscopy (see figure 2.7).

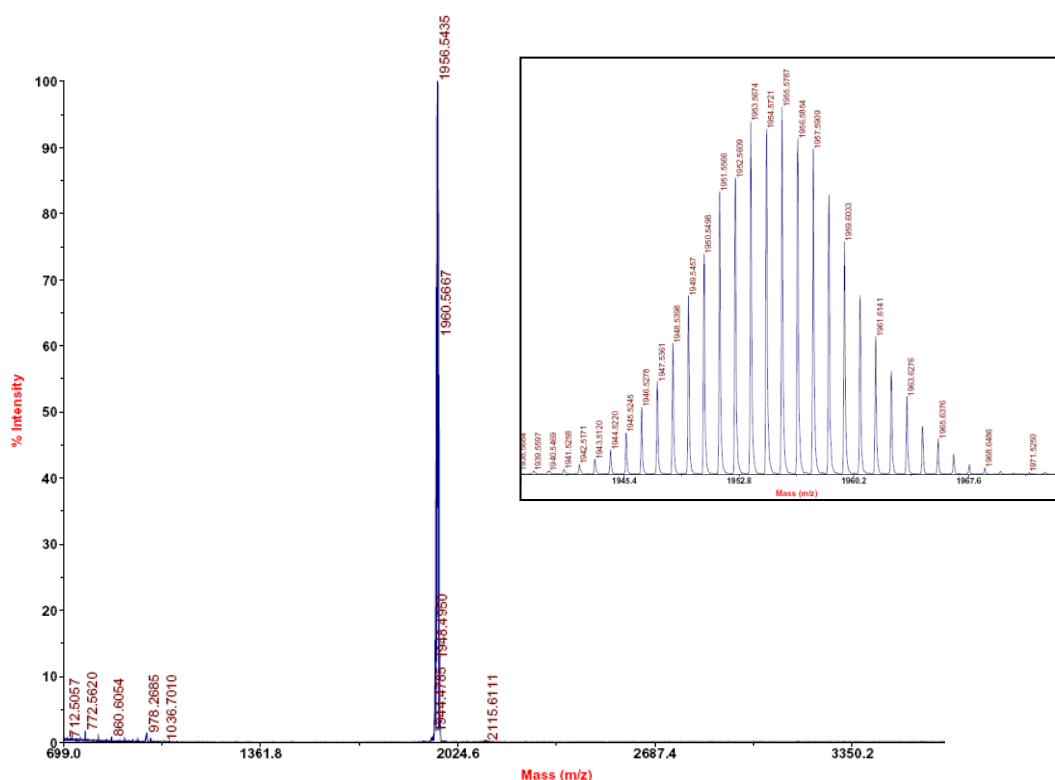


Figure 2.7: Mass spectrum of purified ^{15}N , ^{13}C , ^2H -labeled MBP peptide. The spectrum shows a major peak at ~ 1957 Da which corresponds to deuterated ^{15}N , ^{13}C -labeled MBP peptide. The enlargement of the peak shows a typical mass distribution of a deuterated sample with mass differences of 1 Da derived from different amounts of deuterium incorporation.

2.3.6 Measuring and comparing HSQC spectra of HLA-DR2/ ^{15}N , ^{13}C , ^2H -MBP before and after addition of J10-1

The deuterated ^{15}N - and ^{13}C -labeled MBP peptide was loaded onto DR2 molecules following the protocol described in 2.2.2. The MHCII/peptide complex was concentrated to a final concentration of ~ 36 mg/mL which nearly doubled the peptide concentration compared to the previous DR2/ ^{15}N -MBP complex. At first a tr-HSQC spectrum without MHC II loading enhancer was recorded which can be seen in figure 2.8 in red. The substantial improvement of the spectrum quality can be nicely seen. Many more resonances were detected after increasing the sample concentration and deuterating the peptide. Altogether 18 strong, four intermediate and at least seven weaker peaks were detected for the peptide backbone which results in a total of at least 29 peaks which are more peaks than expected for the 15 amino acid long peptide. Figure 2.8 also shows the spectrum of ^{15}N -labeled MBP peptide free in solution for comparison (black). Only three peaks are potentially overlapping indicating that the ^{15}N , ^{13}C , ^2H -MBP peptide was not free in solution but was bound to DR2 molecule.

Furthermore, the NMR peaks of the MBP peptide in complex with DR2 show a spread over the ^1H axis indicating that the amide protons were surrounded by very distinct chemical environments compared to the amide protons of the free peptide in solution.

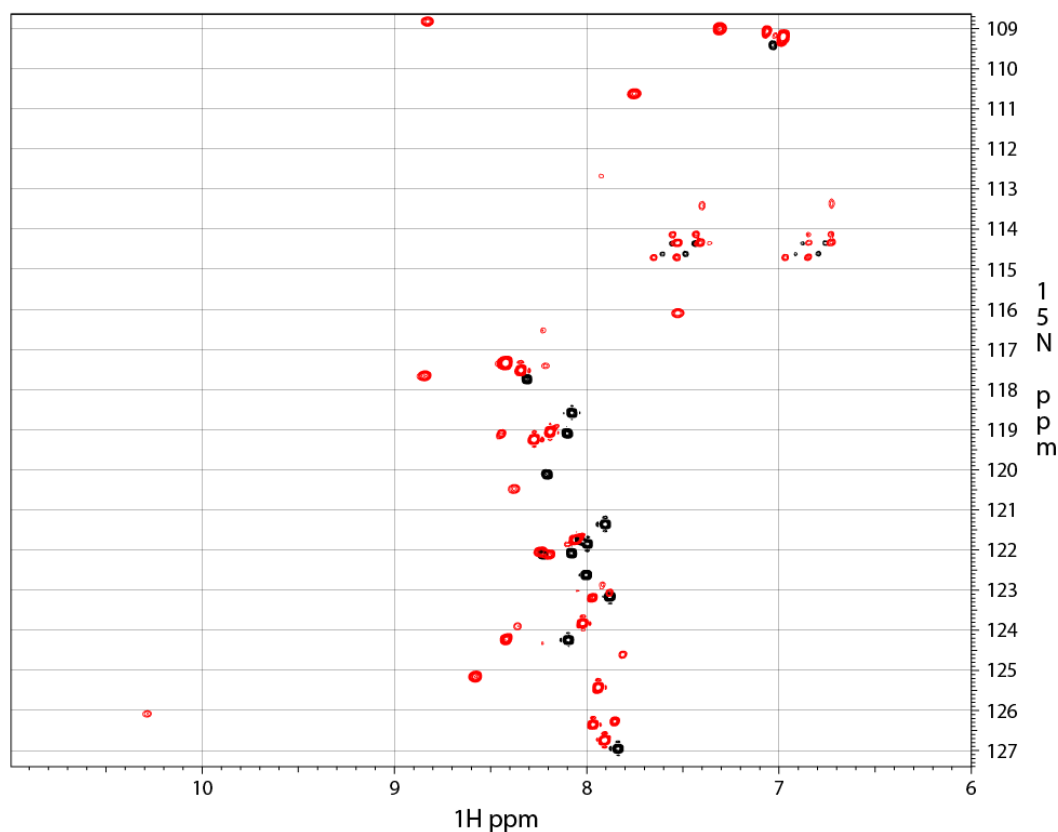
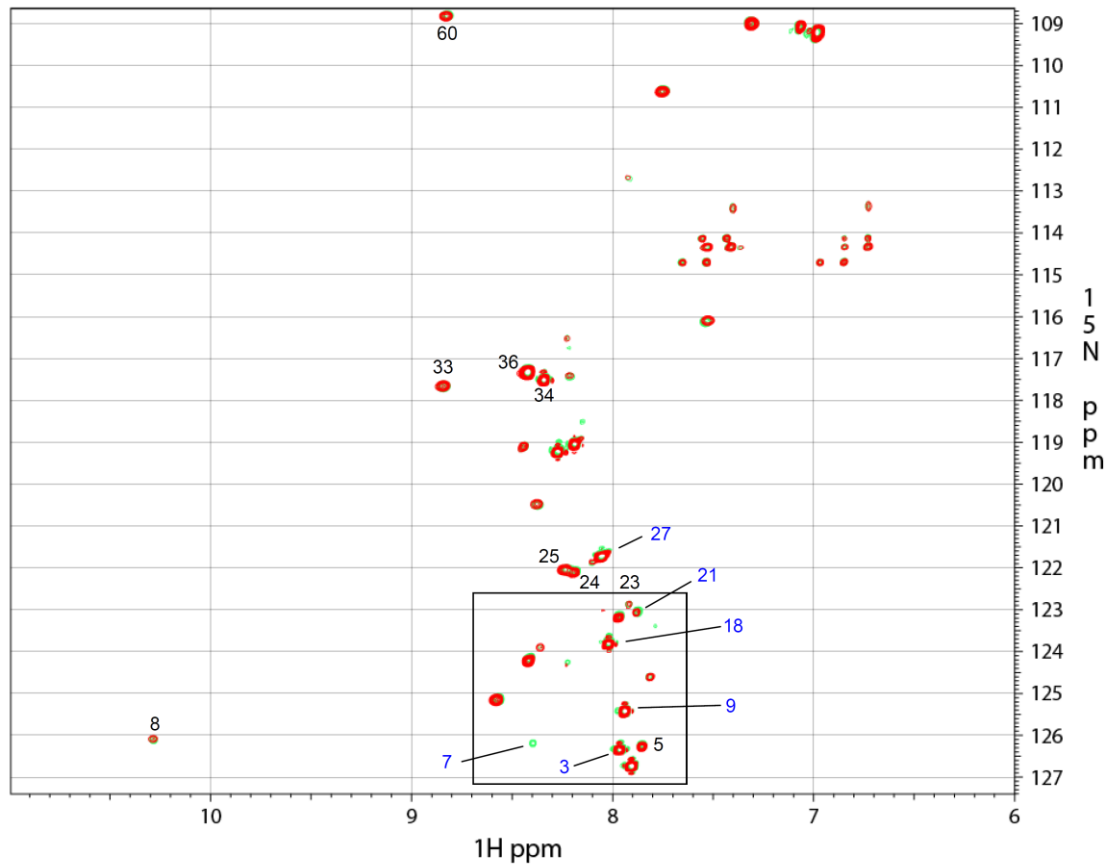


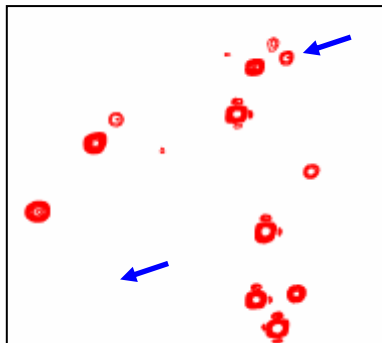
Figure 2.8: Overlay of tr-HSQC spectra of ^{15}N -MBP peptide free in solution (black) and ^{15}N , ^{13}C , ^2H -MBP peptide in complex with DR2 (red). The spectrum of ^{15}N -MBP peptide (black) was measured in 20 mM citrate buffer (pH 5.2) at a concentration of 0.33 mM with a ^1H frequency of 600 MHz at 30 °C. The spectrum of ^{15}N , ^{13}C , ^2H -MBP peptide in complex with DR2 (red) was measured in 50 mM citrate buffer (pH 5.2) at a concentration of 0.6 mM with a ^1H frequency of 750 MHz at 37 °C.

After measuring the spectrum of triple-labeled MBP peptide in complex with DR2 one of the most active MHC II loading enhancers, J10-1, was added at a concentration of 1 mM and the same tr-HSQC experiment carried out. Figure 2.9 shows an overlay of both tr-HSQC spectra with and without MLE. The spectrum in green represents the sample after addition of the MLE. As can be seen from the overlay no major chemical shifts were observed. However minor changes in peak intensities were detected which could be the consequence of small molecule action. Some peaks that were just below threshold in the first spectrum appeared in the latter spectrum and other peaks became stronger which can be seen in (B) and (C) of figure 2.9 showing parts of both spectra.

A



B



C

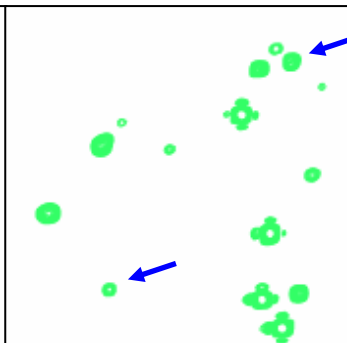


Figure 2.9: Overlay and comparison of tr-HSQC spectra of ^{15}N , ^{13}C , ^2H -MBP peptide in complex with DR2 before (red) and after (green) MLE addition. Both spectra were measured in 50 mM citrate buffer (pH 5.2) at a concentration of 0.6 mM at 37 °C with a ^1H frequency of 750 MHz. After measuring the spectrum of ^{15}N , ^{13}C , ^2H -MBP peptide in complex with DR2 alone (red), 1 mM of MHCII loading enhancer J10-1 was added and the tr-HSQC experiment repeated (green). In (A) an overlay of both spectra can be seen. Peaks with changes in intensity are indicated with blue numbers. (B) and (C) show an enlargement of the indicated area in (A). (B) shows part of the spectrum before MLE addition and (C) part of the spectrum after MLE addition. Arrows are indicating significant intensity changes which are observable.

For quantification relative peak intensities were measured and compared (figure 2.10). Six peaks showed significant changes in peak intensity. Four stronger peaks were affected as well as two weaker peaks. Interestingly all six peaks showed an increase in intensity after MLE addition.

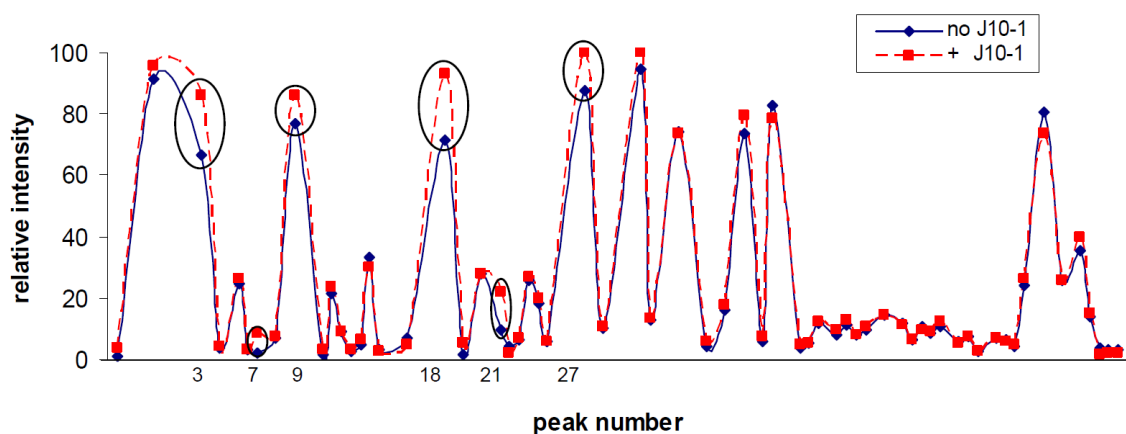


Figure 2.10: Comparison of relative peak intensities of tr-HSQC spectra of ^{15}N , ^{13}C , ^2H -MBP peptide in complex with DR2 before (blue) and after (red) addition of J10-1. Peaks of the tr-HSQC spectra were numbered and relative intensities determined. Blue diamonds indicate peaks of the spectrum without MLE addition. Red squares represent peaks of the spectrum after MLE addition. Significant intensity changes are indicated with black circles.

2.3.7 Performing HNCA and ^{15}N -NOESY experiments of HLA-DR2/ ^{15}N , ^{13}C , ^2H -MBP to determine resonance assignments

To further investigate which parts of the peptide might have been affected by binding of the small molecule J10-1, it was necessary to assign the resonances to specific peptide residues, especially the ones showing a change in intensity. Therefore, using the same DR2/ ^{15}N , ^{13}C , ^2H -MBP sample which was used for measuring the HSQC spectrum of the complex, HNCA and ^{15}N -NOESY experiments were carried out. By matching C_α chemical shifts obtained from the HNCA experiment and additional spatial information from the ^{15}N -NOESY experiment some sequential assignments were made (see table 2.1). But unfortunately the resonance assignments were not unambiguous which can be also seen in table 2.1. As there were more peaks than expected for a 15 amino acid long peptide and apparently several distinct peptide conformations present, it was not clear how many peaks actually arose from each peptide residue and which peaks belonged to a certain peptide conformation. Only some C_α chemical shifts could be matched to C_α chemical shifts of neighboring peptide residues and it was not possible to determine a complete C_α connectivity. Without knowing the C_α connectivity it was also not possible

to assign the chemical shifts to specific peptide residues. Due to this complexity unfortunately it could not be determined which peptide residues might have showed an increase in signal intensity upon small molecule addition.

Table 2.1: Possible peak assignments based on HNCA and ^{15}N -NOESY experiments. The first line displays the peptide sequence. Rows below show peak numbers with possible assignments to specific peptide residues. Numbers in parenthesis show C_{α} chemical shifts in ppm. Numbers with matching color indicate sequences of identical peaks which can be assigned to different peptide residues. Peak numbers refer to peaks indicated in the tr-HSQC spectrum in figure 2.9 (A).

E	N	S	V	V	H	F	F	K	N	I	V	T	S	R
		36 (58)	24 (61)	60 (63)	8 (53)	33 (55)								
		34 (58)	27 (62)											
			34 (58)	27 (62)										
		23 (62)	25 (54)	18 (62)	3 (56)			23 (62)	25 (54)	18 (62)	3 (56)			
							9 (55)	5 (59)					9 (55)	5 (59)
					7 (49)									

2.3.8 Measuring ^{19}F -NMR spectra of J10-11 in the presence of HLA-DR2/MBP and HLA-DR2/CLIP

To further investigate the binding of J10 and its derivatives to DR2 one-dimensional ^{19}F -NMR spectra of the small molecule were measured in the presence of DR2/peptide complexes with different affinities. Some of the J10 derivatives include fluorine atoms which possess NMR active nuclei. ^{19}F atoms are naturally abundant and have a nucleus with spin of $\frac{1}{2}$, same as protons. As nuclei with spin of $\frac{1}{2}$ undergo splitting of spin states in an external magnetic field the nuclei can be excited by electromagnetic radiation yielding measurable NMR signals.

The advantage of measuring ^{19}F -NMR spectra instead of ^1H -NMR spectra is that ^{19}F -NMR signals can only derive from the small molecule as the protein contains no fluorines which simplifies the spectra. A one-dimensional ^1H -NMR spectrum would be

very difficult to interpret because of the large number of proton signals from the protein and the peptide. For the ^{19}F -NMR experiments the small molecule J10-11 was used which contains four fluorine atoms, three at the indole ring and one at the phenyl ring (figure 2.1).

The NMR signal is dependent on the tumbling rate of the molecule as described above and therefore also the binding state of the small molecule. If the small molecule is free in solution it gives rise to very strong NMR signal as it tumbles fast. But as soon as it binds to the DR2 protein it tumbles very slowly and the NMR signal is very weak and broad and can only be detected with a very strong magnetic field and high scan numbers. However, if the small molecule binds to the protein, less small molecule is free in solution resulting in reduced intensity of the NMR signal from the unbound small molecule. Therefore binding of the MHC II loading enhancer J10-11 to DR2 can be measured indirectly.

The analyses of the ^{19}F -NMR experiments were carried out qualitatively by comparing the effect of adding a high (DR2/MBP) versus a low (DR2/CLIP) affinity MHCII/peptide complex to the small molecule J10-11. DR2/MBP and DR2/CLIP were prepared as described in 2.2.2. First the ^{19}F -NMR spectrum of free J10-11 (250 μM) in 50 mM citrate buffer (pH 5.2) was measured (figure 2.11) which gave rise to four strong signals. Afterwards DR2/MBP or DR2/CLIP was added to the small molecule sample at a concentration of 11 μM and the same ^{19}F -NMR experiment carried out.

Figure 2.11 shows an overlay of all three ^{19}F -NMR spectra which were compared by matching the noise level and the signal of TFA which was added separately as a standard. After addition of the high-affinity complex DR2/MBP some reduction in signal intensity was observed compared to the signal of the small molecule without MHC II/peptide present. But in the presence of the low-affinity complex DR2/CLIP even more signal loss was detected. As the lower affinity complex led to more depletion of free J10-11 in solution, indicated by the more pronounced signal loss, a higher affinity of J10-11 to the low-affinity complex was observed than to the high-affinity complex.

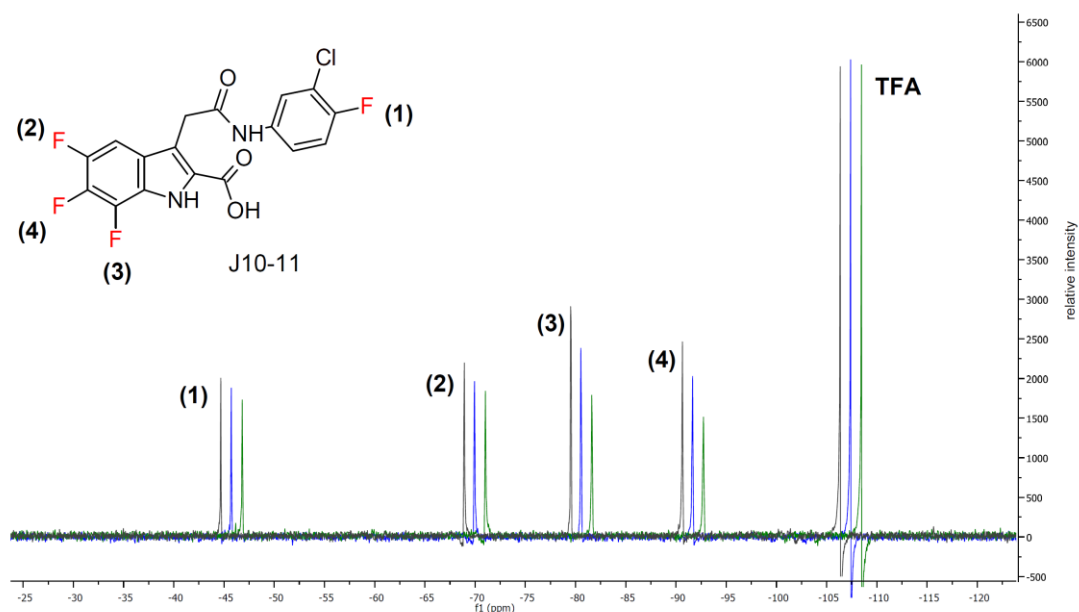


Figure 2.11: Comparison of three different one-dimensional ^{19}F -NMR spectra of the MHC II loading enhancer J10-11 free in solution (grey), in the presence of DR2/MBP (blue) and in the presence of DR2/CLIP (green). The spectra were collected with a small molecule concentration of 0.25 mM in 50 mM citrate buffer (pH 5.2) at 25 °C using a NMR machine with a magnetic field strength of 11.7 Tesla. The five peaks of the three different spectra are overlapping but for comparison the spectra of J10-11 in the presence of 11 μM DR2/MBP (blue) and 11 μM DR2/CLIP (green) were shifted to the right. The signal on the right refers to 1 mM TFA which was added to the NMR tube outside of the microcapillary. The three NMR spectra were compared by matching the peak height of the TFA standard and the noise level. Numbers next to peaks and next to fluorine atoms of the small molecule J10-11 displayed in the top left show the peak assignment.

2.4 Conclusion

To further improve the peptide loading activity of the small molecule J10, which has a potential as adjuvant for peptide therapeutics, a better understanding of the exchange mechanism is necessary. Two different methods were applied to gain a comprehensive understanding of the small molecule interactions with the MHC II/peptide complex and their impact on peptide-binding, i.e. X-ray crystallography and NMR spectroscopy.

First, DR2/MBP was crystallized in the presence of the J10 derivatives J10-1 and J10-12 and the crystals diffracted till 2.9 Å. A data set from a co-crystallization trial showed extra electron density close to the peptide N-terminus in the region around residue Ser α 53. Previous experiments with covalent linkage of the small molecule to the peptide had shown that the small molecule binds in an area close to the peptide N-terminus (Call et al., 2009). Also, mutagenesis studies of the α chain close to the peptide

N-terminus (Trp α 43 to Ser α 53) showed involvement in small molecule binding (unpublished data). Furthermore, J10 and its derivatives show activity on all tested DR alleles (DR1, DR2, DR4) indicating they might bind to the non-polymorphic DR α chain. As this region is also known to be involved in DM binding and activity (Doebele et al., 2000) it is possible that the small molecule and DM might target similar MHC II/peptide interactions. However, unfortunately, the extra electron density could not unambiguously be accounted for by the small molecule. Reasons for the absence of well-defined density for the small molecule could be partial occupancy of the binding site by the small molecule. It is also possible that the small molecule did not bind to the DR2 species which crystallized as it might bind to DR2 conformations only available if the peptide is partially released which has been seen for DM recently (Anders et al., 2011). As the MBP peptide is a high-affinity peptide for DR2 this species might have been small especially as the peptide was still covalently linked to the protein which further increased peptide affinity. In the obtained DR2 structure the MBP peptide was fully bound and showed no conformational changes. Unfortunately, crystals set up with DR2/MBP complex having the linker between peptide and DR2 cleaved did not provide data sets with sufficient resolution, maybe due to higher flexibility. For another group of MHC II loading enhancers (di-peptides, see table 1.1, (Gupta et al., 2008)) some evidence points to the P1 pocket as a possible binding site although a co-crystal structure has not been determined, yet. It is possible that J10 might bind to a similar site, for which partial peptide release would be necessary. In the future co-crystallization experiments with the small molecule could be performed using a MHC II molecule carrying a low-affinity peptide or even an N-terminally truncated peptide (see chapter II). Screening new crystallization conditions might result in well diffracting crystals and reveal a structure presenting a partially filled peptide-binding groove or conformational changes upon small molecule binding.

To investigate the effects of J10 and its derivatives on the dynamics of peptide bound to MHC II molecules ^1H - ^{15}N HSQC spectra of triple-labeled (^2H , ^{13}C , ^{15}N) MBP peptide in complex with DR2 were measured before and after addition of the small molecule J10-1. When the spectra were compared no obvious chemical shifts of the peaks were detected but several changes in peak intensities were observed which could indicate peptide changes resulting from interactions of the small molecule with the MHC II/peptide complex. Furthermore, as there were more peaks (~ 29) than expected for a 15 amino acid long peptide and only three possible overlaps with the spectrum of

the free peptide, the presence of multiple distinct conformations of the bound MBP peptide were observed. ^{15}N -NOESY and HNCA experiments were performed with the sample but unfortunately an unambiguous assignment of the peaks was not possible. Without knowing which sets of peaks belong to certain peptide conformations it was difficult to determine the C_α connectivity. With almost twice as many peaks as peptide residues there could be two distinct peptide conformations or several distinct conformations for particular residues or peptide segments. But even without a distinct peak assignment the NMR spectra show that the MBP peptide although it is bound to the DR2 molecule exhibits conformational dynamics with several distinct peptide conformations which was very surprising, especially as DR2/MBP is a high-affinity complex. So far the structural information we have about DR2/MBP and MHC II/peptide complexes mostly arises from crystal structures which depict the complex in a low energy state. The crystal structures of MHC II/peptide complexes normally show one peptide conformation tightly bound to the MHC II molecule which is energetically very stable as it is stabilized by two main binding features: peptide side chains interact with pockets formed by the MHC II molecule and the peptide backbone forms a hydrogen bond network with conserved MHC II residues. In solution there are likely also more loosely bound peptide conformations present that are energetically less stable but still long-lived to be detected by NMR experiments. In the crystal structure of DR2/MBP (Smith et al., 1998) the C-terminus of the peptide exhibits an overall raised position with P7 and P9 pockets only partially occupied indicating this part of the peptide being more loosely bound. As in solution the complex likely exhibits more flexibility it is possible that multiple distinct conformations of the peptide C-terminus were observed by NMR. To further explore which parts of the peptide exhibit multiple conformations a definite resonance assignment is necessary for which residue-specific labeling would be needed as further triple resonance experiments might be difficult to interpret.

The HSQC spectrum of the triple labeled MBP peptide in complex with DR2 after addition of the small molecule J10-1 showed an increase of peak intensity of four stronger and two weaker peaks. This could be an effect of small molecule addition and could indicate that the small molecule increased the population of a certain peptide conformation. Furthermore, it is also possible that these specific resonances arose from residues showing increased mobility upon small molecule addition leading also to signal enhancement. Whether the observed changes are due to small molecule binding

has to be further investigated and similar as mentioned above without a definite peak assignment it is not clear which part of the peptide could have been affected. In case the observed changes are induced by small molecule binding they are rather subtle as no chemical shifts were observed.

The ^{19}F -NMR experiments showed that the small molecule J10-11 had a higher affinity to the less stable complex DR2/CLIP than to the more stable complex DR2/MBP which could indicate that the small molecule binds to an intermediate MHC II/peptide conformation. Better binding to low- than to high-affinity MHC II/peptide complexes has been also seen for DM (Anders et al., 2011) showing an additional similarity between both molecules. For future experiments it might be interesting to use a lower affinity MHC II/peptide complex as the effect of the small molecule seen by NMR might be more pronounced. But on the other hand the NMR spectra might become even more complex with a low-affinity peptide as more intermediate peptide conformations might be observable.

3 Chapter II: Structural effects of destabilizing peptide-MHC II interactions and implications for the peptide exchange mechanism of HLA-DM

3.1 Introduction

Elucidating the molecular basis for the generation of ligands presented to CD4⁺ T cells requires a deeper understanding of how MHC II molecules are loaded with antigenic peptides catalyzed by DM. Besides susceptibility to proteolytic cleavage resistance to DM catalyzed peptide release is a major factor in determining whether or not a particular peptide is presented on the cell surface. Therefore, understanding the mechanism of DM mediated peptide loading and release would promote efforts to predict immunogenicity of known and emerging pathogens. However, the molecular mechanism of DM catalysis is not well understood.

The co-crystal structure of the DR/DM complex would expose crucial interacting residues and also reveal the overall conformation both proteins adapt in the complex, thus shedding light on the mechanism of how DM catalyzes peptide exchange of MHC II molecules. DM catalyzes exchange of peptides with various sequences (Weber et al., 1996) suggesting that DM might partially target MHC II-peptide interactions that are peptide sequence-independent. Recent studies have shown that release of the peptide N-terminus of the peptide-binding groove of MHC II molecules is necessary in order for DM to bind DR molecules and catalyze peptide exchange (Anders et al., 2011). In particular, disruption of the four N-terminal conserved hydrogen bonds and release of the peptide anchor residue from the P1 pocket seems to be necessary for DM binding. Taking this new information into account, a new approach was designed to crystallize the DR/DM complex using a modified DR molecule missing the three N-terminal peptide residues which exhibited higher affinity for DM than DR complexes with full length peptide. As the complex was not covalently linked the affinity between both molecules had to be optimized to favor crystallization of the complex versus the individual components. Therefore, surface plasmon resonance experiments were carried out to determine the dissociation constant of the complex at different pH to direct crystallization screens.

Furthermore, the structure of the DR1 molecule carrying an N-terminally truncated peptide was pursued, as the implications of the partial peptide release for the DR1 conformation were unknown. The structure of the modified DR1/peptide complex could indicate whether conformational changes occur in the DR region around the missing peptide N-terminus or whether the DR conformation is stable, even if the N-terminal peptide residues are missing and several hydrogen bonds are not formed. Of particular interest is the conformation of the extended strand of the DR α chain around residues Ser α 53 and Phe α 51, which is adjacent to the peptide N-terminus and forms an anti-parallel β -sheet with the peptide. This region includes residues shown to be involved in DM activity (Anders et al., 2011; Doebele et al., 2000). The DR1 structure, with a partially filled peptide-binding groove, might reveal a DM receptive DR conformation giving further insight into the process of peptide exchange by MHC II molecules. To prepare DR1 complex with the very low-affinity HA peptide variant, the peptide is covalently linked to the DR α chain in the peptide-binding groove via a disulfide bond. However, the yield of complex formation was very low. Since large amounts of DR1/peptide complex are needed for crystallization experiments, the protocol for the peptide loading and covalent linkage reaction had to first be optimized.

3.2 Materials and Methods

3.2.1 Preparation of biotinylated HLA-DM and HLA-DM mutant

Soluble DM and DM mutant (DM α R98A-R194A, DM mut), which shows no binding to DR, were expressed in *Sf9* insect cells. The cells were infected with recombinant Baculovirus (MOI > 5) and proteins purified after 3 days. Both proteins carried a C-terminal BirA tag (GLNDIFEAQKIEWHE) at the α -chain and a protein C tag at the β -chain. Two N-linked glycosylation sites (DM α N165D and DM β N92D) were removed to diminish heterogeneity leaving the DM α Asn15 glycosylation site. Proteins were purified by anti-Protein C affinity chromatography (Roche Applied Science) and aggregates were removed by gel filtration (Superose 6, GE Healthcare).

BirA was added at a molar ratio of 1:20 (BirA:protein) for site-specific biotinylation of the BirA tag. The reaction was incubated for 2 h at 30 °C at a protein concentration of 2-3 mg/mL in the presence of biotin (100 μ M), ATP (10 mM) and protease inhibitors.

Excess biotin was removed by dialysis and successful biotinylation was confirmed with native polyacrylamide electrophoresis determining mobility shift with streptavidin.

3.2.2 Preparation of HLA-DM used for crystallization

Soluble DM was produced using stably transfected CHO cells in hollow fiber bioreactors (Day et al., 2003) and purified by affinity chromatography using protein C tag on DM α chain. Protein C tag as well as Jun and HA tags on DM β chain were cleaved using 50 units thrombin per 1 mg protein while incubating at 37 °C for 7 hours. To exclude interference with introduced cysteines of the DR molecule, which was later mixed with DM for co-crystallization experiments, free cysteines on the DM surface were alkylated by incubating DM under reducing conditions (1 mM DTT) at 25 °C for 1 hour and subsequent dialysis in 20 mM Tris (pH 8), 50 mM NaCl containing 10 mM iodoacetamide. Excess iodoacetamide was removed by gel filtration chromatography and DM further purified by ion exchange chromatography.

3.2.3 Preparation of covalently linked HLA-DR1/peptide complexes and of HLA-DR1 mutant

DR1 molecules with a low-affinity CLIP peptide (CLIP_{low}, SKARMATGALAQA), covalently linked to the DR β chain, were expressed as a secreted protein in *Sf9* insect cells. After three days the protein was purified by affinity chromatography with monoclonal antibody to DR (L243; American Type Culture Collection). Aggregates were removed with a Superose 6 gel filtration column. The covalently linked CLIP_{low} peptide and C-terminal leucine zippers were cleaved with V8 protease (endoproteinase Glu-C, New England BioLabs Inc.) containing a His-tag. The protease was removed with Ni²⁺-NTA beads and protein was further purified by ion-exchange column (MonoQ). Cleaved CLIP_{low} peptide was exchanged versus synthesized HA peptide variants (Peptide2.0 Inc., 21st century biochemicals) containing a cysteine at P6 position using redox conditions allowing formation of a disulfide bond between the peptide and a cysteine introduced at position 65 of DR α chain in the peptide-binding groove. The variants of HA peptide were labeled with a DNP group linked to a lysine side chain at the peptide C-terminus. Before protein addition HA peptides were reduced in 500 μ M glutathione. 20-fold molar excess of peptide was used in 50 mM citrate-phosphate buffer (pH 5.3), 150 mM NaCl in the presence of 50 μ M of the small molecule J10-1

and incubated for 2 hours in the presence of 750 μM glutathione. Reactions were then shifted for 2 hours to oxidizing conditions (950 μM oxidized glutathione) to promote disulfide bond formation. Excess peptide was removed with a Superose 12 gel filtration column. As the truncated HA peptide was labeled with a DNP group the complex was purified with an α -DNP affinity column. Disulfide linkage of HA peptides was confirmed on the basis of lower motility of the DR α chain by SDS-PAGE. After a final purification with a second MonoQ ion exchange column the purified complex was concentrated to a final concentration of ~ 10 mg/mL. The yield was $\sim 8\%$.

The DR1 mutation was introduced using the QuikChange Lightning site-directed mutagenesis kit (Agilent Technologies) and the DR1 mutant was expressed in *Sf9* insect cells. Aggregates were removed by size exclusion chromatography (Superose 6). C-terminal leucine zippers were removed by V8 (endoproteinase Glu-C, New England BioLabs Inc.) cleavage. The peptide exchange protocol was followed as described above, excess peptide was removed by size exclusion chromatography (Superose 12) and the protein finally purified with α -DNP affinity chromatography.

3.2.4 Preparation of HLA-DM with an N-terminally truncated α chain

DM missing eleven residues at the N-terminus of the DM α chain was expressed in *Sf9* insect cells and purified by protein C-affinity chromatography. After removing aggregates with gel filtration (Superose 6) the protein was further purified by ion exchange chromatography (MonoQ) and biotinylated using the protocol as described in 3.2.1.

3.2.5 Surface plasmon resonance experiments

Surface plasmon resonance (SPR) experiments were conducted on a BIAcore 3000 machine (GE Healthcare) using streptavidin chips (GE Healthcare), which were primed and normalized before immobilization of biotinylated protein. For immobilization biotinylated DM wild-type (wt) and DM mutant (α R98A, α R194A; mut) were separately injected in two consecutive flow cells after diluting the protein to a concentration of 0.5 mg/mL in HBS-EP buffer (GE Healthcare). 500 RU (response units) of protein were immobilized in each flow cell using a flow rate of 10 $\mu\text{L}/\text{min}$ at 25 $^{\circ}\text{C}$. Experiments were carried out in degassed 50 mM citrate phosphate buffer (pH 5.3), 150 mM NaCl and 0.06 % C₁₂E₉ detergent (Calbiochem; EMD Chemicals).

DR/peptide complexes (analyte) were diluted into the running buffer before injection and injected at the appropriate concentration followed by buffer. Chips were regenerated by injection of HA peptide (50 μM). Binding of the reference flow cell (DM mut) was subtracted from binding in the flow cell of DM wt. Dissociation constants were determined by curve fitting (1:1 Langmuir model) using the BIAevaluation software. For experiments with DM possessing an N-terminally truncated DM α chain, the DM variant was immobilized in flow chamber three; whereas, the DM mutant was immobilized in flow chamber two and DM wild type in flow chamber four. For analysis flow chamber two was subtracted from flow chambers three and four, respectively.

3.2.6 Protein crystallization, collection of diffraction data and structure solving

For co-crystallization experiments purified DM and DR1/HA were mixed using a 1:1 ratio, dialyzed against 10 mM MES buffer (pH 6) and concentrated until a total protein concentration of ~ 10 mg/mL was reached. Initial screening plates were set up at the Collaborative Crystallization Center in Melbourne, Australia, using the nano-dispensing crystallization robots mosquito Crystal (TTP LabTech) and Phoenix (Rigaku). Customized screens were prepared with a Freedom Evo liquid handling robot (Tecan Group Ltd.) preparing crystallization conditions with a pH equal or lower than 6.5. Around 480 crystallization conditions were screened. Final crystals of DR1/HA(P_{1,Val}-P₁₁) were grown in 2.5 M ammonium sulfate, 10 % DMSO or 100 mM sodium acetate (pH 4.3), 9% PEG 10,000 at 20 °C. Protein crystallization was performed using hanging-drop vapor diffusion. The crystals were mounted using CryoLoops (Hampton Research) or MicroLoops E (Mitegen) and transferred into a solution containing the crystallization condition and ~ 5 M xylitol or 38% ethylene glycol as cryo-protectant. Crystals were flash-cooled in liquid nitrogen. X-ray diffraction data were collected at beamline 24-ID-E of NE-CAT or beamline 23-ID-D of GM/CA-CAT at the Advanced Photon Source of Argonne National Laboratory, IL, USA. Crystals were stepwise exposed to X-ray radiation by moving the X-ray beam along the crystal to minimize radiation damage. Crystals diffracted up to 3.1 Å and 2.14 Å, respectively, and several complete data sets were collected from individual crystals.

Diffraction data were indexed and scaled using the software HKL2000 (Otwinowski and Minor, 1997). The structure of DR1 with the truncated HA peptide was solved by

molecular replacement with the program Phaser (McCoy et al., 2007) using the previously solved DR1/HA structure (PDB: 1DLH, (Stern et al., 1994)) as a search model. The structure was refined using Phenix (Adams et al., 2010) and evaluation of the structure was carried out with MolProbity (Chen et al., 2010). During refinement manual adjustments of the structure were performed using the software Coot (Emsley and Cowtan, 2004). To assess the accuracy of the crystal structure the statistical quantities R_{free} and R_{work} were used (Brunger, 1992). Figures depicting protein structures are generated with PYMOL (Schrodinger, 2010).

3.2.7 Eluting covalently linked peptide from HLA-DR1

To release the covalently linked peptide from DR1 the complex was incubated for 1 hour at 25 °C in the presence of 4 mM DTT. After addition of full length HA peptide, using twenty times molar excess, the complex was incubated at 25 °C for an additional hour. The sample was injected to an α -DNP affinity column and the separated peptide carrying a DNP-label eluted with 50 mM CAPS buffer (pH 11.5). The eluted peptide was lyophilized, dissolved in water and submitted for mass spectrometry.

3.2.8 Mass spectrometry

Lyophilized peptide sample was dissolved in water and separated by a nano-liquid chromatography system (Nano-Acquity UPLC system from Waters Corporation) and analyzed by an ABI model 4800 TOF/TOF Matrix Assisted Laser Desorption mass spectrometer and by a Thermo Scientific LTQ Orbitrap XL (Thermo Fisher Scientific).

3.3 Results and discussion

3.3.1 Preparing HLA-DM and HLA-DR1 carrying a truncated HA peptide, both used for crystallization experiments

DM used for crystallization experiments was expressed in CHO cells and purified following the scheme described in figure 3.1. First, DM was purified by affinity chromatography and protein tags were proteolytically removed. After incubation under reducing conditions, free cysteines of DM were alkylated using iodoacetamide. DM was further purified by gel filtration and ion exchange chromatography before mixing with

DR1 protein. DR1 molecules carrying covalently linked HA peptide variants were prepared as described in figure 3.2. Initially, DR1 molecules carrying a low-affinity CLIP peptide were expressed in *Sf9* insect cells and purified by affinity chromatography. Aggregates were removed by gel filtration and the linker between peptide and DR β chain, as well as C-terminal leucine zippers, were proteolytically cleaved. DR1/CLIP_{low} was further purified by ion exchange chromatography. As for protein crystallization, large amounts of covalently linked DR1/peptide complex are required, the peptide exchange protocol had to be improved as the yield amounted to only 5 %. By using a milder reducing agent (glutathione instead of DTT), balancing redox conditions and longer incubation times favoring the formation of the disulfide bond between DR1 and peptide, the yield of the peptide exchange step was improved up to 30 %. Following the optimized peptide exchange protocol described in 3.2.1, the low-affinity CLIP peptide was exchanged versus an N-terminally truncated HA peptide. After peptide exchange under redox conditions excess peptide was removed by gel filtration. By improving the yield of the peptide exchange reaction it was feasible to prepare enough protein for crystallization experiments. In the end the covalently linked MHC II/peptide complex was purified by ion exchange chromatography and the overall yield was ~ 8 %.

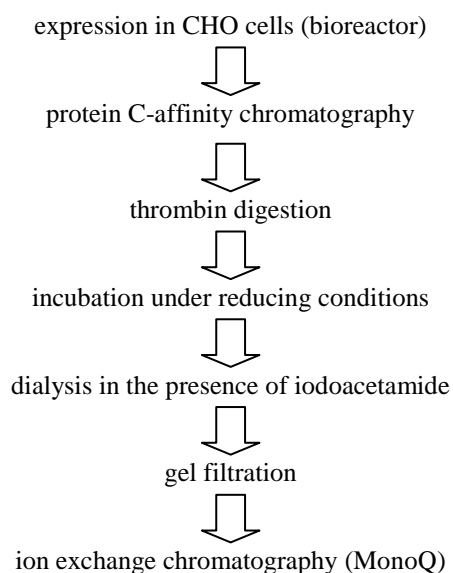


Figure 3.1: Preparation of DM used for crystallization trials. DM was expressed in CHO cells using hollow fiber bioreactors. After protein purification using protein C-affinity chromatography protein tags were removed by thrombin digestion. Following incubation under reducing conditions DM was dialyzed in the presence of iodoacetamide to alkylate free cysteines. DM was further purified by gel filtration and ion exchange chromatography.

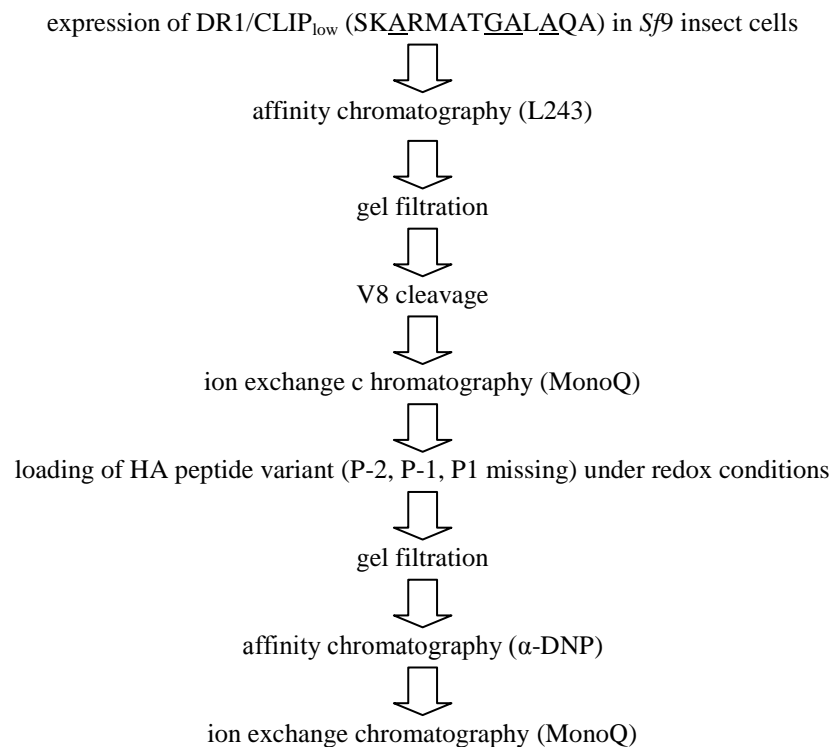


Figure 3.2: Preparation of DR1 carrying an N-terminally truncated HA peptide. DR1/CLIP_{low} was expressed in *S9* insect cells as a secreted protein. The protein was purified by L243 affinity chromatography and aggregates removed by gel filtration chromatography. The linker between peptide and DR β chain as well as C-terminal leucine zippers were cleaved by V8 protease. After ion exchange chromatography the cleaved peptide was exchanged versus an HA peptide variant missing residues P-2, P-1 and P1 under redox conditions. Excess peptide was removed by gel filtration and the DR1 complex carrying a covalently linked HA peptide variant further purified by affinity chromatography and ion exchange chromatography.

3.3.2 Measuring pH-dependent affinity of HLA-DM to HLA-DR1 carrying an N-terminally truncated HA peptide using surface plasmon resonance

To determine optimal conditions for crystallizing the non-covalently linked complex of DM and DR1, surface plasmon resonance experiments were carried out at different pH. As can be seen in figure 3.3 the strongest affinity of DM to the covalent complex of DR1 and an N-terminally truncated HA peptide was measured at pH 5.5 with a dissociation constant of $\sim 1.6 \mu\text{M}$. With increasing pH, DM affinity decreased with a dissociation constant of $4.7 \mu\text{M}$ at pH 6.5 and $15.4 \mu\text{M}$ at neutral pH. To favor crystallization of the non-covalent complex of DM and DR1 crystallization conditions with pH lower than 6.5 were preferentially screened.

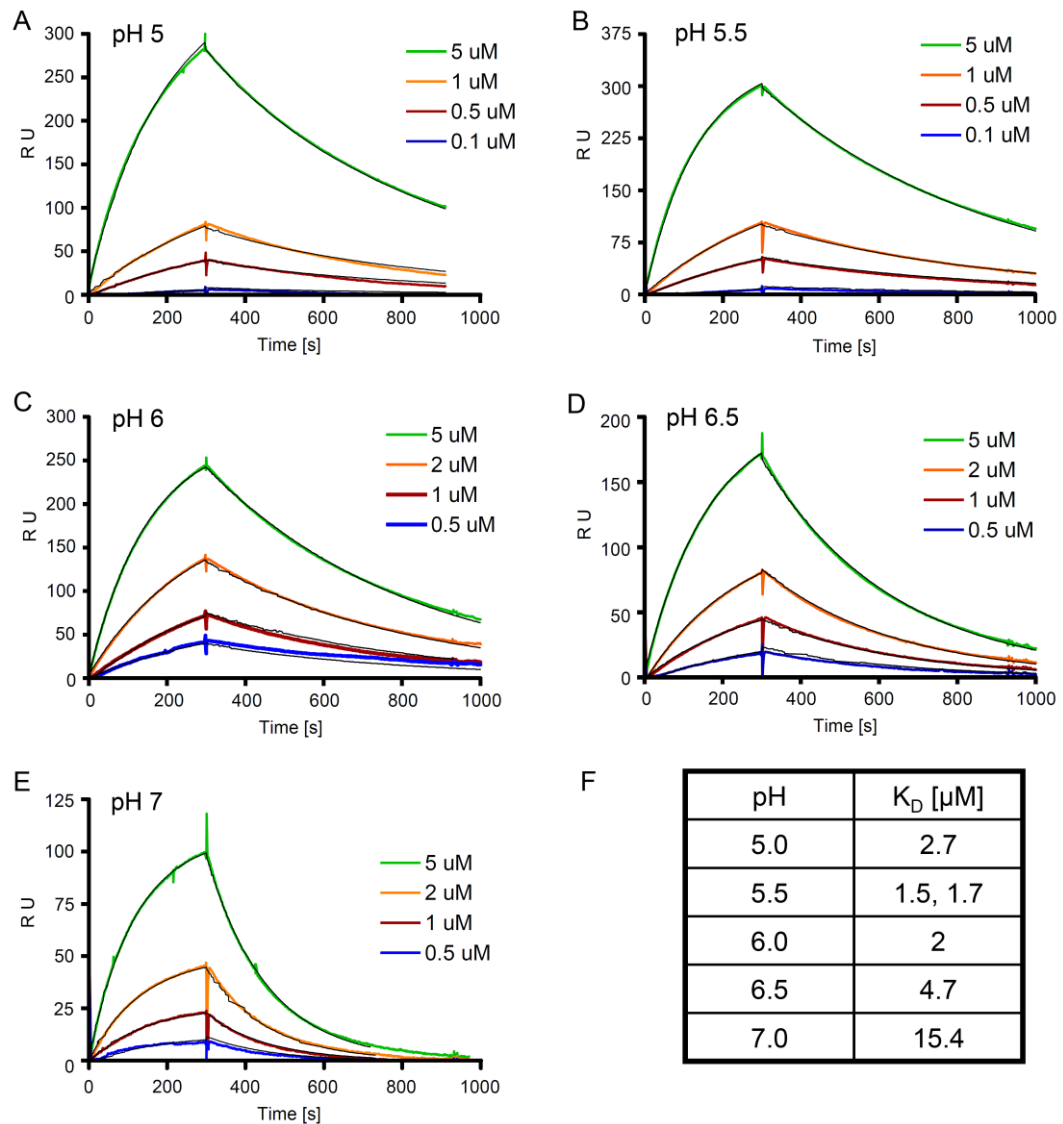


Figure 3.3: Measuring affinity of DM to DR1 carrying an N-terminally truncated HA peptide at different pH using surface plasmon resonance. (A-E) DM and DM mutant (αR98A , αR194A) were immobilized in consecutive flow cells of streptavidin chips. DR1 carrying an N-terminally truncated HA peptide variant was injected for five minutes at the indicated concentrations at 25 °C in citrate phosphate buffer with the indicated pH. After protein injection, buffer with the indicated pH was injected to measure dissociation. Binding in the DM mutant flow cell was subtracted from measurements in the DM wild type flow cell. Dissociation constants were determined by curve fitting using 1:1 Langmuir model (black curves). The table in (F) shows the calculated dissociation constants at different pH.

3.3.3 Crystallizing HLA-DR1 carrying a truncated HA peptide, in the presence of HLA-DM and alone

For co-crystallization experiments purified DM and DR1 carrying an N-terminally truncated HA peptide were mixed at a 1 to 1 ratio and concentrated to a total concentration of ~ 10 mg/mL. As SPR experiments showed strongest DM affinity to the covalent DR1/peptide complex at acidic pH (see 3.3.2), a sparse matrix screen containing conditions with pH lower than 6.5 was prepared. Around 480 initial crystallization conditions were screened.

Of the initial screens two crystallization conditions were of further interest, one containing ammonium sulfate and DMSO, the other one sodium acetate and PEG 10,000. However both conditions, although set up with a DM/DR1 mixture, yielded only DR1 crystals. The ammonium sulfate condition looked very promising as initial crystallization drops already resulted in small but single protein crystals. The crystals were further optimized and in the end reached a size of 200 μm x 80 μm x 80 μm . However, as will be described in the next paragraph, data obtained from crystals grown in this condition were difficult to analyze due to crystallographic problems. Therefore, the second crystallization condition was pursued as well.

The sodium acetate condition initially yielded only fine needles. However, upon optimization by varying pH and the concentration of the precipitant, longer and thicker needle/rod-shaped crystals were obtained with dimensions of up to 700 μm x 70 μm x 50 μm .

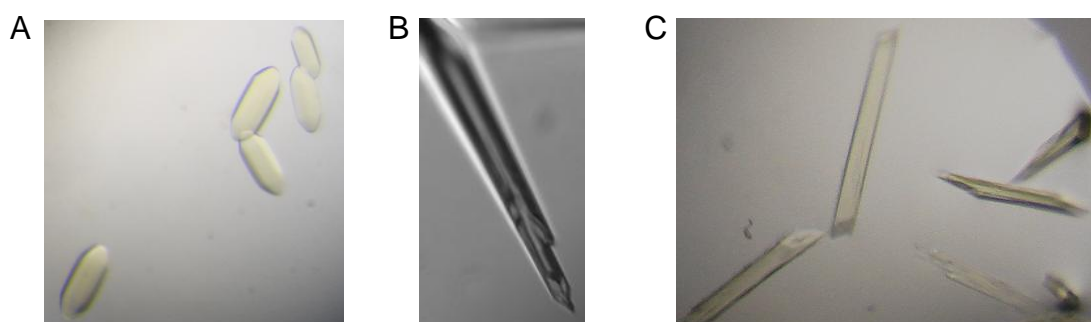


Figure 3.4: Crystals of DR1 carrying an N-terminally truncated HA peptide. (A) DR1 crystals were grown in 2.5 M ammonium sulfate and 10 % DMSO at 20 °C. The dimensions of the crystals were 200 μm x 80 μm x 80 μm . (B+C) DR1 crystals were grown in 100 mM sodium acetate (pH 4.3), 9 % PEG 10,000 at 20 °C. The largest crystals had dimensions of 700 μm x 70 μm x 50 μm .

3.3.4 Solving the structure of HLA-DR1 carrying an N-terminally truncated HA peptide

DR1 crystals obtained with the ammonium sulfate condition were measured by X-ray synchrotron radiation and diffracted up to 3.1 Å. Indexing of the diffraction data revealed that the DR1 molecules crystallized in a hexagonal lattice. However, determining the unit cell was not straight forward as the data could be indexed in a small ($a = b = 118$ Å, $c = 359$ Å) and a large unit cell ($a = b = 204$ Å, $c = 359$ Å) indicating pseudo-translation, which was further confirmed by the presence of a strong off-origin peak in the native Patterson map. The structure was finally solved by molecular replacement, but potential twinning made it difficult to definitively determine the space group and refine the structure. The R_{free} factor was stalled at ~ 32 % and for some parts of the molecule it was difficult to unambiguously interpret the electron density.

Because of these crystallographic problems crystals of another crystallization condition were pursued containing sodium acetate. The needle/rod-shaped crystals were stepwise exposed to synchrotron radiation to minimize radiation damage and several complete data sets were collected from single crystals with a resolution of up to 2.14 Å (table 2.1). The DR1 protein crystallized in a monoclinic lattice with space group $C222_1$ and cell dimensions were unambiguously determined ($a = 96$ Å, $b = 111$ Å, $c = 211$ Å). Applying molecular replacement, the structure was solved and two molecules were found in the asymmetric unit. No indications of pseudo-translation or twinning were detected and the structure was refined without involvement of crystallographic problems. In the end an R_{work} factor of 20.8 % and an R_{free} factor of 23.5 % were reached.

Table 3.1: Data collection and refinement statistics of DR1 carrying an N-terminally truncated HA peptide. The data set was collected at beamline 23-ID-D at GM/CA-CAT at the Advanced Photon Source of the Argonne National Laboratory, IL, USA. The crystal was grown in 100 mM sodium acetate (pH 4.3) and 9 % PEG 10,000 at 20 °C and its dimensions were 700 μm x 70 μm x 50 μm . Values in parenthesis refer to the highest resolution shell.

Data collection	
Space group	C222 ₁
Cell dimensions	
a, b, c (Å)	95.8, 111.4, 211.4
Resolution (Å)	50.0-2.14 (2.18-2.14)
R _{merge} (%)	8.4 (34.4)
I/ σ I	31.7 (5.4)
Completeness (%)	94.6 (90.6)
Redundancy	6.4 (6.2)
Refinement	
Resolution (Å)	38-2.14
No. unique reflections	59393 (2862)
R _{work} /R _{free} (%)	20.8/23.5
Number of atoms (ASU)	
Protein	6159
Peptide	159
Water	362
B-factors (Å²)	
Protein	35.0
Peptide	40.3
Water	38.1
R.m.s. deviations	
Bond lengths (Å)	0.007
Bonds angles (°)	1.055

3.3.5 Structure of HLA-DR1 carrying an N-terminally truncated HA peptide

Using molecular replacement the structure of DR1 carrying an N-terminally truncated HA peptide was solved to 2.14 Å resolution. The two DR1 molecules found in the asymmetric unit exhibit similar protein conformations with different crystal contacts with one crystal contact being of particular interest. As can be seen in figure 3.5, the flexible C-terminus of the DR α chain of a DR1 molecule binds to the partially empty peptide-binding groove of an adjacent DR1 molecule where normally the peptide N-terminus is bound. This intermolecular contact, which occupies only one of the two peptide-binding grooves in the asymmetric unit, is stabilized by hydrogen bonds between the DR α C-terminus and conserved MHC II residues. The same MHC II residues are involved in the conserved hydrogen bond network between peptide N-terminus and MHC II molecule. For example His β 81, which generally interacts with the peptide backbone of residue P-1, builds a hydrogen bond to the carboxyl group of the DR α C-terminus. Furthermore, the side chain of residue Ser α 53 forms a hydrogen bond

to the peptide backbone of residue Leu α 211 of the C-terminal DR α chain. Overall the DR α C-terminus is not as closely and tightly packed in the DR binding groove as can be observed for the peptide N-terminus in crystal structures of MHC II/peptide complexes (figure 3.9). However the extended intermolecular interactions show the ability of this DR region to bind protruding protein parts and might bind certain DM regions in a similar way during DM/DR interaction after partial peptide release. One hypothesis was that the N-terminus of the DM α chain could interact with the partially empty peptide-binding groove of DR in a similar way and was further investigated by surface plasmon resonance experiments as described in section 3.3.7.

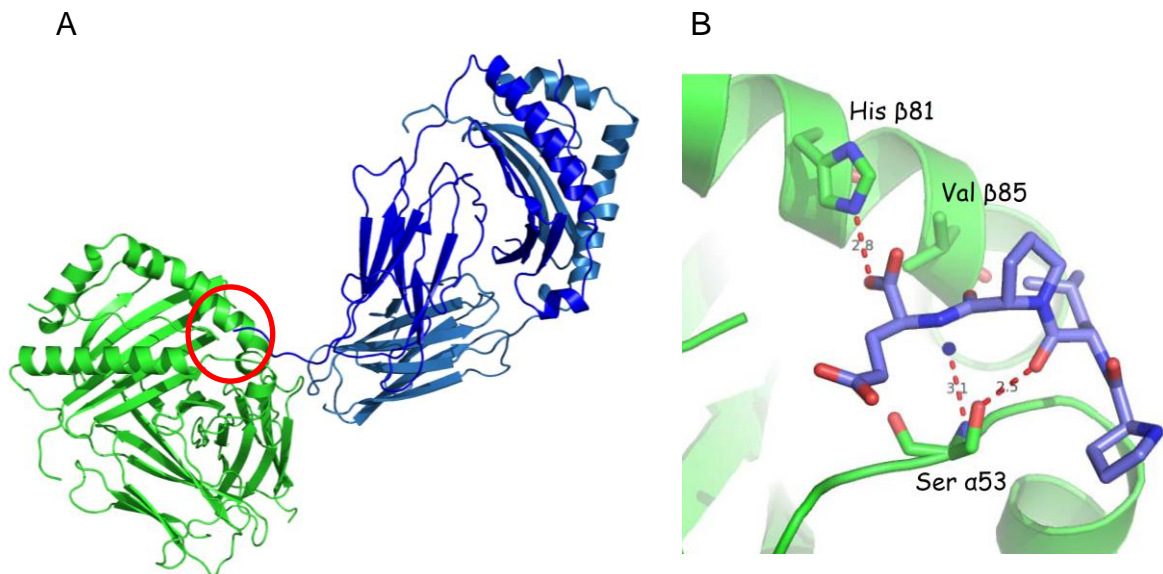


Figure 3.5: C-terminus of DR α chain of one DR1 molecule in the asymmetric unit binds in the partially empty peptide-binding group of the other DR1 molecule. (A) The two DR1 molecules of the asymmetric unit are shown in cartoon representation. The red circle indicates where the flexible C-terminus of the α chain of one DR1 molecule (blue) binds in the partially empty peptide-binding groove of the other DR1 molecule (green), normally filled with the peptide N-terminus. (B) In green as cartoon representation part of the peptide-binding groove is shown where normally the peptide N-terminus binds. DR residues His β 81, Val β 85 and Ser α 53 are indicated and shown as stick representation. In blue the C-terminus of the α chain of an adjacent DR1 molecule is shown as stick model. Dotted lines indicate hydrogen bonds whereas black numbers display the lengths of the hydrogen bonds in Angstrom. The filled circle in blue indicates a coordinated water molecule.

During refinement of the DR1 structure the peptide and a region of the DR α chain next to the peptide N-terminus were omitted to reduce model bias as these parts could possibly reveal conformational changes. After building missing protein and peptide residues into the observable electron density, extra electron density was visible at the site where normally the P1 peptide residue is bound (figure 3.6). As the HA peptide

which was covalently linked to the DR α chain should be N-terminally truncated with residues P1, P-1 and P-2 missing (VKQNCLKLATK) this site should be empty unless other small molecules bound in the P1 pocket. Therefore, small molecules (e.g. TFA, acetate), which could fit into the extra electron density and were present during crystallization, were built into the extra electron density. However, none of the small molecules sufficiently explained the extra electron density as still negative or positive electron density was observable after model refinement including the small molecules. Upon closer inspection of the extra electron density it looked like the missing part was covalently linked to the peptide N-terminus, i.e. an additional residue would be present at the peptide N-terminus. In fact, when an additional valine was built at the peptide N-terminus the extra electron density was well explained. The additional valine at the peptide N-terminus (VVKQNCLKLATK) likely resulted from a peptide contaminant during peptide synthesis. Such a peptide would preferentially bind to DR1 molecules as it has higher affinity to DR1 due to the additional valine as P1 anchor compared to the primarily present peptide lacking a P1 anchor residue (VKQNCLKLATK). To further prove the presence of an additional valine at P1 position the peptide was eluted from DR1 molecules used for crystallization experiments and was analyzed by mass spectrometry (see 3.3.6).

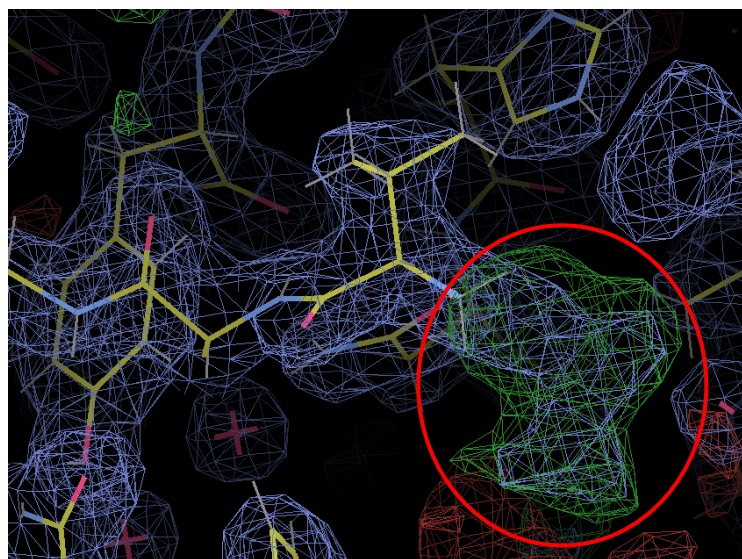


Figure 3.6: Electron density ($2F_o-F_c$) of the peptide N-terminus showing extra electron density (F_o-F_c) for an additional peptide residue. The peptide N-terminus and parts of the DR1 molecule are shown as stick model. The electron density is shown in mesh representation ($2F_o-F_c$: blue, F_o-F_c : green). The peptide extends horizontally with the N-terminus at the right side. In the front parts of residues of the DR α chain and in the background residue His β 81 of the DR β chain can be seen. The red circle indicates extra electron density accounting for an additional valine at the peptide N-terminus.

Figure 3.7 (A, B) shows an overlay of the peptide-binding groove of the newly solved DR1 structure carrying an N-terminally truncated HA peptide (green) with the previously published DR1 structure carrying a full length HA peptide (orange). As can be seen from the superimposition no major conformational change was observed in the DR1 region around the partially empty peptide-binding groove and the overall conformation of the DR α and DR β chains stayed intact. However, the DR α and DR β helices normally next to the peptide N-terminus were further apart (0.8-0.9 Å) in the DR1/HA(P_{1,Val}-P₁₁) structure compared to the DR1 structure carrying a full length HA peptide (figure 3.7, B) and also carrying a CLIP(106-120) peptide missing residue P-2 (figure 3.10).

It was surprising that greater conformational changes were not observed since in the absence of two N-terminal peptide residues (P-2, P-1) several peptide/MHC II interactions were missing resulting in possible destabilization of the respective DR1 region. For example, two hydrogen bonds normally formed between peptide residue P-2 and DR residues Ser α 53 and Phe α 51 could not be formed (figure 3.7, C, D). Furthermore, the hydrogen bond between peptide residue P-1 and His β 81 could not be built and instead His β 81 formed a bridged hydrogen bond to the amine group of the peptide N-terminus (P1 residue) that was mediated by a coordinated water molecule. However, the other three N-terminal hydrogen bonds formed by peptide residues P2 and P1 with DR1 residues Asn β 82 and Ser α 53 were unmodified. Concerning the peptide conformation, peptide residue valine at position P2 exhibited a different rotamer in the DR1/HA(P_{1,Val}-P₁₁) structure as had been seen for the same peptide residue in the DR1 structure carrying a full length HA peptide (figure 3.7, C, D).

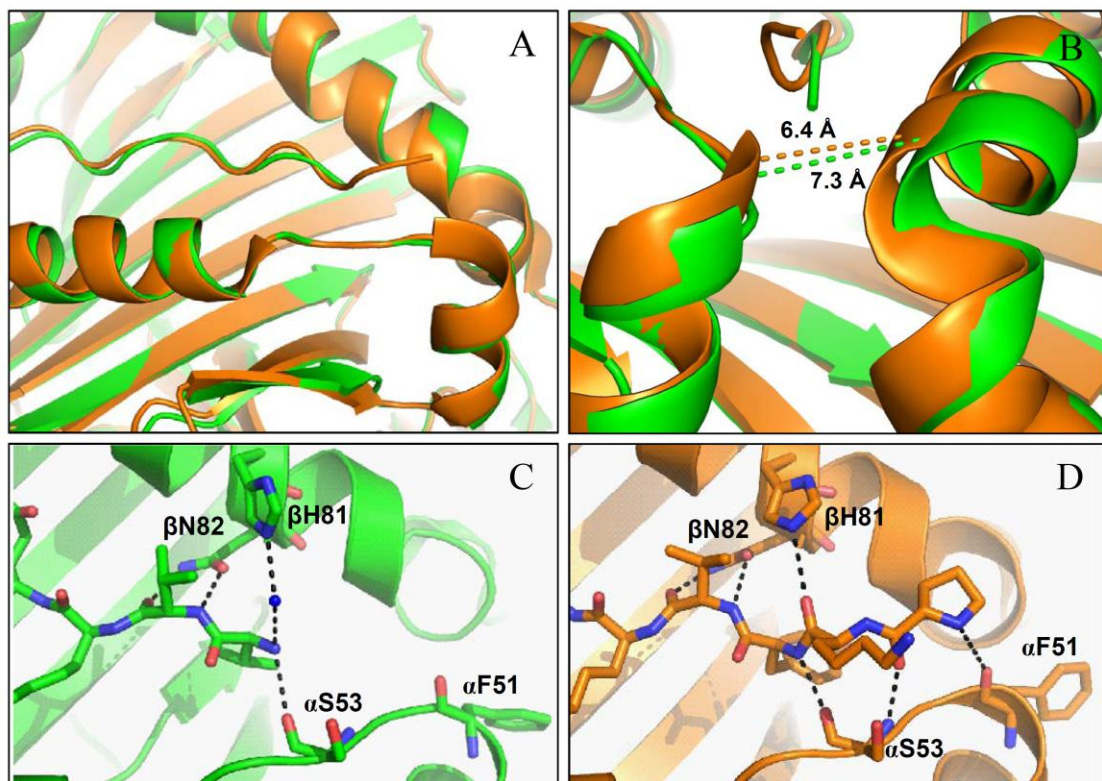


Figure 3.7: Comparison of the peptide-binding groove of DR1 carrying a full length HA peptide versus carrying an N-terminally truncated HA peptide. (A, B) The new DR1 structure carrying an N-terminally truncated HA peptide (green) is superimposed with the previously published DR1 structure carrying a full length HA peptide (PDB: 1DLH, orange). (A) No major conformational changes of the peptide-binding groove were observed. (B) The helices of the DR α and DR β chains adjacent to the peptide N-terminus are further apart in the DR1 structure missing two N-terminal peptide residues, 7.3 Å versus 6.4 Å. Distances were measured between C α atoms of residues Ala α 52 and Val β 85. (A, B) DR1 molecules and peptides are shown as cartoon representation. (A, B, C, D) Part of the peptide-binding groove is shown which binds the N-terminal part of the peptide. (A, C, D) DR α chain can be seen in the foreground and DR β chain in the background. The peptide extends horizontally with the N-terminus at the right side. (B) DR α chain can be seen on the left and DR β chain on the right. The peptide N-terminus is pointing towards the observer. (C) The peptide-binding groove of the DR1 structure is shown binding an N-terminally truncated HA peptide with an additional valine at P1 position and residues P-2 and P-1 missing. A coordinating water molecule between His β 81 and the peptide N-terminus is shown as filled circle in blue. (D) The peptide-binding groove of the previously published DR1 structure (1DLH) is shown binding a full length HA peptide. (C, D) DR molecules are shown as cartoon representation and bound peptides as stick model. DR1 residues interacting with the peptide N-terminus are labeled and shown as stick representation. Hydrogen bonds between DR1 and peptide are shown as dotted lines.

Next, the conformations of conserved DR residues around the peptide-binding groove of DR1/HA(P_{1,Val}-P₁₁) were compared with the conformations of DR residues of previously published DR structures to detect minor changes of the partially empty peptide-binding groove. Most of the conserved residues in the peptide-binding area either overlapped quite well with the conformation of the residues of the newly solved DR1/HA(P_{1,Val}-P₁₁) structure or showed general conformational variability like residue Phe α 51. However residue Val β 85, which showed a conserved conformation for previously published DR structures (see figure 3.8, A), revealed a different conformation with the valine rotated outwards from the peptide-binding groove (see figure 3.8, B). At first, the rotation seems to be a subtle conformational change, but is of particular relevance as Val β 85 is involved in forming the crucial P1 pocket which is important for peptide-binding. By rotation of Val β 85 the pocket is opened up on one side (figure 3.8, B). This can be nicely seen in the surface representation of the peptide-binding groove of DR1/HA(P_{1,Val}-P₁₁) (figure 3.8, C) and is further illustrated by comparison with the fully closed P1 pocket exhibited by the DR1 structure carrying a full length HA peptide (figure 3.8, D). The rotated conformer of Val β 85 was also observed for the DR1/HA(P_{1,Val}-P₁₁) molecule exhibiting a peptide-binding groove interacting with the C-terminus of an adjacent DR1 molecule as described above. As the C-terminus binds further away than the peptide N-terminus the peptide-binding site is still destabilized as the tight peptide/MHC II interactions are not compensated (figure 3.9). The conformational change of Val β 85 might occur as the tight interactions with peptide residues P-1 and P1 are absent and diminished, respectively. The altered rotamer of Val β 85 was not observed for the DR1/CLIP structure missing residue P-2 (Gunther et al., 2010) and may be dependent on the absence of residue P-1 (figure 3.10). With regard to the entire process of peptide release a partial opening of the P1 pocket in consequence of the release of the two N-terminal peptide residues (P-2, P-1) likely destabilizes the P1 anchor residue and might further facilitate release of the entire peptide.

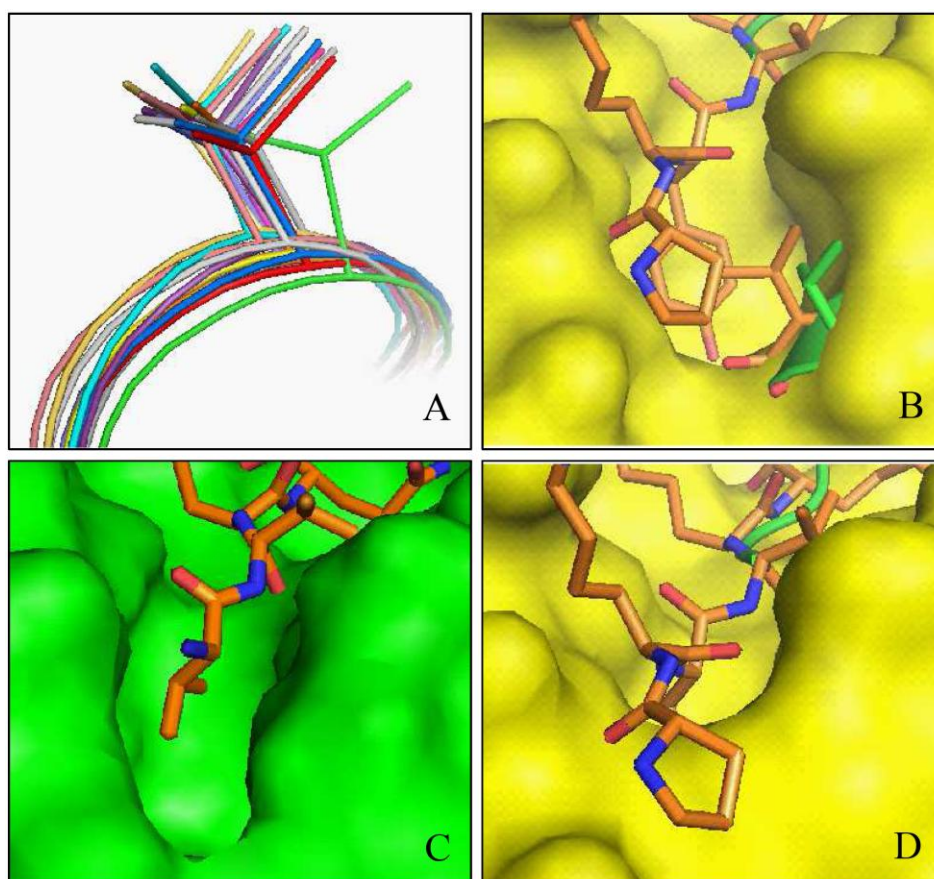


Figure 3.8: Minor conformational changes of Val β 85 were observed affecting the P1 pocket. (A) The newly solved structure DR1/HA(P_{1,Val}-P₁₁) was superimposed with other DR structures and the conserved residue Val β 85 is shown as stick model. It can be seen that the conformation (rotamer) of Val β 85 is conserved for DR molecules carrying a peptide containing residue P-1. However Val β 85 of DR1/HA(P_{1,Val}-P₁₁) exhibits a different conformer. The distance between C $_{\beta}$ -atoms of Val β 85 of DR1/HA(P_{1,Val}-P₁₁) and other DR molecules is 0.9-1.7 Å. DR1/HA(P_{1,Val}-P₁₁) (green), DR1/HA (1DLH, cyan), DR2/MBP (1BX2, purple), DR3/CLIP (1A6A, yellow), DR4/human collagen II peptide (2SEB, light pink), DR1/CLIP(106-120)_{flipped} (3PGC, grey), DR1/CLIP(102-120) (3PDO, purple blue), DR1/CLIP(106-120)_{canonical} (3PGD, orange), DR1/A2(103-117) (1AQD, red), DR2/MBP (1HQR, pink), DR1/HA (1HXY, pale yellow), DR4/HA (1J8H, purple), DR1/TPI(23-37) (1KLU, grey). (B) In the crystal structure of DR1/HA(P_{1,Val}-P₁₁) which is missing two N-terminal peptide residues (P-2, P-1), Val β 85 is rotated outwards from the binding groove opening up the P1 pocket on one side (C). In the crystal structure of DR1 with a full length HA peptide (orange/yellow, 1DLH) the P1 pocket is fully closed (D). (B) In yellow the surface representation of DR1 (1DLH) is shown except Val β 85 which is shown as stick model (orange). The structure DR1/HA(P_{1,Val}-P₁₁) was superimposed and residue Val β 85 is shown as stick model (green). The full length HA peptide of DR1/HA (1DLH) is shown as stick model (orange). (C) The DR molecule of DR1/HA(P_{1,Val}-P₁₁) is shown as surface representation (green) and the N-terminally truncated HA peptide P_{1,Val}-P₁₁ is shown as stick model (orange). (D) The DR molecule of DR1/HA (1DLH) is shown as surface representation (yellow) and the full length HA peptide as stick model (orange).

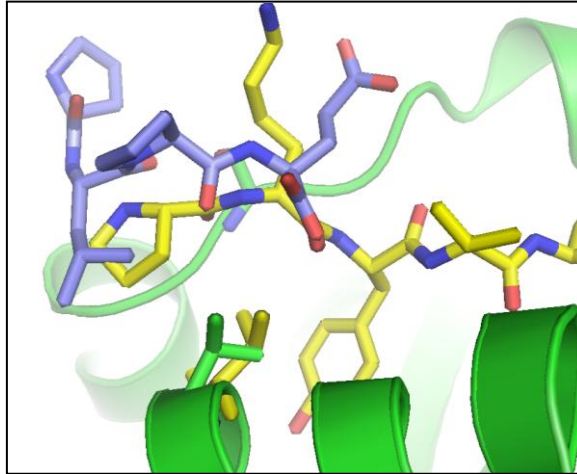


Figure 3.9: C-terminus of adjacent DR1 molecule binds further away than N-terminal part of full length HA peptide binds to DR1. The rotated conformer of Val β 85 was also observed for the DR1 molecule, which exhibits a peptide-binding site that interacts with a C-terminus of an adjacent DR1 molecule. As the C-terminus binds further away than the peptide N-terminus the tight interactions between peptide and MHC II molecule are not imitated. In green as cartoon representation, DR α (background) and DR β chain (foreground) can be seen of DR1/HA(P_{1,Val}-P₁₁) forming part of the peptide-binding groove. Residue Val β 85 is shown as stick model. The previously published DR1/HA structure (1DLH) was superimposed and the full length HA peptide and residue Val β 85 are shown as yellow stick representation. In blue as stick representation the DR α C-terminus of the adjacent DR1 molecule of DR1/HA(P_{1,Val}-P₁₁) can be seen.

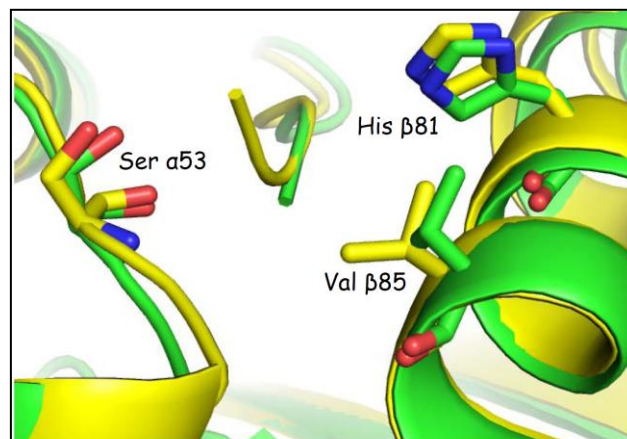


Figure 3.10: Comparison of the DR1 peptide-binding groove carrying an N-terminally truncated HA(P_{1,Val}-P₁₁) peptide and a CLIP(106-120) peptide missing P-2. The new DR1/HA(P_{1,Val}-P₁₁) structure (green) is superimposed with the previously published DR1 structure carrying a CLIP(106-120) peptide (3PGD, yellow). The helices of the DR α and β chains adjacent to the peptide N-terminus are further apart in the DR1/HA(P_{1,Val}-P₁₁) structure and the altered conformer of Val β 85 is not observed for the DR1/CLIP(106-120) structure. DR1 molecules and peptides are shown as cartoon representation and relevant DR residues are indicated and represented as stick model.

3.3.6 Eluting N-terminally truncated HA peptide from HLA-DR1 protein used for crystallization and analyzing by mass spectrometry

The peptide stock solution, used to prepare the crystallized DR1/peptide complex, was analyzed to investigate whether a peptide contaminant derived from peptide synthesis exhibited an additional valine at position P1 seen in the electron density (3.3.5). Therefore, the peptide solution was analyzed by mass spectrometry in combination with liquid chromatography and individual peptide sequences were determined by identifying resulting peptide fragments. Indeed a minor peptide component was found that included an additional valine at position P1 (VVKQNCLKLTK) besides the primary peptide with sequence VKQNCLKLTK.

To further investigate whether the peptide contaminant also bound to DR1, bound peptide was eluted from DR1 protein used for crystallization. Under reducing conditions the covalently linked peptide was released from DR1 and as the peptide carried a C-terminal DNP-label the peptide was separated from protein using α -DNP affinity chromatography. The eluted peptide sample was analyzed by mass spectrometry and the peptide contaminant was detected in addition to the primary peptide species. As can be seen in the mass spectrum in figure 3.11, the particular peptide contaminant carrying a valine at P1 position was even enriched on DR1 after peptide loading likely due to the higher affinity to DR1 compared to the primary peptide missing a P1 anchor.

Therefore, DR1 protein used for crystallization contained both peptide species and DR1 carrying the peptide contaminant including a P1 anchor might have crystallized preferentially as it presumably exhibits higher stability.

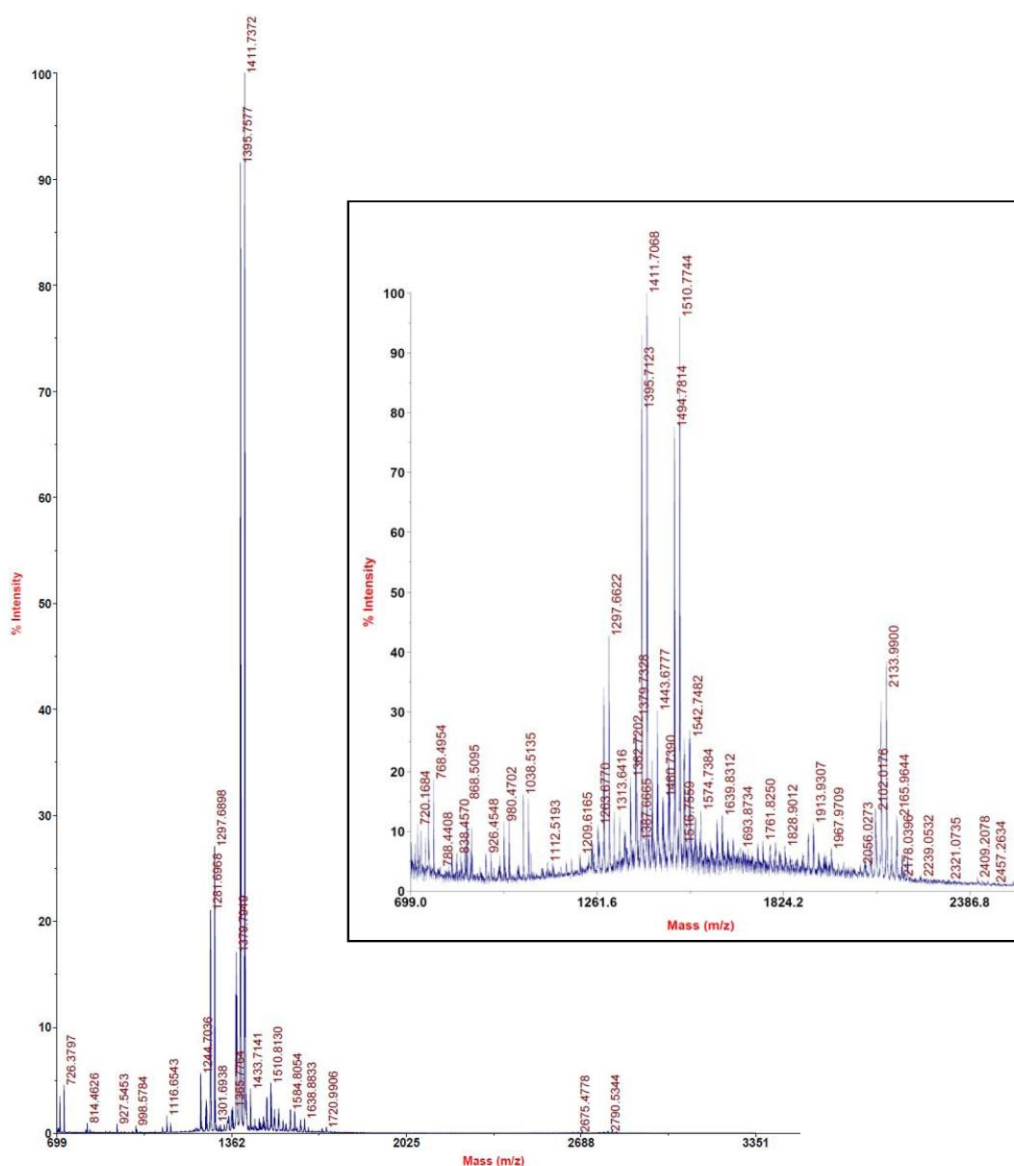


Figure 3.11: Mass spectra of a synthesized HA peptide variant prior to DR1 binding and eluted from DR1 protein used for crystallization (inset). Mass spectrum of a sample of the stock solution of synthesized N-terminally truncated HA peptide used for loading DR1 molecules. The main peak at 1412 Da corresponds to the main peptide species, an HA peptide variant missing residues P-2, P-1 and P1 (VKQNCLKLATK-DNP). A minor peak at 1511 Da can be seen representing an HA peptide variant missing residues P-2, P-1 and containing an additional valine at P1 position (VVKQNCLKLATK-DNP). Inset: The covalently linked HA peptide variants were eluted from DR1 molecules under reducing conditions. An enrichment of the HA peptide variant with a mass of 1510 Da is observed. High background signal can be seen due to low peptide concentration.

3.3.7 Measuring HLA-DR binding to N-terminally truncated HLA-DM using surface plasmon resonance

As one of the two peptide-binding sites in the structure of DR1/HA(P_{1,Val}-P₁₁) interacts with the flexible C-terminus of an adjacent DR1 molecule (3.3.5), the question was raised whether the N-terminus of the DM α chain might bind to DR in a similar way and could be involved in peptide exchange. The N-terminus is present on the outer face of DM and could reach the DM/DR binding site. Therefore, eleven residues of the DM α chain were truncated and DR binding assays were performed using surface plasmon resonance. However, as can be seen in figure 3.12, the truncated DM bound as well as the unmodified DM molecule to DR1 carrying a low-affinity CLIP peptide. Therefore, the possibility can be excluded that the N-terminus of the DM α chain is involved in DR binding.

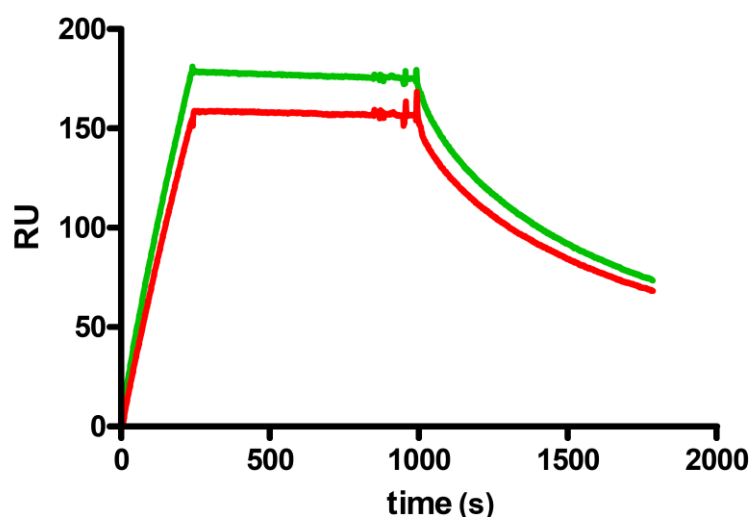


Figure 3.12: Measuring DR binding to N-terminally truncated DM using surface plasmon resonance. In consecutive flow cells 500 RU of DM mutant (α R98A, α R194A), DM with N-terminally truncated α chain and DM wild type, respectively, were immobilized and DR1/CLIP_{low} (2 μ M, V8 cleaved) injected for four minutes at a flow rate of 15 μ L/min. After buffer injection full length HA peptide (50 μ M) was injected. The experiments were carried out in 50 mM citrate phosphate buffer (pH 5.3), 150 mM NaCl at 25 $^{\circ}$ C. The green line displays DR binding to truncated DM (third flow cell) and the red line DR binding to DM wild type (fourth flow cell). DR binding in the second flow cell (DM mutant) was subtracted from measurements in the third (DM with N-terminally truncated α chain) or fourth flow cell (DM wt), respectively. The DR solution consecutively passed through flow chambers one to four, which can be also the reason why less DR binding was observed for flow cell four.

3.3.8 Measuring HLA-DM binding to HLA-DR1 carrying an HA peptide variant with a valine at P1 position and two N-terminal peptide residues absent

As the DR1/peptide complex used for SPR (figure 3.3) and crystallization experiments (figure 3.4) contained two HA peptide variants, one missing a P1 residue and the other one containing a valine at P1 position, shown by mass spectrometry (figure 3.11), it had to be determined whether both or only one of the complexes bind to DM. Previous experiments (Anders et al., 2011) had shown that if the DR1 molecule carried an HA peptide variant missing two N-terminal residues and contained a tyrosine at P1 position, no DM binding was observed. The question was whether DM binding could be detected with a DR1/peptide complex including a smaller anchor residue as valine. Therefore, DR1/peptide complexes were prepared with synthesized HA peptide variants missing residues P-2, P-1 and one peptide specifically containing a valine at P1 position and another one containing a glycine at P2 position and no P1 residue. Both complexes were used to carry out SPR experiments. The HA peptide with a glycine at position P2 (P-2, P-1, P1 missing) was synthesized by a different company and highly purified after synthesis to avoid contaminations. A glycine was chosen for the P2 position to ensure that even if a by-product of the peptide synthesis would include an additional glycine at position P1 it would not represent an anchor residue.

As can be seen in figure 3.13 DM binding was observed for the DR1 complex carrying an HA peptide missing two N-terminal peptide residues and containing a valine at P1 position although significantly less than for the previously used DR1 complex containing a mixture of HA(P_{1,Val}-P₁₁) and HA(P₂-P₁₁) peptides. More DM binding than to the previously used DR1 complex was observed with the DR1/peptide complex carrying an HA peptide with a glycine at P2 position and most probably no P1 residue. In figure 3.13 (B) it can be seen that DM binding to the DR1/complex containing an HA peptide with a valine at P1 position (HA(P_{1,Val}-P₁₁)) is concentration dependent. Interestingly, the off-rate of DR1/HA(P_{1,Val}-P₁₁) is slower compared to the off-rates of DR1/HA(P₂-P₁₁) and DR1/HA(P_{2,Gly}-P₁₁) which could indicate that the valine at P1 position may stabilize a DR conformer that binds to DM.

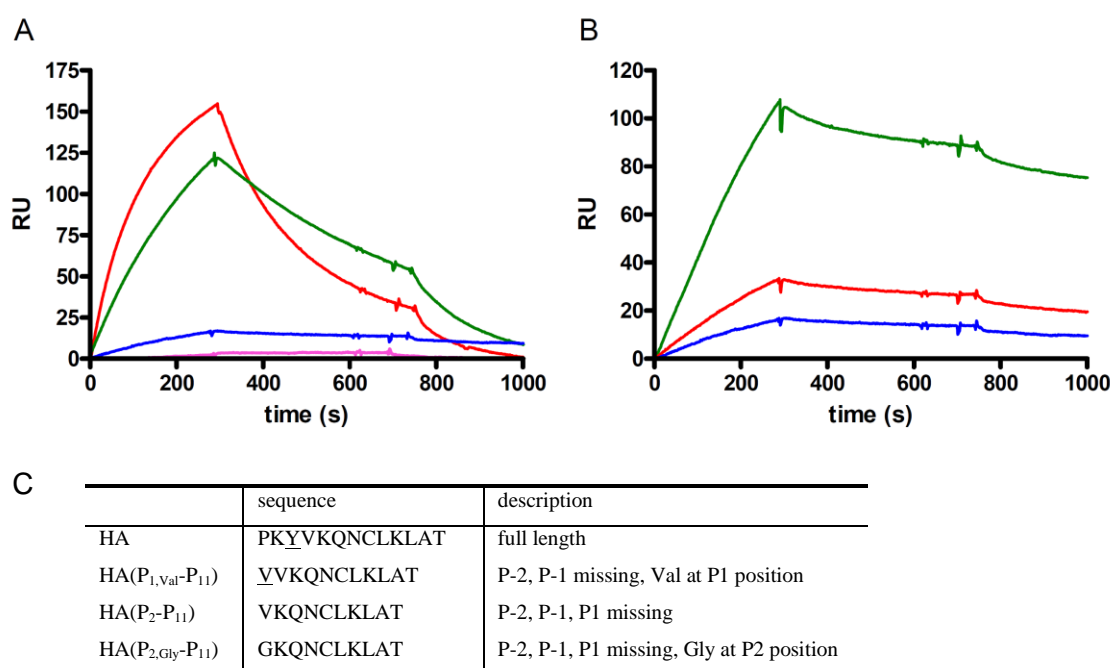


Figure 3.13: Measuring DM binding of DR1 molecules carrying various HA peptide variants using surface plasmon resonance. (A) DR1 molecules (2 μ M) were injected carrying various covalently bound HA peptide variants, full length HA peptide (pink), HA(P_{1,Val}-P₁₁) (blue), mixture of HA(P₂-P₁₁) and HA(P_{1,Val}-P₁₁) (green), HA(P_{2,Gly}-P₁₁) (red). (B) DR1 with covalently linked HA(P_{1,Val}-P₁₁) peptide was injected at various concentrations, 2 μ M (blue), 4 μ M (red) and 10 μ M (green). (A, B) DR1/peptide complexes were injected for 5 minutes with a flow rate of 15 μ L/min following buffer injection for 5 minutes and injection of full length HA peptide (50 μ M). The experiments were carried out in 50 mM citrate phosphate buffer (pH 5.3), 150 mM NaCl at 25 °C. Binding in the DM mutant flow cell was subtracted from measurements in the DM wild type flow cell. The table in (C) shows the peptide sequences and a description of the different HA peptide variants. The position of the P1 anchor is underlined.

3.3.9 Measuring HLA-DM binding to HLA-DR1 mutant (Val β 85Asp) using surface plasmon resonance

As described in 3.3.5 the crystal structure of DR1/HA(P_{1,Val}-P₁₁) revealed no major conformational changes although the two N-terminal peptide residues were missing. However, as a consequence of the absent peptide residues, DR residues that normally make contact with the peptide N-terminus became exposed. These residues are alanine 52 and serine 53 of the DR α chain and valine 85 and histidine 81 of the DR β chain (figure 3.14). As release of the peptide N-terminus is crucial (Anders et al., 2011) for DM binding, DM may bind in the DR region where normally the peptide N-terminus binds and make contact to some of the newly exposed DR residues, which could stabilize the region. To test this hypothesis residue Val β 85, which is usually buried

under the peptide N-terminus (residues P-2, P-1), was mutated to aspartic acid introducing a charged residue at that site. DM binding of the DR1 mutant was compared to DM binding of the DR1 wild type using surface plasmon resonance. Both molecules carried a covalently linked HA peptide missing residues P-2, P-1, P1 and containing a glycine at position P2 to ensure the respective DR1 region is exposed.

As can be seen in figure 3.15 less DM binding was observed for DR1 mutant than for DR1 wild type indicating DM binding occurred more slowly for the mutant than for the wild type. However, the off-rate of the mutant was also slower than the off-rate of the wild type making it difficult to determine whether the overall affinity of the mutant is lower. More mutations in the respective DR region have to be tested for DM binding to further investigate this hypothesis

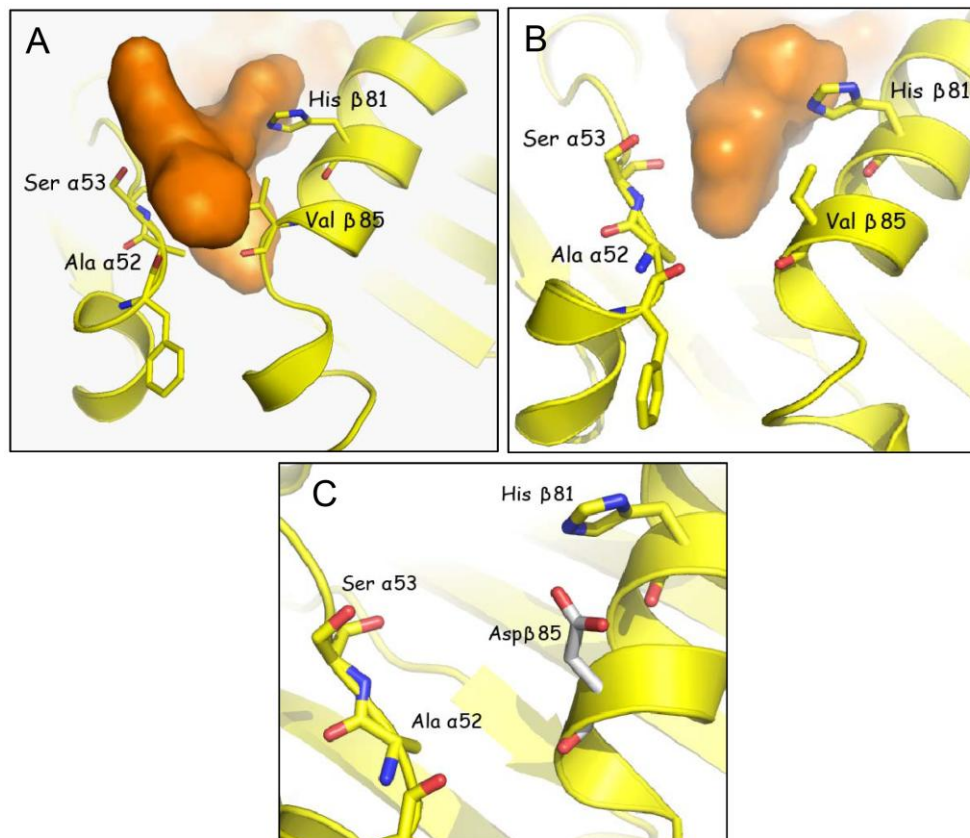


Figure 3.14: DR1 residues become accessible once the two N-terminal peptide residues (P-2, P-1) are absent. The DR1 residues Ser α 53, Ala α 52, His β 81 and Val β 85, which are covered by peptide residues in the complex of DR1 with full-length HA-peptide, (A) become exposed once the two N-terminal peptide residues (P-2, P-1) are absent (B). Peptide N-termini with part of the peptide-binding groove of DR1/HA (1DLH) (A) and DR1/HA(P_{1,Val}-P₁₁) (B) are shown. (C) Model showing an aspartic acid residue at position 85 of DR β chain. (A, B, C) DR molecules are shown as cartoon depictions and peptides are shown as surface representations.

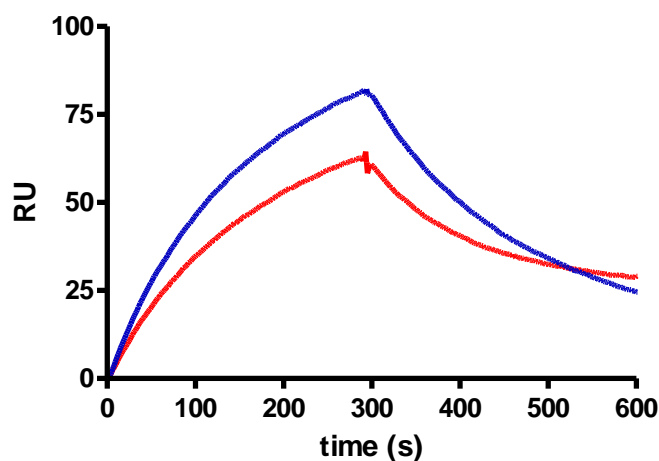


Figure 3.15: Comparing DM binding of DR1 wild type and DR1 mutant with residue Val885 mutated to aspartic acid. DR1 wild type and DR1 mutant (Val885Asp) carrying HA(P_{2,Gly}-P₁₁) peptide were injected at 1 μ M. As can be seen DR1 mutant (red) binds to DM with a slower on-rate and a slower off-rate than DR1 wild type (blue). DR1/peptide complexes were injected for 5 minutes with a flow rate of 15 μ L/min following buffer injection for 5 minutes and injection of full length HA peptide (50 μ M). The experiments were carried out in 50 mM citrate phosphate buffer (pH 5.3), 150 mM NaCl at 25 $^{\circ}$ C. Binding in the flow cell of DM mutant was subtracted from measurements in the DM wild type flow cell.

3.4 Conclusion

To determine the co-crystal structure of DR and DM co-crystallization experiments were set up with a modified DR1/peptide complex carrying an N-terminally truncated HA peptide, which showed higher affinity to DM than DR molecules carrying full length peptides. To determine conditions favoring crystallization of the non-covalently linked DR/DM complex versus the individual proteins, the affinity of the DR/DM complex was measured at different pH applying surface plasmon resonance. The experiments revealed that the pH optimum for DM/DR binding is around pH 5.5 and a major drop in DM binding was observed between pH 6.5 and pH 7.0 with dissociation constants of 4.7 μ M and 15.4 μ M, respectively. The results agree with previous data measuring increased DM activity at acidic pH present in the late endosome (Sloan et al., 1995) where DM catalysis happens. Therefore, crystallization experiments were set up using customized crystallization conditions with pH lower than 6.5.

Unfortunately, the DM/DR complex did not crystallize, however, the DR1 molecule with an N-terminally truncated HA peptide yielded crystals which revealed a DR1 structure (2.14 \AA resolution) carrying a peptide missing two N-terminal peptide residues (P-2, P-1) and containing an additional valine at position P1. That the peptide included a

P1 residue was surprising as a synthesized HA peptide variant was used for the preparation of the DR/peptide complex lacking all three N-terminal peptide residues. As was confirmed later by mass spectrometry, a side-product of the peptide synthesis likely bound to DR1 carrying an additional valine at P1 position. The minor species was probably enriched due to two selection processes, i.e. preferential binding during the peptide loading step based on higher peptide affinity and favored crystallization based on higher stability of the DR/peptide complex. SPR experiments revealed that the DR1 complex carrying an HA peptide variant with a valine at P1 position and two N-terminal peptide residues missing binds to DM, although the extent of DM binding is lower than that of DR1/peptide complex lacking a P1 anchor. Previously DR1 with an HA peptide variant containing a tyrosine as P1 anchor (P-2, P-1 missing) displayed only marginal binding to DM; however, it seems that the presence of valine at P1 position allows DM binding maybe due to its smaller size. Alternatively the valine may more readily leave the pocket due to fewer interactions with the pocket in case DM binding requires an empty P1 pocket to bind DR. That even a full length peptide bound to a DR molecule exhibits extensive mobility has been observed during the studies described in chapter I. The inhomogeneity of the DR1/peptide complex carrying at least two different HA peptide variants may have made it more difficult to crystallize the DR/DM complex, as DM also exhibits lower affinity to the DR/peptide complex containing a P1 anchor.

The DR1 crystal structure revealed an interesting crystal contact with the flexible C-terminus of the DR α chain binding to the empty part of the peptide-binding groove of a neighboring DR1 molecule demonstrating the affinity of this region for extended peptide strands and protruding protein parts. The resulting hypothesis that DM may bind to DR in a similar way with the solvent exposed N-terminus of the DM α chain possibly reaching the DM/DR interface was excluded by SPR experiments in these studies.

Surprisingly, no major conformational change of DR1 was observed as had been expected due to loss of DR/peptide interactions and lack of three conserved hydrogen bonds. However, smaller conformational changes were observed. First, the helices of the DR α and β chains normally next to the peptide N-terminus were further apart than in the DR1 structure carrying a full length HA peptide (Stern et al., 1994) or a CLIP peptide missing residue P-2 (Gunther et al., 2010). The divergence of the helices is likely due to the missing interactions with the peptide in between them normally holding the helices closer together. Although the DR1 structure can not directly be

compared with the molecular dynamics simulations that were carried out with DR1 molecules lacking the entire peptide (Painter et al., 2008; Rupp et al., 2011), the observations are different as a small divergence and not a narrowing or partially collapsing of the helices around the peptide N-terminus was observed. However, it is also possible that a larger part of the peptide has to be absent for collapse of the groove.

Furthermore, a small conformational change of residue valine $\beta 85$ was observed which is a conserved residue forming part of the P1 pocket and exhibits a conserved rotamer. In the presented structure Val $\beta 85$ is rotated outwards opening up part of the P1 pocket, which probably further destabilizes the P1 residue and may facilitate release of the entire peptide. The altered rotamer of Val $\beta 85$ was not observed for the DR1/CLIP structure missing residue P-2 (Gunther et al., 2010) and may be dependent on the absence of residue P-1.

The absence of two N-terminal peptide residues led to exposure of DR residues (Ala $\alpha 52$, Ser $\alpha 53$, His $\beta 81$ and Val $\beta 85$) that are normally covered by or in contact with the peptide, raising the question whether DM may interact with these newly exposed DR residues and may bind to the DR region normally covered by the peptide N-terminus. To test this hypothesis residue Val $\beta 85$, which is usually covered by peptide residue P-1, was mutated to an aspartic acid introducing a charged residue and SPR experiments revealed a slower on-rate, but also slower off-rate for DM binding of the DR mutant compared to DR wild type. To further investigate this hypothesis more SPR experiments with different mutations in the respective DR region need to be carried out. Summarizing, we can say that if the two N-terminal peptide residues are missing (P-2, P-1) and with it three conserved hydrogen bonds between peptide N-terminus and DR, no major conformational change of the peptide-binding groove is observed. Whether DM binds to the newly exposed DR region and whether release of the P1 anchor residue induces a major conformational change of the DR molecule still has to be determined. However, the presented DR1 structure carrying an HA peptide missing two N-terminal peptide residues reveals a relevant intermediate state during peptide release contributing to a detailed understanding of peptide exchange by MHC II molecules.

4 Chapter III: Investigating HLA-DM binding to high-affinity MHC II/peptide complexes

4.1 Introduction

DM plays an important role as peptide editor of MHC II molecules ensuring the generation of high-stability MHC II/peptide complexes. The presence of MHC II/peptide complexes with a long half-life on the cell surface is important for multiple T cell encounters and potential antigen recognition. Previous studies have shown that low-stability complexes are good substrates for DM-mediated peptide release whereas high-stability complexes are poor substrates with some high-affinity complexes believed to be DM insensitive (Kropshofer et al., 1996). For example, DR1/HA was believed to be resistant to DM action as no DM-facilitated peptide exchange could be observed (Kropshofer et al., 1996; Sloan et al., 1995). Experiments carried out in our lab using an N-terminally truncated peptide revealed that DM binds to a MHC II conformer with a critical part of the binding groove empty (Anders et al., 2011). These novel data suggested that spontaneous release of the peptide N-terminus may be required for initial DM binding and also implied that in contrast to previous assumptions DM theoretically should bind to any MHC II/peptide complex, even if to a small extent, as peptide motion is always present.

It had been shown before that peptide exchange in the presence or absence of DM is dependent on both temperature and pH (Denzin and Cresswell, 1995; Reay et al., 1992; Sloan et al., 1995). Furthermore, previous data revealed that dissociation of the peptide N-terminus represents a crucial component of the energy barrier which has to be overcome explaining the strong temperature dependence of DM binding (Anders et al., 2011). To test whether DM binding to high-stability MHC II/peptide complexes could be enhanced by higher temperature also increasing peptide mobility, SPR experiments were carried out at 25 °C and 37 °C. The SPR experiments at 37 °C were substantially more challenging than experiments at room temperature and had to be carried out carefully as the machine used for measuring surface plasmon resonance is very sensitive and high temperature, for example, can cause spontaneous bubble formation in the flow chambers.

Additionally, to test the functional relevance of the DM binding assay carried out using surface plasmon resonance, data obtained by SPR were compared to functional experiments measuring DM catalyzed peptide exchange by fluorescence polarization. For this purpose, DM binding to a low- and a high-affinity DR/peptide complex was measured by SPR and compared to DM catalyzed peptide exchange of both complexes monitored by fluorescence polarization.

4.2 Materials and Methods

4.2.1 Preparation of HLA-DR/peptide complexes

Soluble DR1/CLIP complexes were produced using stably transfected CHO cells in hollow fiber bioreactors (Day et al., 2003) and purified by affinity chromatography (L243, American Type Culture Collection). Aggregates were removed by gel filtration (Superose 6, GE Healthcare) and the linker between peptide and N-terminus of DR β chain cleaved with thrombin (20 units thrombin/mg protein, 1.5 h, 25 °C). HA(306-318) peptide was synthesized by Peptide 2.0 with a DNP label linked to a lysine group at the peptide C-terminus. For peptide exchange DR1/CLIP was incubated (30 °C, 8 hours) with 50 μ M HA peptide and 50 μ M J10-1 in 50 mM citrate phosphate buffer (pH 5.3), 150 mM NaCl at a protein concentration of 0.3 mg/mL including protease inhibitors. Unbound peptide was removed by gel filtration (Superose 12, GE Healthcare) and DR1/HA further purified by anti-DNP chromatography.

DR2/MBP and DR2/CLIP were expressed in *Sf9* insect cells after infection with recombinant Baculovirus (MOI > 5, pAcDB3 plasmid with BaculoGold Baculovirus; BD Biosciences). Proteins were purified by affinity chromatography (L243, American Type Culture Collection) and the linker between peptide and DR β chain cleaved with thrombin (20 units thrombin/mg protein, 1.5 h, 25 °C). The complexes were further purified by ion exchange chromatography (MonoQ, GE Healthcare) and aggregates were removed by gel filtration (Superose 6, GE Healthcare). Purified proteins were buffer exchanged to the final buffer for SPR experiments (50 mM citrate phosphate buffer, pH 5.3, 150 mM NaCl, 0.06 % C₁₂E₉ detergent).

4.2.2 Surface plasmon resonance experiments

SPR experiments were prepared and carried out as described in 3.2.5. Chips were regenerated by injection of either HA peptide (50 μM) or MBP peptide (5 μM). For experiments at different temperatures than 25 $^{\circ}\text{C}$ the chip was again normalized after temperature change. Biotinylated DM wt and DM mut were prepared as described in 3.2.1. Binding of the reference flow cell (DM mut) was subtracted from binding in the experimental flow cell (DM wt).

4.2.3 Fluorescence polarization experiments

Fluorescence polarization (FP) experiments were conducted on a Victor³ V multilabel plate reader (PerkinElmer) using black polystyrene 384-well flat-bottomed plates (Corning). DR/peptide complexes were incubated with MBP(85-99) peptide which was labeled at position P5 (lysine-to-cysteine substitution) with a maleimide derivative of Alexa Fluor 488 (Molecular Probes). Measurements were performed in triplicates in a volume of 40 μL in 50 mM citrate phosphate buffer (pH 5.3) containing 150 mM NaCl.

4.3 Results and discussion

4.3.1 Preparing the high-affinity complexes HLA-DR2/MBP and HLA-DR1/HA

The high-affinity complexes DR1/HA and DR2/MBP were prepared to be tested for DM binding in SPR experiments at different temperatures. HA peptide is a high-affinity influenza hemagglutinin peptide of amino acid 306-318. MBP peptide is part of myelin basic protein (residues 85-99) and has a high-affinity to DR2. DR2/MBP was produced in *Sf9* insect cells and purified using affinity, ion exchange and gel filtration chromatography. The linker between MBP peptide and DR was proteolytically cleaved. To prepare the high-affinity DR1/HA complex, DR1/CLIP was produced in CHO cells and the linker between peptide and DR proteolytically cleaved after affinity chromatography. Following the peptide exchange protocol described in 4.2.1, HA peptide was loaded onto DR1 molecules and DR1/HA further purified by gel filtration and affinity chromatography.

4.3.2 Measuring HLA-DM binding to HLA-DR2/MBP and HLA-DR1/HA using surface plasmon resonance

Surface plasmon resonance experiments at 25 °C showed only little DM binding to the high-affinity DR/peptide complexes DR2/MBP and DR1/HA (see figure 4.1, A, B). To test whether DM binding to the high-affinity complexes is enhanced with higher temperature SPR experiments were carried out at 37 °C. As can be seen in figure 4.1 (D) definitive DR2/MBP binding to DM was measured at 37 °C with 69, 155 and 273 response units for 10 μ M, 20 μ M and 40 μ M DR2/MBP, respectively. DR1/HA was injected at 10 μ M, 20 μ M and 40 μ M, as well, at 37 °C and DM binding of 13, 22 and 39 response units was measured, respectively, (figure 4.1, C).

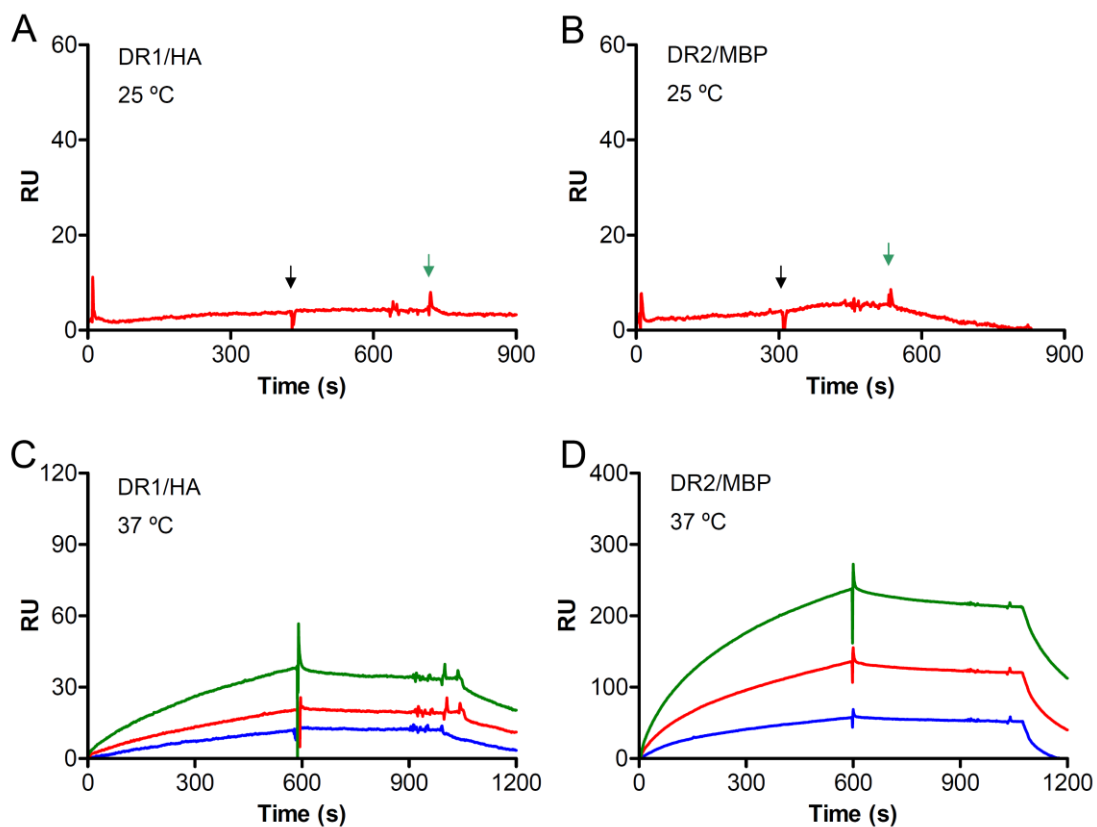


Figure 4.1: DM binding to high-affinity MHC II/peptide complexes at 25 °C and 37 °C. (A, B) DR1/HA (10 μ M) was injected for 7 minutes (A) and DR2/MBP (2 μ M) for 5 minutes (B) at a flow rate of 15 μ L/min at 25 °C, followed by buffer injection (black arrow) and peptide injection (green arrow), 50 μ M HA peptide (A) and 10 μ M CLIP peptide (A), respectively. (C, D) At 37 °C, DR1/HA (C) and DR2/MBP (D), respectively, were injected for 10 minutes at a flow rate of 15 μ L/min at 10 μ M (blue), 20 μ M (red) and 40 μ M (green), followed by injection of buffer and injection of 50 μ M HA peptide (C) or 5 μ M MBP peptide (D). (A-D) SPR assays were carried out in consecutive flow cells with 500 RU of immobilized DM wt and DM mut, respectively, in citrate phosphate buffer (pH 5.3). Binding in the DM mut flow cell was subtracted from measurements in the DM wt flow cell. (experiments in A and B were carried out by Anne-Kathrin Anders)

The SPR data show that increased DM binding to high-affinity MHC II/peptide complexes is detected at higher temperature suggesting that peptide mobility which is increased at higher temperature may play an important role for DM binding.

4.3.3 Comparing HLA-DM binding detected by surface plasmon resonance with HLA-DM catalysis measured by fluorescence polarization

To test the functional relevance of the DM binding assay conducted by surface plasmon resonance, SPR data were compared with fluorescence polarization experiments measuring DM catalysis. Therefore, DM binding and DM catalyzed peptide exchange of the low-affinity complex DR2/CLIP and the high-affinity complex DR2/MBP were measured and set in comparison. Comparing the initial binding rates of DM binding to DR2/CLIP and DR2/MBP measured by SPR, 8.7-fold slower DM binding was detected to DR2/MBP compared to DR2/CLIP (figure 4.2, A).

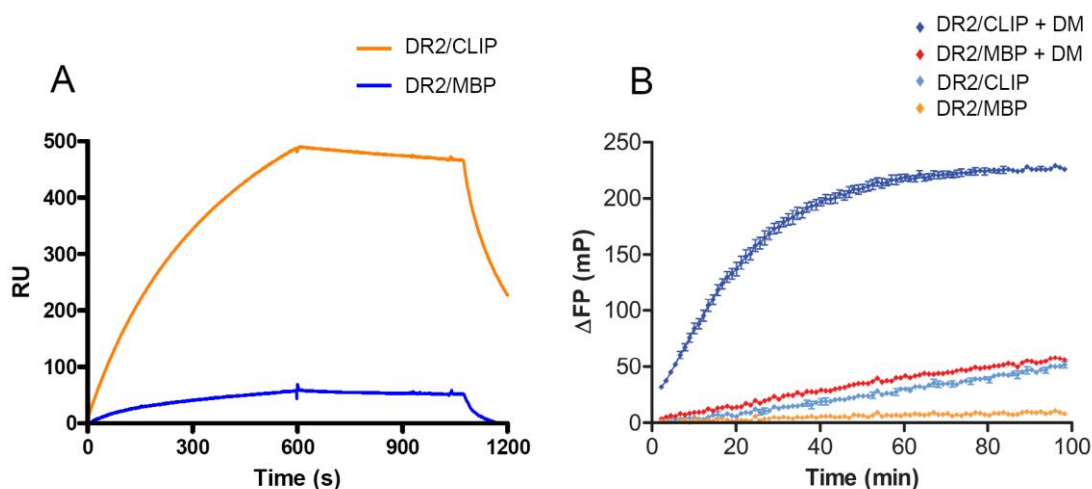


Figure 4.2: Comparison of the kinetics of DM binding and DM catalysis for low-affinity versus high-affinity DR/peptide complexes. (A) DM binding by low-affinity (DR2/CLIP) and high-affinity complexes (DR2/MBP). DR2 complexes preloaded with the indicated peptides (10 μ M) were injected for 10 minutes followed by injection of buffer and 5 μ M MBP peptide. The SPR experiments were carried out in citrate phosphate buffer (pH 5.3) at 37 $^{\circ}$ C at a flow rate of 15 μ L/min in consecutive flow cells with 500 RU of immobilized DM wt and DM mut, respectively. Measurements from the DM mut flow cell were subtracted from data obtained from the DM wt flow cell. DM binding by DR2/MBP was 8.7-fold slower compared to DR2/CLIP, based on measurements of the initial rates. (B) DM catalyzed peptide exchange of DR2/CLIP and DR2/MBP complexes. Binding of 200 nM Alexa488-labeled MBP to DR2 (200 nM) preloaded with the indicated peptides was measured in the presence or absence of 100 nM DM in 50 mM citrate phosphate buffer (pH 5.3), 150 mM NaCl. The initial rate of DM catalyzed peptide-binding was 11.8-fold slower when DR2/MBP rather than DR2/CLIP was used as the input protein in the reaction.

Measuring DM catalyzed peptide exchange of both MHC II/peptide complexes by FP in the presence of fluorophore-labeled MBP peptide and comparing again initial exchange rates, DM catalyzed peptide exchange was 11.8-fold slower when DR2/MBP rather than DR2/CLIP was used as the input protein in the reaction (figure 4.2, B).

As can be seen, the kinetics of DM binding and DM catalysis for low-affinity versus high-affinity DR/peptide complexes agree very well indicating data obtained by the DM binding assay have strong functional significance and can be related to DM activity.

4.4 Conclusion

In these studies temperature-dependent DM binding was demonstrated to high-affinity MHC II/peptide complexes previously exhibiting no or only little DM susceptibility. Surface plasmon resonance experiments at 37 °C showed increased DM binding to DR2/MBP and interestingly also definitive DM binding to DR1/HA, which was previously believed to be resistant to DM action (Kropshofer et al., 1996; Sloan et al., 1995). The presented data support the model of a common transient MHC II/peptide conformation for high- and low-affinity MHC II/peptide complexes dependent on kinetic parameters and more abundant at higher temperature. Furthermore, the data assist the hypothesis that increased peptide mobility may be necessary for initial DM binding as stated previously (Anders et al., 2011). The functional relevance of the applied DM binding assay was demonstrated by comparing SPR data with FP experiments measuring DM activity. Comparing initial rates of DM binding and DM catalysis of a low- and a high-affinity MHC II/peptide complex revealed high congruence. Showing that data obtained by the DM binding assay can be related to DM activity was important to demonstrate the functional relevance of the results.

Generation of high-affinity MHC II/peptide complexes *in vivo* is important for long-term presentation of MHC II/peptide complexes on the cell surface which is necessary for multiple T cell encounters. Here we show that DM can bind to high-affinity MHC II/peptide complexes and also exchange high-affinity peptides. However, we also demonstrate that DM interaction with high-affinity MHC II/peptide complexes is dependent on kinetic parameters and requires higher temperature compared to low-affinity MHC II/peptide complexes.

5 Final discussion and outlook

As antigen presentation by MHC II molecules plays a pivotal role in the adaptive immune response it is important to understand how antigenic peptides are selected and loaded onto MHC II molecules which is catalyzed by DM. The crystal structures of MHC II and DM are already known since 1993 and 1998, respectively, (Brown et al., 1993; Mosyak et al., 1998) and mutagenesis studies mapped a large lateral surface on both molecules required for interaction which has been confirmed by tethering experiments (Busch et al., 2002; Stratikos et al., 2002). However, the molecular mechanism of how DM catalyzes peptide exchange on MHC II molecules is still unknown and different models have been proposed including DM targeting the hydrogen bond network between peptide and MHC II (Mosyak et al., 1998; Weber et al., 1996) as well as global conformational changes (Belmares et al., 2002).

Recent studies in the lab showed strong DM binding to a low stability DR/peptide complex missing three N-terminal peptide residues (Anders et al., 2011) and thereby disrupting conserved MHC II-peptide interactions. The question arose whether the truncated peptide represented an intermediate state of a DR/peptide complex with the peptide N-terminus partially released due to peptide mobility. However, some high-affinity complexes, e.g. DR1/HA, were believed to be resistant to DM action as no DM-facilitated peptide exchange had been observed (Kropshofer et al., 1996; Sloan et al., 1995) arguing against this model which implied DM binding to any MHC II/peptide complex, even if to a small extent. Crucial surface plasmon resonance experiments undertaken during this study revealed concentration- and temperature-dependent DM binding to the high-affinity complexes DR1/HA and DR2/MBP, previously exhibiting no and only little DM binding, respectively. These data demonstrated that at high temperature DM binding can be detected to high-affinity MHC II/peptide complexes previously believed to be DM resistant substantiating the relevance of peptide mobility for DM catalyzed peptide exchange and supporting the model of spontaneous release of peptide N-terminus (Anders et al., 2011). Furthermore, the functional significance of the SPR data was demonstrated during these studies by comparing DM binding experiments with DM activity data measured by fluorescence polarization displaying an agreement between both assays.

NMR experiments performed during this work further addressed peptide mobility in the peptide-binding groove revealing the presence of multiple peptide conformations for

MBP peptide bound to DR2 molecule and advanced the image of MHC II/peptide complexes which is so far mainly influenced by the static picture of crystal structures. In the future, a distinct peak assignment of the NMR spectra could provide more detailed information about peptide dynamics in the peptide-binding groove.

Besides peptide mobility which probably plays an important role in the peptide exchange mechanism of MHC II molecules, another important factor for understanding the interaction between DM and MHC II might be the presence of multiple conformers of both molecules (Busch et al., 1998; Chou and Sadegh-Nasseri, 2000; Zarutskie et al., 1999). For example, empty MHC II molecules are known to rapidly lose their ability to bind peptides and aggregate (Germain and Rinker, 1993; Rabinowitz et al., 1998). Molecular dynamics simulations of empty MHC II molecules predict a partial collapse of the peptide-binding groove (Painter et al., 2008; Rupp et al., 2011) suggesting that major conformational changes may occur once the peptide leaves the binding groove. The MHC II receptive conformation which rapidly binds peptide is of special interest as it may reveal important features of the peptide exchange mechanism and likely represents the conformation DM binds to but on the other hand is probably also short-lived. During this study a DR1 structure is presented carrying an HA peptide variant missing two N-terminal peptide residues that reveals an intermediate state of a MHC II molecule during peptide release. As has been shown that the peptide N-terminus has to leave the binding groove in order for DM to bind (Anders et al., 2011) it is crucial to know what conformation MHC II molecules adapt once the peptide N-terminus is absent as that might be a conformation DM readily binds to and could give insight into the peptide exchange mechanism. Concerning the structure surprisingly no major but small conformational changes were observed including a small divergence of the α and β helices normally adjacent to the peptide N-terminus and an altered conformer of the conserved residue Val β 85 which partially opens up the P1 pocket. A narrowing of the binding groove was not observed as predicted by molecular dynamics simulations for empty MHC II molecules (Painter et al., 2008; Rupp et al., 2011), but might require a larger part of the peptide to be absent. Overall the DR1 structure seems to be relatively stable even if three conserved hydrogen bonds are disrupted and small conformational changes appear to destabilize the P1 anchor that may facilitate further release of the peptide. Although SPR data showed that the crystallized DR1/peptide complex binds to DM, it is not clear, yet, whether the crystallized structure represents the DR conformer DM binds to as DM may bind to a more dynamic and energetically less stable

conformer present in solution which may be exposed after further peptide release, e.g. release of the P1 anchor. That peptide-binding induces conformational changes of MHC II molecules has been observed before (Zarutskie et al., 1999) and also indications of alterations in the P1 pocket (Chou and Sadegh-Nasseri, 2000). Recently, a structure was published of a DR1 mutant carrying a full length CLIP peptide showing increased susceptibility to DM and revealing conformational alterations near the N-terminus of the bound peptide involving a reorientation of a helical region of the DR α chain for one of the two molecules in the asymmetric unit (Painter et al., 2011). Similar as discussed above the problem exists not knowing whether the crystallized DR form with the bound peptide binds to DM or whether part of the peptide first leaves the binding groove before DM binding occurs. As the mutation alters the P1 pocket and thereby destabilizes the bound peptide apparent by an increased intrinsic rate of peptide release (Painter et al., 2011) enhanced DM susceptibility could be also partially due to increased peptide mobility. To further address the receptive MHC II conformation which seems to be challenging to crystallize due to its short-lived state and potential structural diversity other methods might be necessary like NMR spectroscopy to investigate the dynamic state of the complex in solution. For example, the system established during this study involving isotope labeled peptide bound to MHC II molecule can be further developed and used to track the bound peptide N-terminus upon DM binding in solution. In addition, further crystallization experiments should be performed with a DR1 molecule carrying an N-terminally truncated HA peptide variant with a glycine at P2 position and no P1 anchor residue which showed enhanced DM binding during this study and could reveal whether conformational changes occur once the P1 anchor is absent.

The co-crystallization experiments of DR2 with the small molecule J10, a MHC loading enhancer, carried out in this study may involve a similar challenge as the small molecule may bind to and stabilize a different DR conformation than the form that crystallized. Functional experiments in this study already revealed a higher affinity of the small molecule to low-stability MHC II/peptide complexes and co-crystallization experiments should be repeated with a low-affinity DR/peptide complex. Especially, DR complexes with N-terminally truncated peptides should be analyzed for J10 binding and used for co-crystallization experiments as the small molecule may function by stabilizing the empty peptide-binding groove and a partially empty groove may expose

a potential binding site. Dipeptides, another group of MLE, for example, showed some evidence for binding in the P1 pocket (Gupta et al., 2008).

In general, investigating the mechanism of peptide exchange of MHC II molecules is very challenging as it involves breaking and reforming of tight interactions between the bound peptide and MHC II which probably involves multiple intermediate states. As peptide exchange is a dynamic process methods investigating protein dynamics should be explored besides X-ray crystallography. For example, NMR spectroscopy could be used to track peptide release and binding in solution as proposed above to gain insight into the dynamics of the process. X-ray crystallography, however, can provide important information about structural details of the process and the crystal structure of the MHC II/DM complex could display how MHC II and DM interact and reveal important details about the peptide exchange mechanism. However, so far it has been not possible to crystallize the MHC II/DM complex which is maybe also due to structural diversity of both molecules. DM exhibits highest affinity to empty DR molecules (Anders et al., 2011) but as empty MHC II molecules themselves are not stable and as even a partial empty peptide-binding groove attracts and binds extended protein parts (as has been shown in this study by a prominent crystal contact) an approach based on empty DR molecules may introduce inhomogeneity which could interfere with crystallization. A MHC II molecule with a covalently linked peptide which is N-terminally truncated provides a highly receptive DR form for the DR/DM complex without exposing an empty peptide-binding groove that may bind various contaminants. Therefore, the DR1 molecule carrying an HA peptide variant with a glycine at P2 position (missing residues P-2, P-1 and P1) which showed enhanced DM binding during this study could provide a new approach for crystallizing the DR/DM complex. To favor crystallization of the complex further studies could also explore covalent linkage between both molecules.

6 References

- Adams, P.D., Afonine, P.V., Bunkoczi, G., Chen, V.B., Davis, I.W., Echols, N., Headd, J.J., Hung, L.W., Kapral, G.J., Grosse-Kunstleve, R.W., *et al.* (2010). PHENIX: a comprehensive Python-based system for macromolecular structure solution. *Acta Crystallogr D Biol Crystallogr* 66, 213-221.
- Anders, A.K., Call, M.J., Schulze, M.S., Fowler, K.D., Schubert, D.A., Seth, N.P., Sundberg, E.J., and Wucherpfennig, K.W. (2011). HLA-DM captures partially empty HLA-DR molecules for catalyzed removal of peptide. *Nat Immunol* 12, 54-61.
- Anderson, K.S., and Cresswell, P. (1994). A role for calnexin (IP90) in the assembly of class II MHC molecules. *EMBO J* 13, 675-682.
- Bartels, C., Xia, T.H., Billeter, M., Güntert, P., and Wüthrich, K. (1995). The program XEASY for computer-supported NMR spectral analysis of biological macromolecules. *J. Biomolecular NMR* 5, 1-10.
- Behrens, G.M., Li, M., Davey, G.M., Allison, J., Flavell, R.A., Carbone, F.R., and Heath, W.R. (2004). Helper requirements for generation of effector CTL to islet beta cell antigens. *J Immunol* 172, 5420-5426.
- Belmares, M.P., Busch, R., Wucherpfennig, K.W., McConnell, H.M., and Mellins, E.D. (2002). Structural factors contributing to DM susceptibility of MHC class II/peptide complexes. *J Immunol* 169, 5109-5117.
- Brown, J.H., Jardetzky, T.S., Gorga, J.C., Stern, L.J., Urban, R.G., Strominger, J.L., and Wiley, D.C. (1993). Three-dimensional structure of the human class II histocompatibility antigen HLA-DR1. *Nature* 364, 33-39.
- Brunger, A.T. (1992). Free R value: a novel statistical quantity for assessing the accuracy of crystal structures. *Nature* 355, 472-475.
- Brunger, A.T. (2007). Version 1.2 of the Crystallography and NMR system. *Nat Protoc* 2, 2728-2733.
- Brunger, A.T., Adams, P.D., Clore, G.M., DeLano, W.L., Gros, P., Grosse-Kunstleve, R.W., Jiang, J.S., Kuszewski, J., Nilges, M., Pannu, N.S., *et al.* (1998). Crystallography & NMR system: A new software suite for macromolecular structure determination. *Acta Crystallogr D Biol Crystallogr* 54, 905-921.
- Busch, R., Pashine, A., Garcia, K.C., and Mellins, E.D. (2002). Stabilization of soluble, low-affinity HLA-DM/HLA-DR1 complexes by leucine zippers. *J Immunol Methods* 263, 111-121.
- Busch, R., Reich, Z., Zaller, D.M., Sloan, V., and Mellins, E.D. (1998). Secondary structure composition and pH-dependent conformational changes of soluble recombinant HLA-DM. *J Biol Chem* 273, 27557-27564.
- Call, M.J. (2011). Small molecule modulators of MHC class II antigen presentation: Mechanistic insights and implications for therapeutic application. *Mol Immunol* 48, 1735-1743.

- Call, M.J., Xing, X., Cuny, G.D., Seth, N.P., Altmann, D.M., Fugger, L., Krogsgaard, M., Stein, R.L., and Wucherpennig, K.W. (2009). In vivo enhancement of peptide display by MHC class II molecules with small molecule catalysts of peptide exchange. *J Immunol* *182*, 6342-6352.
- Chen, V.B., Arendall, W.B., 3rd, Headd, J.J., Keedy, D.A., Immormino, R.M., Kapral, G.J., Murray, L.W., Richardson, J.S., and Richardson, D.C. (2010). MolProbity: all-atom structure validation for macromolecular crystallography. *Acta Crystallogr D Biol Crystallogr* *66*, 12-21.
- Chen, X., Laur, O., Kambayashi, T., Li, S., Bray, R.A., Weber, D.A., Karlsson, L., and Jensen, P.E. (2002). Regulated expression of human histocompatibility leukocyte antigen (HLA)-DO during antigen-dependent and antigen-independent phases of B cell development. *J Exp Med* *195*, 1053-1062.
- Cho, S.G., Attaya, M., and Monaco, J.J. (1991). New class II-like genes in the murine MHC. *Nature* *353*, 573-576.
- Chou, C.L., and Sadegh-Nasseri, S. (2000). HLA-DM recognizes the flexible conformation of major histocompatibility complex class II. *J Exp Med* *192*, 1697-1706.
- Cresswell, P. (1996). Invariant chain structure and MHC class II function. *Cell* *84*, 505-507.
- Day, C.L., Seth, N.P., Lucas, M., Appel, H., Gauthier, L., Lauer, G.M., Robbins, G.K., Szczepiorkowski, Z.M., Casson, D.R., Chung, R.T., *et al.* (2003). Ex vivo analysis of human memory CD4 T cells specific for hepatitis C virus using MHC class II tetramers. *J Clin Invest* *112*, 831-842.
- De Wall, S.L., Painter, C., Stone, J.D., Bandaranayake, R., Wiley, D.C., Mitchison, T.J., Stern, L.J., and DeDecker, B.S. (2006). Noble metals strip peptides from class II MHC proteins. *Nat Chem Biol* *2*, 197-201.
- Delaglio, F., Grzesiek, S., Vuister, G.W., Zhu, G., Pfeifer, J., and Bax, A. (1995). NMRPipe: a multidimensional spectral processing system based on UNIX pipes. *J Biomol NMR* *6*, 277-293.
- Denzin, L.K., and Cresswell, P. (1995). HLA-DM induces CLIP dissociation from MHC class II alpha beta dimers and facilitates peptide loading. *Cell* *82*, 155-165.
- Denzin, L.K., Sant'Angelo, D.B., Hammond, C., Surman, M.J., and Cresswell, P. (1997). Negative regulation by HLA-DO of MHC class II-restricted antigen processing. *Science* *278*, 106-109.
- Deshaies, F., Brunet, A., Diallo, D.A., Denzin, L.K., Samaan, A., and Thibodeau, J. (2005). A point mutation in the groove of HLA-DO allows egress from the endoplasmic reticulum independent of HLA-DM. *Proc Natl Acad Sci U S A* *102*, 6443-6448.
- Deussing, J., Roth, W., Saftig, P., Peters, C., Ploegh, H.L., and Villadangos, J.A. (1998). Cathepsins B and D are dispensable for major histocompatibility complex class II-mediated antigen presentation. *Proc Natl Acad Sci U S A* *95*, 4516-4521.
- Doebele, R.C., Busch, R., Scott, H.M., Pashine, A., and Mellins, E.D. (2000). Determination of the HLA-DM interaction site on HLA-DR molecules. *Immunity* *13*, 517-527.
- Emsley, P., and Cowtan, K. (2004). Coot: model-building tools for molecular graphics. *Acta Crystallogr D Biol Crystallogr* *60*, 2126-2132.

- Falk, K., Lau, J.M., Santambrogio, L., Esteban, V.M., Puentes, F., Rotzschke, O., and Strominger, J.L. (2002). Ligand exchange of major histocompatibility complex class II proteins is triggered by H-bond donor groups of small molecules. *J Biol Chem* 277, 2709-2715.
- Ferrante, A., and Gorski, J. (2010). Cutting edge: HLA-DM-mediated peptide exchange functions normally on MHC class II-peptide complexes that have been weakened by elimination of a conserved hydrogen bond. *J Immunol* 184, 1153-1158.
- Germain, R.N. (1994). MHC-dependent antigen processing and peptide presentation: providing ligands for T lymphocyte activation. *Cell* 76, 287-299.
- Germain, R.N., and Rinker, A.G., Jr. (1993). Peptide binding inhibits protein aggregation of invariant-chain free class II dimers and promotes surface expression of occupied molecules. *Nature* 363, 725-728.
- Goronzy, J.J., and Weyand, C.M. (2005). Rheumatoid arthritis. *Immunol Rev* 204, 55-73.
- Gunther, S., Schlundt, A., Sticht, J., Roske, Y., Heinemann, U., Wiesmuller, K.H., Jung, G., Falk, K., Rotzschke, O., and Freund, C. (2010). Bidirectional binding of invariant chain peptides to an MHC class II molecule. *Proc Natl Acad Sci U S A* 107, 22219-22224.
- Gupta, S., Hopner, S., Rupp, B., Gunther, S., Dickhaut, K., Agarwal, N., Cardoso, M.C., Kuhne, R., Wiesmuller, K.H., Jung, G., *et al.* (2008). Anchor side chains of short peptide fragments trigger ligand-exchange of class II MHC molecules. *PLoS One* 3, e1814.
- Hauptmann, G., and Bahram, S. (2004). Genetics of the central MHC. *Curr Opin Immunol* 16, 668-672.
- Hopner, S., Dickhaut, K., Hofstatter, M., Kramer, H., Ruckerl, D., Soderhall, J.A., Gupta, S., Marin-Esteban, V., Kuhne, R., Freund, C., *et al.* (2006). Small organic compounds enhance antigen loading of class II major histocompatibility complex proteins by targeting the polymorphic P1 pocket. *J Biol Chem* 281, 38535-38542.
- Hornell, T.M., Burster, T., Jahnsen, F.L., Pashine, A., Ochoa, M.T., Harding, J.J., Macaubas, C., Lee, A.W., Modlin, R.L., and Mellins, E.D. (2006). Human dendritic cell expression of HLA-DO is subset specific and regulated by maturation. *J Immunol* 176, 3536-3547.
- Inoko, H., Ando, A., Kimura, M., and Tsuji, K. (1985). Isolation and characterization of the cDNA clone and genomic clones of a new HLA class II antigen heavy chain, DO alpha. *J Immunol* 135, 2156-2159.
- Jones, T.A., Zou, J.Y., Cowan, S.W., and Kjeldgaard, M. (1991). Improved methods for building protein models in electron density maps and the location of errors in these models. *Acta Crystallogr A* 47 (Pt 2), 110-119.
- Jonsson, A.K., and Rask, L. (1989). Human class II DNA and DOB genes display low sequence variability. *Immunogenetics* 29, 411-413.
- Kalandadze, A., Galleno, M., Foncerrada, L., Strominger, J.L., and Wucherpfennig, K.W. (1996). Expression of recombinant HLA-DR2 molecules. Replacement of the hydrophobic transmembrane region by a leucine zipper dimerization motif allows the assembly and secretion of soluble DR alpha beta heterodimers. *J Biol Chem* 271, 20156-20162.
- Keller, R.L.J. (2004). The computer aided resonance assignment tutorial. Cantina Verlag, Goldau, Switzerland.

- Kelly, A.P., Monaco, J.J., Cho, S.G., and Trowsdale, J. (1991). A new human HLA class II-related locus, DM. *Nature* 353, 571-573.
- Kleid, D.G., Yansura, D., Small, B., Dowbenko, D., Moore, D.M., Grubman, M.J., McKercher, P.D., Morgan, D.O., Robertson, B.H., and Bachrach, H.L. (1981). Cloned viral protein vaccine for foot-and-mouth disease: responses in cattle and swine. *Science* 214, 1125-1129.
- Kropshofer, H., Vogt, A.B., Moldenhauer, G., Hammer, J., Blum, J.S., and Hammerling, G.J. (1996). Editing of the HLA-DR-peptide repertoire by HLA-DM. *Embo J* 15, 6144-6154.
- Kropshofer, H., Vogt, A.B., They, C., Armandola, E.A., Li, B.C., Moldenhauer, G., Amigorena, S., and Hammerling, G.J. (1998). A role for HLA-DO as a co-chaperone of HLA-DM in peptide loading of MHC class II molecules. *EMBO J* 17, 2971-2981.
- Lamb, C.A., and Cresswell, P. (1992). Assembly and transport properties of invariant chain trimers and HLA-DR-invariant chain complexes. *J Immunol* 148, 3478-3482.
- Lanzavecchia, A., Reid, P.A., and Watts, C. (1992). Irreversible association of peptides with class II MHC molecules in living cells. *Nature* 357, 249-252.
- Leddon, S.A., and Sant, A.J. (2010). Generation of MHC class II-peptide ligands for CD4 T-cell allorecognition of MHC class II molecules. *Curr Opin Organ Transplant* 15, 505-511.
- Liljedahl, M., Kuwana, T., Fung-Leung, W.P., Jackson, M.R., Peterson, P.A., and Karlsson, L. (1996). HLA-DO is a lysosomal resident which requires association with HLA-DM for efficient intracellular transport. *EMBO J* 15, 4817-4824.
- Liljedahl, M., Winqvist, O., Surh, C.D., Wong, P., Ngo, K., Teyton, L., Peterson, P.A., Brunmark, A., Rudensky, A.Y., Fung-Leung, W.P., and Karlsson, L. (1998). Altered antigen presentation in mice lacking H2-O. *Immunity* 8, 233-243.
- Lindstedt, R., Liljedahl, M., Peleraux, A., Peterson, P.A., and Karlsson, L. (1995). The MHC class II molecule H2-M is targeted to an endosomal compartment by a tyrosine-based targeting motif. *Immunity* 3, 561-572.
- Marin-Esteban, V., Falk, K., and Rotzschke, O. (2003). Small-molecular compounds enhance the loading of APC with encephalitogenic MBP protein. *J Autoimmun* 20, 63-69.
- Marin-Esteban, V., Falk, K., and Rotzschke, O. (2004). "Chemical analogues" of HLA-DM can induce a peptide-receptive state in HLA-DR molecules. *J Biol Chem* 279, 50684-50690.
- Marks, M.S., Roche, P.A., van Donselaar, E., Woodruff, L., Peters, P.J., and Bonifacio, J.S. (1995). A lysosomal targeting signal in the cytoplasmic tail of the beta chain directs HLA-DM to MHC class II compartments. *J Cell Biol* 131, 351-369.
- McCoy, A.J., Grosse-Kunstleve, R.W., Adams, P.D., Winn, M.D., Storoni, L.C., and Read, R.J. (2007). Phaser crystallographic software. *J Appl Crystallogr* 40, 658-674.
- Mehra, N.K., and Kaur, G. (2003). MHC-based vaccination approaches: progress and perspectives. *Expert Rev Mol Med* 5, 1-17.
- Miozzari, G.F., and Yanofsky, C. (1978). Translation of the leader region of the Escherichia coli tryptophan operon. *J Bacteriol* 133, 1457-1466.

- Morris, P., Shaman, J., Attaya, M., Amaya, M., Goodman, S., Bergman, C., Monaco, J.J., and Mellins, E. (1994). An essential role for HLA-DM in antigen presentation by class II major histocompatibility molecules. *Nature* 368, 551-554.
- Mosyak, L., Zaller, D.M., and Wiley, D.C. (1998). The structure of HLA-DM, the peptide exchange catalyst that loads antigen onto class II MHC molecules during antigen presentation. *Immunity* 9, 377-383.
- Nagarajan, U.M., Lochamy, J., Chen, X., Beresford, G.W., Nilsen, R., Jensen, P.E., and Boss, J.M. (2002). Class II transactivator is required for maximal expression of HLA-DOB in B cells. *J Immunol* 168, 1780-1786.
- Nakagawa, T., Roth, W., Wong, P., Nelson, A., Farr, A., Deussing, J., Villadangos, J.A., Ploegh, H., Peters, C., and Rudensky, A.Y. (1998). Cathepsin L: critical role in Ii degradation and CD4 T cell selection in the thymus. *Science* 280, 450-453.
- Narayan, K., Chou, C.L., Kim, A., Hartman, I.Z., Dalai, S., Khoruzhenko, S., and Sadegh-Nasseri, S. (2007). HLA-DM targets the hydrogen bond between the histidine at position beta81 and peptide to dissociate HLA-DR-peptide complexes. *Nat Immunol* 8, 92-100.
- Naruse, T.K., Kawata, H., Anzai, T., Takashige, N., Kagiya, M., Nose, Y., Nabeya, N., Isshiki, G., Tatsumi, N., and Inoko, H. (1999). Limited polymorphism in the HLA-DOA gene. *Tissue Antigens* 53, 359-365.
- Naruse, T.K., Kawata, H., Inoko, H., Isshiki, G., Yamano, K., Hino, M., and Tatsumi, N. (2002). The HLA-DOB gene displays limited polymorphism with only one amino acid substitution. *Tissue Antigens* 59, 512-519.
- Newcomb, J.R., and Cresswell, P. (1993). Structural analysis of proteolytic products of MHC class II-invariant chain complexes generated in vivo. *J Immunol* 151, 4153-4163.
- Nicholson, M.J., Moradi, B., Seth, N.P., Xing, X., Cuny, G.D., Stein, R.L., and Wucherpennig, K.W. (2006). Small molecules that enhance the catalytic efficiency of HLA-DM. *J Immunol* 176, 4208-4220.
- Otwinowski, Z., and Minor, W. (1997). Processing of X-ray diffraction data collected in oscillation mode. *Methods Enzymol* 276, 307-326.
- Painter, C.A., Cruz, A., Lopez, G.E., Stern, L.J., and Zavala-Ruiz, Z. (2008). Model for the peptide-free conformation of class II MHC proteins. *PLoS One* 3, e2403.
- Painter, C.A., Negroni, M.P., Kellersberger, K.A., Zavala-Ruiz, Z., Evans, J.E., and Stern, L.J. (2011). Conformational lability in the class II MHC 310 helix and adjacent extended strand dictate HLA-DM susceptibility and peptide exchange. *Proc Natl Acad Sci U S A* 108, 19329-19334.
- Pashine, A., Busch, R., Belmares, M.P., Munning, J.N., Doebele, R.C., Buckingham, M., Nolan, G.P., and Mellins, E.D. (2003). Interaction of HLA-DR with an acidic face of HLA-DM disrupts sequence-dependent interactions with peptides. *Immunity* 19, 183-192.
- Peaper, D.R., Wearsch, P.A., and Cresswell, P. (2005). Tapasin and ERp57 form a stable disulfide-linked dimer within the MHC class I peptide-loading complex. *EMBO J* 24, 3613-3623.

- Pervushin, K., Riek, R., Wider, G., and Wuthrich, K. (1997). Attenuated T2 relaxation by mutual cancellation of dipole-dipole coupling and chemical shift anisotropy indicates an avenue to NMR structures of very large biological macromolecules in solution. *Proc Natl Acad Sci U S A* *94*, 12366-12371.
- Rabinowitz, J.D., Vrljic, M., Kasson, P.M., Liang, M.N., Busch, R., Boniface, J.J., Davis, M.M., and McConnell, H.M. (1998). Formation of a highly peptide-receptive state of class II MHC. *Immunity* *9*, 699-709.
- Reay, P.A., Wettstein, D.A., and Davis, M.M. (1992). pH dependence and exchange of high and low responder peptides binding to a class II MHC molecule. *EMBO J* *11*, 2829-2839.
- Reith, W., and Mach, B. (2001). The bare lymphocyte syndrome and the regulation of MHC expression. *Annu Rev Immunol* *19*, 331-373.
- Riese, R.J., Wolf, P.R., Bromme, D., Natkin, L.R., Villadangos, J.A., Ploegh, H.L., and Chapman, H.A. (1996). Essential role for cathepsin S in MHC class II-associated invariant chain processing and peptide loading. *Immunity* *4*, 357-366.
- Roche, P.A., Marks, M.S., and Cresswell, P. (1991). Formation of a nine-subunit complex by HLA class II glycoproteins and the invariant chain. *Nature* *354*, 392-394.
- Runnels, H.A., Weber, D.A., Moore, J.C., Westerman, L.E., and Jensen, P.E. (1997). Intact proteins can bind to class II histocompatibility molecules with high affinity. *Mol Immunol* *34*, 471-480.
- Rupp, B., Gunther, S., Makhmoor, T., Schlundt, A., Dickhaut, K., Gupta, S., Choudhary, I., Wiesmuller, K.H., Jung, G., Freund, C., *et al.* (2011). Characterization of structural features controlling the receptiveness of empty class II MHC molecules. *PLoS One* *6*, e18662.
- Sadasivan, B., Lehner, P.J., Ortmann, B., Spies, T., and Cresswell, P. (1996). Roles for calreticulin and a novel glycoprotein, tapasin, in the interaction of MHC class I molecules with TAP. *Immunity* *5*, 103-114.
- Sadegh-Nasseri, S., Chen, M., Narayan, K., and Bouvier, M. (2008). The convergent roles of tapasin and HLA-DM in antigen presentation. *Trends Immunol* *29*, 141-147.
- Sakaguchi, S. (2010). Immunology: Conditional stability of T cells. *Nature* *468*, 41-42.
- Sato, A.K., Zarutskie, J.A., Rushe, M.M., Lomakin, A., Natarajan, S.K., Sadegh-Nasseri, S., Benedek, G.B., and Stern, L.J. (2000). Determinants of the peptide-induced conformational change in the human class II major histocompatibility complex protein HLA-DR1. *J Biol Chem* *275*, 2165-2173.
- Schrodinger, LLC (2010). The PyMOL Molecular Graphics System, Version 1.3r1.
- Schulze, M.S., and Wucherpfennig, K.W. (2012). The mechanism of HLA-DM induced peptide exchange in the MHC class II antigen presentation pathway. *Curr Opin Immunol* *24*, 105-111.
- Schuttelkopf, A.W., and van Aalten, D.M. (2004). PRODRG: a tool for high-throughput crystallography of protein-ligand complexes. *Acta Crystallogr D Biol Crystallogr* *60*, 1355-1363.

- Servenius, B., Rask, L., and Peterson, P.A. (1987). Class II genes of the human major histocompatibility complex. The DO beta gene is a divergent member of the class II beta gene family. *J Biol Chem* 262, 8759-8766.
- Sloan, V.S., Cameron, P., Porter, G., Gammon, M., Amaya, M., Mellins, E., and Zaller, D.M. (1995). Mediation by HLA-DM of dissociation of peptides from HLA-DR. *Nature* 375, 802-806.
- Smith, K.J., Pyrdol, J., Gauthier, L., Wiley, D.C., and Wucherpfennig, K.W. (1998). Crystal structure of HLA-DR2 (DRA*0101, DRB1*1501) complexed with a peptide from human myelin basic protein. *J Exp Med* 188, 1511-1520.
- Staley, J.P., and Kim, P.S. (1994). Formation of a native-like subdomain in a partially folded intermediate of bovine pancreatic trypsin inhibitor. *Protein Sci* 3, 1822-1832.
- Stern, L.J., Brown, J.H., Jardetzky, T.S., Gorga, J.C., Urban, R.G., Strominger, J.L., and Wiley, D.C. (1994). Crystal structure of the human class II MHC protein HLA-DR1 complexed with an influenza virus peptide. *Nature* 368, 215-221.
- Stratikos, E., Mosyak, L., Zaller, D.M., and Wiley, D.C. (2002). Identification of the lateral interaction surfaces of human histocompatibility leukocyte antigen (HLA)-DM with HLA-DR1 by formation of tethered complexes that present enhanced HLA-DM catalysis. *J Exp Med* 196, 173-183.
- Stratikos, E., Wiley, D.C., and Stern, L.J. (2004). Enhanced catalytic action of HLA-DM on the exchange of peptides lacking backbone hydrogen bonds between their N-terminal region and the MHC class II alpha-chain. *J Immunol* 172, 1109-1117.
- Studier, F.W., Rosenberg, A.H., Dunn, J.J., and Dubendorff, J.W. (1990). Use of T7 RNA polymerase to direct expression of cloned genes. *Methods Enzymol* 185, 60-89.
- Svejgaard, A. (2008). The immunogenetics of multiple sclerosis. *Immunogenetics* 60, 275-286.
- Tonnelle, C., DeMars, R., and Long, E.O. (1985). DO beta: a new beta chain gene in HLA-D with a distinct regulation of expression. *EMBO J* 4, 2839-2847.
- Trowsdale, J., and Kelly, A. (1985). The human HLA class II alpha chain gene DZ alpha is distinct from genes in the DP, DQ and DR subregions. *EMBO J* 4, 2231-2237.
- Vagin, A., and Teplyakov, A. (2010). Molecular replacement with MOLREP. *Acta Crystallogr D Biol Crystallogr* 66, 22-25.
- van Ham, M., van Lith, M., Lillemeier, B., Tjin, E., Gruneberg, U., Rahman, D., Pastoors, L., van Meijgaarden, K., Roucard, C., Trowsdale, J., *et al.* (2000). Modulation of the major histocompatibility complex class II-associated peptide repertoire by human histocompatibility leukocyte antigen (HLA)-DO. *J Exp Med* 191, 1127-1136.
- van Ham, S.M., Tjin, E.P., Lillemeier, B.F., Gruneberg, U., van Meijgaarden, K.E., Pastoors, L., Verwoerd, D., Tulp, A., Canas, B., Rahman, D., *et al.* (1997). HLA-DO is a negative modulator of HLA-DM-mediated MHC class II peptide loading. *Curr Biol* 7, 950-957.
- van Lith, M., van Ham, M., and Neefjes, J. (2002). Novel polymorphisms in HLA-DOA and HLA-DOB in B-cell malignancies. *Immunogenetics* 54, 591-595.

-
- Vinuesa, C.G., Tangye, S.G., Moser, B., and Mackay, C.R. (2005). Follicular B helper T cells in antibody responses and autoimmunity. *Nat Rev Immunol* 5, 853-865.
- Vogt, A.B., Kropshofer, H., Kalbacher, H., Kalbus, M., Rammensee, H.G., Coligan, J.E., and Martin, R. (1994). Ligand motifs of HLA-DRB5*0101 and DRB1*1501 molecules delineated from self-peptides. *J Immunol* 153, 1665-1673.
- Wearsch, P.A., and Cresswell, P. (2007). Selective loading of high-affinity peptides onto major histocompatibility complex class I molecules by the tapasin-ERp57 heterodimer. *Nat Immunol* 8, 873-881.
- Wearsch, P.A., and Cresswell, P. (2008). The quality control of MHC class I peptide loading. *Curr Opin Cell Biol* 20, 624-631.
- Weber, D.A., Evavold, B.D., and Jensen, P.E. (1996). Enhanced dissociation of HLA-DR-bound peptides in the presence of HLA-DM. *Science* 274, 618-620.
- Zarutskie, J.A., Sato, A.K., Rushe, M.M., Chan, I.C., Lomakin, A., Benedek, G.B., and Stern, L.J. (1999). A conformational change in the human major histocompatibility complex protein HLA-DR1 induced by peptide binding. *Biochemistry* 38, 5878-5887.
- Zhou, Z., Callaway, K.A., Weber, D.A., and Jensen, P.E. (2009). Cutting edge: HLA-DM functions through a mechanism that does not require specific conserved hydrogen bonds in class II MHC-peptide complexes. *J Immunol* 183, 4187-4191.